eCAM Evidence-Based Complementary and Alternative Medicine

Medicinal Herbs and Their Active Compounds for Fatty Liver Diseases

Lead Guest Editor: Chang G. Son
Guest Editors: Zhang Wei, H. Balaji Raghavendran, Jing-Hua Wang, and Elzbieta Janda

Medicinal Herbs and Their Active Compounds for Fatty Liver Diseases

Evidence-Based Complementary and Alternative Medicine

Medicinal Herbs and Their Active Compounds for Fatty Liver Diseases

Special Issue Editor in Chief: Chang G. Son
Guest Editors: Zhang Wei, H. Balaji Raghavendran, Jing-Hua Wang, and Elzbieta Janda

Editorial Board

Contents

Hindawi
Evidence-Based Complementary and Alternative Medicine
Volume 2017, Article ID 3612478, 2 pages
https://doi.org/10.1155/2017/3612478

Editorial

Medicinal Herbs and Their Active Compounds for Fatty Liver Diseases

Chang Gue Son,[1] Zhang Wei,[2] H. Balaji Raghavendran,[3] Jing-Hua Wang,[4] and Elzbieta Janda[5]

[1]*Liver & Immunology Research Center, Daejeon Oriental Hospital of Daejeon University, Daejeon, Republic of Korea*
[2]*Shanghai University of Traditional Chinese Medicine, Shanghai, China*
[3]*Department of Orthopedic Surgery, University of Malaya, Faculty of Medicine, Kuala Lumpur, Malaysia*
[4]*Key Laboratory of Xin'an Medicine, Ministry of Education, Clinical College of TCM, Anhui University of TCM, Hefei, Anhui Province, China*
[5]*Department of Health Sciences, Magna Graecia University, Campus Germaneto, Catanzaro, Italy*

Correspondence should be addressed to Chang Gue Son; ckson@dju.ac.kr

Received 7 November 2017; Accepted 8 November 2017; Published 7 December 2017

Fatty liver disease (FLD), also called commonly as fatty liver or hepatic steatosis, is a condition of the excessive accumulation of lipids in hepatocytes. The prevalence of FLD in the general population ranges from 10% to 24% in various countries [1]. Fatty liver is generally classified as alcoholic steatosis (alcoholic FLD) or nonalcoholic fatty liver disease (NAFLD), depending on the contribution of alcohol to the FLD pathogenesis [2]. Due to decreased number of hepatic viruses carriers and increased population with obesity, FLD has become the most common cause of abnormal liver function tests in developed countries recently [3].

Fatty liver is a leading step to chronic liver diseases including steatohepatitis (nonalcoholic steatohepatitis, NASH, and alcoholic steatohepatitis, ASH), liver fibrosis, and cirrhosis worldwide [4]. In addition, FLD is also associated with other diseases such as metabolic syndrome and diabetes mellitus [5]. FLD has a complex pathology involving the imbalance between lipogenesis and lipolysis, followed by inflammatory response [6]. The high prevalence of FLD is considered as a medical issue worldwide; yet there are no currently available drug-based therapies. For this reason medicinal herbs-derived remedies are emerging as potential therapeutics against FLD due to high efficacy and low risk of side effects [7, 8].

This special issue is an attempt to contribute to the knowledge on CAM treatments for fatty liver diseases and its associated disorders. We called for articles that have explored effectiveness and mechanisms of medicinal herbs and their compounds on FLD. A collection of seven original research articles are presented, which address the animal (six articles) or cell-based (one article) pharmacological effects of herbal drugs or their compounds on FLD. This issue presets herbal resources which consisted of three multiherbal formulae (Dahuang Zexie Decoction, Yinchen Linggui Zhugan Decoction, and Seyoeum), three of medicinal plants *(Artemisia iwayomogi* plus *Curcuma longa,* Salvia-Nelumbinis Naturalis, and *Euphorbia kansui),* and one citrus bioflavonoid (Hesperidin) against NAFLD, nonalcoholic steatohepatitis (NASH), and lipid metabolic disorders, respectively.

This special issue provides valuable information to practitioners and researchers working in the field of FLD regarding new potential medicinal herbs and pathophysiological features of multitargets in FLD. We hope that it will become their inspiration or reference to develop new therapeutic strategies against FLD based on herbal-derived multidrugs and bioactive compounds.

Acknowledgments

We, the editorial team, sincerely thank all the authors for submitting their valuable manuscripts and for their patience,

and we are also grateful to the reviewers for their timely responses. All the credits for developing this issue go to all its contributors and the guest editors.

Chang Gue Son
Zhang Wei
H. Balaji Raghavendran
Jing-Hua Wang
Elzbieta Janda

References

[1] W. Dunn, P. Angulo, S. Sanderson et al., "Utility of a new model to diagnose an alcohol basis for steatohepatitis," *Gastroenterology*, vol. 131, no. 4, pp. 1057–1063, 2006.

[2] P. Angulo, "Medical progress: nonalcoholic fatty liver disease," *The New England Journal of Medicine*, vol. 346, no. 16, pp. 1221–1231, 2002.

[3] D. R. LaBrecque, Z. Abbas, F. Anania et al., "World gastroenterology organisation global guidelines: nonalcoholic fatty liver disease and nonalcoholic steatohepatitis," *Journal of Clinical Gastroenterology*, vol. 48, no. 6, pp. 467–473, 2014.

[4] M. Blachier, H. Leleu, M. Peck-Radosavljevic, D.-C. Valla, and F. Roudot-Thoraval, "The burden of liver disease in Europe: a review of available epidemiological data," *Journal of Hepatology*, vol. 58, no. 3, pp. 593–608, 2013.

[5] J. C. Bae, S. K. Kim, J. M. Han et al., "Additive effect of nonalcoholic fatty liver disease on the development of diabetes in individuals with metabolic syndrome," *Diabetes Research and Clinical Practice*, vol. 129, pp. 136–143, 2017.

[6] A. E. Feldstein, N. W. Werneburg, and A. Canbay, "Free fatty acids promote hepatic lipotoxicity by stimulating TNF-α expression via a lysosomal pathway," *Hepatology*, vol. 40, no. 1, pp. 185–194, 2004.

[7] M. Parafati, A. Lascala, V. M. Morittu et al., "Bergamot polyphenol fraction prevents nonalcoholic fatty liver disease via stimulation of lipophagy in cafeteria diet-induced rat model of metabolic syndrome," *The Journal of Nutritional Biochemistry*, vol. 26, no. 9, pp. 938–948, 2015.

[8] H. Yao, Y.-J. Qiao, Y.-L. Zhao et al., "Herbal medicines and nonalcoholic fatty liver disease," *World Journal of Gastroenterology*, vol. 22, no. 30, pp. 6890–6905, 2016.

Hindawi
Evidence-Based Complementary and Alternative Medicine
Volume 2017, Article ID 2945803, 13 pages
https://doi.org/10.1155/2017/2945803

Research Article

Dahuang Zexie Decoction Protects against High-Fat Diet-Induced NAFLD by Modulating Gut Microbiota-Mediated Toll-Like Receptor 4 Signaling Activation and Loss of Intestinal Barrier

Jing Fang,[1] Xiaoqi Sun,[2] Boyu Xue,[1] Nanyuan Fang,[1,3] and Min Zhou[1,3]

[1] *The First College of Clinical Medicine, Nanjing University of Chinese Medicine, Nanjing 210023, China*
[2] *Department of Police Tactics, Nanjing Forest Police College, Nanjing 210023, China*
[3] *Department of Infectious Disease, Jiangsu Province Hospital of Traditional Chinese Medicine, Affiliated Hospital of Nanjing University of Chinese Medicine, Nanjing 210029, China*

Correspondence should be addressed to Min Zhou; zhoumdoctor@163.com

Received 20 July 2017; Revised 24 September 2017; Accepted 4 October 2017; Published 12 November 2017

Academic Editor: Chang G. Son

Increasing evidence suggests that intestinal dysbiosis, intestinal barrier dysfunction, and activated Toll-like receptor 4 (TLR4) signaling play key roles in the pathogenesis of NAFLD. Dahuang Zexie Decoction (DZD) has been verified to be effective for treating NAFLD, but the mechanisms remain unclear. In this study, we investigated the effects of DZD on NAFLD rats and determined whether such effects were associated with change of the gut microbiota, downregulated activity of the TLR4 signaling pathway, and increased expressions of tight junction (TJ) proteins in the gut. Male Sprague Dawley rats were fed high-fat diet (HFD) for 16 weeks to induce NAFLD and then given DZD intervention for 4 weeks. We found that DZD reduced body and liver weights of NAFLD rats, improved serum lipid levels and liver function parameters, and relieved NAFLD. We further found that DZD changed intestinal bacterial communities, inhibited the intestinal TLR4 signaling pathway, and restored the expressions of TJ proteins in the gut. Meanwhile ten potential components of DZD had been identified. These findings suggest that DZD may protects against NAFLD by modulating gut microbiota-mediated TLR4 signaling activation and loss of intestinal barrier. However, further studies are needed to clarify the mechanism by which DZD treats NAFLD.

1. Introduction

Nonalcoholic fatty liver disease (NAFLD), as the hepatic manifestation of metabolic syndrome [1], is typified by fat accumulation in the liver without significant alcohol consumption [2]. Recently, NAFLD has become the most common cause for chronic liver disease worldwide [3–5]. The prevalence rate of NAFLD is 25.24% globally, being highest in the Middle East and South America and lowest in Africa. NAFLD has been associated with obesity, type 2 diabetes mellitus, hyperlipidemia, hypertension, fibrosis, and hepatocellular carcinoma [6]. However, the pathogenesis of NAFLD has not been completely clarified. It is well-established that the gut microbiota is significantly involved in the pathogenesis of NAFLD [7, 8]. The gut is open to the outer environment, and the gut microbiota is a complex microbial community inhabiting the intestinal tract that includes 100 trillion bacteria with over 1000 species. It contains genetic materials severalfold those of human genome and produces considerable metabolites and peptides. Accumulating evidence has proven that NAFLD increased energy harvesting upon intestinal dysbiosis or bacterial overgrowth [9, 10]. Patients with NAFLD have lower percentages of Bacteroidetes and Ruminococcaceae than those in normal subjects [11, 12]. Besides, damage of the intestinal barrier also significantly contributes to NAFLD. The intestinal mucosal mechanical barrier is the first defense of intestinal barrier, which is composed of intestinal epithelial cells (IECs), tight junction (TJ), and the mucous layer that covers the surface of IECs. TJ plays a crucial role in maintaining the integrity of the

intestinal barrier, which promotes nutrient and water transport and also protects against gut-derived pathogens [13]. In the case of NAFLD, intestinal bacterial overgrowth generates gut-derived pathogens such as endotoxin or lipopolysaccharide (LPS) which are the main components of cell walls in Gram-negative bacteria. Meanwhile, they can activate the Toll-like receptor 4 (TLR4) signaling pathway. After binding TLR4 on the cell membrane, they increase the intestinal permeability by downregulating TJ proteins. As we all know, the liver is located in the proximity of the gut, receiving 75% of its blood supply through the portal vein. The portal vein flow not only carries nutrients, but also translocates microbial products and bacteria. Due to increased intestinal permeability (leaky gut), gut-derived pathogens can penetrate the intestinal barrier into the portal vein and cause NAFLD by inducing liver inflammation and fat deposition.

In Western countries, there is still no proven medical therapy for NAFLD hitherto. In contrast, traditional Chinese medicine drugs have exhibited remarkable therapeutic effects on NAFLD. Dahuang Zexie Decoction (DZD), as a Chinese herbal formula, consists of three herbs, Zexie *(Alisma orientale)*, Baizhu *(Atractylodes macrocephala)*, and Dahuang *(Rheum palmatum)*. It was developed from Zexie Decoction, a classical prescription documented in Synopsis of the Golden Chamber, which was completed in the Chinese Han dynasty (206 BC-220 AD). Zexie Decoction only has two herbs, Zexie *(A. orientale)* and Baizhu *(A. macrocephala)*. It can obviously mitigate NAFLD and decrease blood lipid levels [14]. Thereby motivated, we established a rat model of high-fat diet- (HFD-) induced NAFLD and then evaluated the effects of DZD on the liver function and gut microbiota, together with the expressions of intestinal TJ proteins and members in the TL4 signaling pathway in these rats.

2. Materials and Methods

2.1. Preparation of DZD. We prepared DZD by a mixture comprising the following three dried herbs: Zexie (*Alisma orientalis*, 30 g), Baizhu (*Atractylodes macrocephala*, 12 g), and Dahuang (*Rheum palmatum*, 15 g). The herbs were extracted with water, concentrated to the density of 1 g crude herb/ml, and stored at −20°C until further use. All the herbal components were purchased from Baicaotang Outpatient Department, Nanjing University of Chinese Medicine (Nanjing, China). Herbs were obtained from qualified suppliers on the basis of standards specified in the Chinese Pharmacopoeia (2010 Edition).

2.2. Animals. The protocols for animal studies were reviewed and approved by the Animal Studies Ethics Committee of Nanjing University of Chinese Medicine. Eight-week-old male Sprague Dawley (SD) rats ($n = 24$) were housed in a controlled environment (12 h–12 h light–dark cycle) in the Animal Center of Nanjing University of Chinese Medicine. After one week of acclimation on normal diet, the rats were randomly divided into three groups and fed either normal diet or HFD. Normal diet (fat contributed 10% calories) and HFD (fat contributed 45% calories) were purchased from Jiangsu Medicine Biological & Pharmaceutical Co., Ltd. (Yangzhou, China). A control group was fed normal diet for 16 weeks ($n = 8$), and the remaining sixteen rats were fed HFD for 16 weeks. After 16 weeks of HFD feeding, the sixteen rats were further divided into 2 groups: NAFLD group and DZD group ($n = 8$). The DZD group received daily gavage of 5.13 g/kg DZD (density: 1 g crude herb/ml) in addition to HFD for four weeks, while the NAFLD group was gavaged with the same volume of saline for four weeks. The control group was fed normal diet and saline for four weeks. Body weight gain was assessed once a week. After 4 weeks of gavage, the animals were anesthetized with 4% chloral hydrate and then sacrificed. Blood was drawn and collected into tubes. Liver tissue was weighed and collected. Intestine and feces samples were also collected.

2.3. Reagents. Antibody against TLR4 was purchased from Abnova (TW, China). Antibodies against myeloid differentiation factor 88 (MyD88), *p*-JNK, JNK, *p*-ERK, and ERK were purchased from Cell Signaling Technology (MA, USA). Antibody against occludin and goat anti-mouse secondary antibody were purchased from Abcam (MA, USA). Antibody against zonula occludens-1 (ZO-1) was purchased from Thermo Fisher Scientific (MA, USA). Antibody against β-actin and goat anti-rabbit secondary antibody were purchased from Santa Cruz Biotechnology (CA, USA).

2.4. Biochemical Assays. Triglyceride (TG), total cholesterol (TC), low density lipoprotein-cholesterol (LDL-C), high density lipoprotein-cholesterol (HDL-C), alanine aminotransferase (ALT), and aspartate aminotransferase (AST) in serum were measured by commercial kits (Nanjing Jiancheng Institute of Biotechnology, Nanjing, China) according to the manufacturer's instructions.

2.5. Histopathological Examination. Liver pieces of about 5 mm in all dimensions were obtained from rats and fixed in 4% formaldehyde for 15 min. Afterwards, the specimens were sequentially equilibrated in 30% sucrose, 15% sucrose/50% optimal cutting temperature medium (OCT, Sakura Finetek, Torrance, CA, USA), and 100% OCT. Liver pieces were subsequently frozen in OCT and 10 μm-thick sections were cut with a cryostat. The sections were then stained with hematoxylin/eosin (HE) and visualized by light microscopy.

2.6. Immunohistochemical Assay. Ileum and colon tissues were obtained to detect ZO-1 and occludin. The above sections were used for immunohistochemistry, and rehydrated before immunostaining. After blocking, the sections were incubated with rabbit anti-rat ZO-1 and occludin antibodies (Invitrogen, USA). The immunostaining results were reviewed and scored independently by two pathologists.

2.7. Western Blotting. The protein expressions of ZO-1, occludin, TLR4, MyD88, *p*-JNK, JNK, *p*-ERK, and ERK in the gut were detected by Western blotting. In brief, total protein was extracted from distal ileum and colon tissues, and the concentrations of supernatants were measured using the BCA protein assay (Thermo Fisher). Aliquots of supernatants containing 30 μg of protein were electrophoresed on 10% (w/v)

sodium dodecyl sulfate-polyacrylamide gels and transferred onto polyvinylidene difluoride membranes. After blocking for 1 h with 5% (w/v) skimmed milk, the membranes were incubated with primary antibodies at 4°C overnight and then washed by tris-buffered saline and incubated with secondary antibodies for 1 h. Protein bands were analyzed with image analysis software Quantity one. The results were expressed as ratios relative to β-actin as the internal control.

2.8. DNA Extraction, 16S Ribosomal RNA (rRNA) Gene Sequencing, and Microbial Analysis of Fecal Samples. Fecal samples were collected and frozen at −80°C within 3 h after sampling. DNA extraction was performed using a QIAamp Fast DNA Stool Mini kit (Qiagen, California, USA). Purity was determined and concentration was calculated. The V3 region of bacterial 16S rRNA gene was amplified by PCR. The bacterial genomic DNA was amplified by PCR with forward primer (5′-TCGTCGGCAGCGTCAGATGTGTATAAGAGACAGCCTACGGGNGGCWGCAG) and reverse primer (5′-GTCTCGTGGGCTCGGAGATGTGTATAAGAGACAGGACTACHVGGGTATCTAATCC) for the V3 hypervariable region. Purified amplicons were pooled into equimolar concentrations, and paired-end sequencing was performed using an Illumina MiSeq instrument (Illumina, San Diego, California, USA). The representative sequences of OTUs were used to analyze α-diversity (Chao index and Shannon diversity index) on the basis of their relative abundances. A heatmap was generated according to the relative abundances of OTUs by R software (https://www.R-project.org). Phylogenetic β-diversity measures such as unweighted UniFrac significance test, principal coordinate analysis, and nonmetric multidimensional scaling were performed using the representative sequences of OTUs for each sample by the Mothur program to analyze community and phylogenesis. Taxonomy-based analyses were performed for taxonomic classification using the ribosomal database project classifier with a 60% bootstrap score.

2.9. High-Performance Liquid Chromatography Coupled with Mass Spectrometry (HPLC-MS). DZD water extract was analyzed by high-performance liquid chromatography with hybrid linear ion trap Orbitrap mass spectrometry (HPLC-LTQ/Orbitrap) (Thermo Fisher Scientific, USA) with an Accucore C chromatographic column (182.1 mm × 150 mm, 0.26 μm, Thermo Fisher Scientific, USA) and a 5 cm Lot 13375 guard column (Thermo Fisher Scientific, USA). The mobile phase consisted of (A) 100% acetonitrile and (B) 100% water with 0.1% formic acid. Gradient elution was conducted by using 5%–12% (0–30 min), 40% (35 min), 40% (52 min), 70% (63 min), 85% (67 min), and 85% acetonitrile (70 min). The flow rate was 1 mL/min and the detection range was full wavelength. The mass spectrometry (MS) method consisted of positive and negative ion detection model. The ESI source parameters were set as follows: ion spray voltage 2.4 kV, capillary temperature 300°C, source heater temperature 110°C, sheath gas (N2) 40 arbitrary units, auxiliary gas (N2) 10 arbitrary units, and sweep gas (N2) 0 arbitrary units. The Orbitrap analyzer scanned the mass with the range of m/z 120–900.

2.10. Statistical Analysis. SPSS 18.0 and GraphPad Prism 5 were used for statistical analysis. Data were expressed as mean ± standard error of mean (SEM). One-way analysis of variance with Tukey's correction was applied for differences between two groups, and $P < 0.05$ was accepted as statistically significant.

3. Results

(1) Therapeutic Effect of DZD on Rat Model of HFD-Induced NAFLD. To evaluate the therapeutic effect of DZD on NAFLD in the HFD-fed rat model, we detected the body weight, liver weight, serum lipid levels, liver function parameters, and pathological changes of three groups. Compared to the control group, the HFD group had higher body weight, liver weight, and serum ALT, AST, TG, TC, HDL-C, and LDL-C levels (Figures 1(a)–1(h)). DZD treatment for 4 weeks significantly decreased body and liver weights and restored serum lipid levels and liver function parameters compared with those of the HFD group (Figures 1(a)–1(h)). Meanwhile, the body weight, liver weight, serum lipids, and liver function parameters of the DZD group were similar to those of the control group. The three groups also had similar serum glucose levels (Figure 1(i)). Consistently, the liver sections of the HFD group showed extensive macrosteatosis and hepatocyte ballooning which were relieved in those of DZD-treated rats (Figure 1(j)). Collectively, DZD exerted beneficial effects on the NAFLD rat model.

(2) Effects of DZD Therapy on the Gut Microbiota Composition of NAFLD Rats. NAFLD is associated with intestinal dysbiosis, so we analyzed the effects of HDF and DZD on the gut microbiota composition. We used MiSeq technology to conduct bacterial 16S rRNA sequencing after 4 weeks of treatment. The quality of sequencing, which included microbial richness and biodiversity, met the requirements for subsequent analysis. Both HFD and DZD decreased the Shannon index compared with that of the control group (Figure 2(a)), so they significantly reduced the diversity of gut microbiota. Meanwhile, the three groups had similar richness, as indicated by the Chao index (Figure 2(b)). Samples from the three groups formed distinct clusters in the ordination plot, suggesting that HFD and DZD induced main changes in the gut microbiota (Figure 2(c)). The HFD group had a higher relative abundance of Firmicutes and a lower relative abundance of Bacteroidetes than those of the control group, and DZD decreased the proportion of Firmicutes and increased that of Bacteroidetes on the phylum level (Figures 2(d) and 2(e)). Besides, principle component analysis (PCoA) was performed to compare the differences in bacterial communities between different groups on the OTU level (Figure 2(f)). In addition, changes of intestinal microbiota on the family level showed that Ruminococcaceae significantly decreased and Desulfovibrionaceae significantly increased in the HFD group compared to those in the control group (Figures 3(a) and 3(b)). In contrast, DZD administration restored these proportions (Figures 3(a) and 3(b)). On the genus level, the relative abundances of *Desulfovibrio* and *Escherichia/Shigella* were significantly higher in the NAFLD

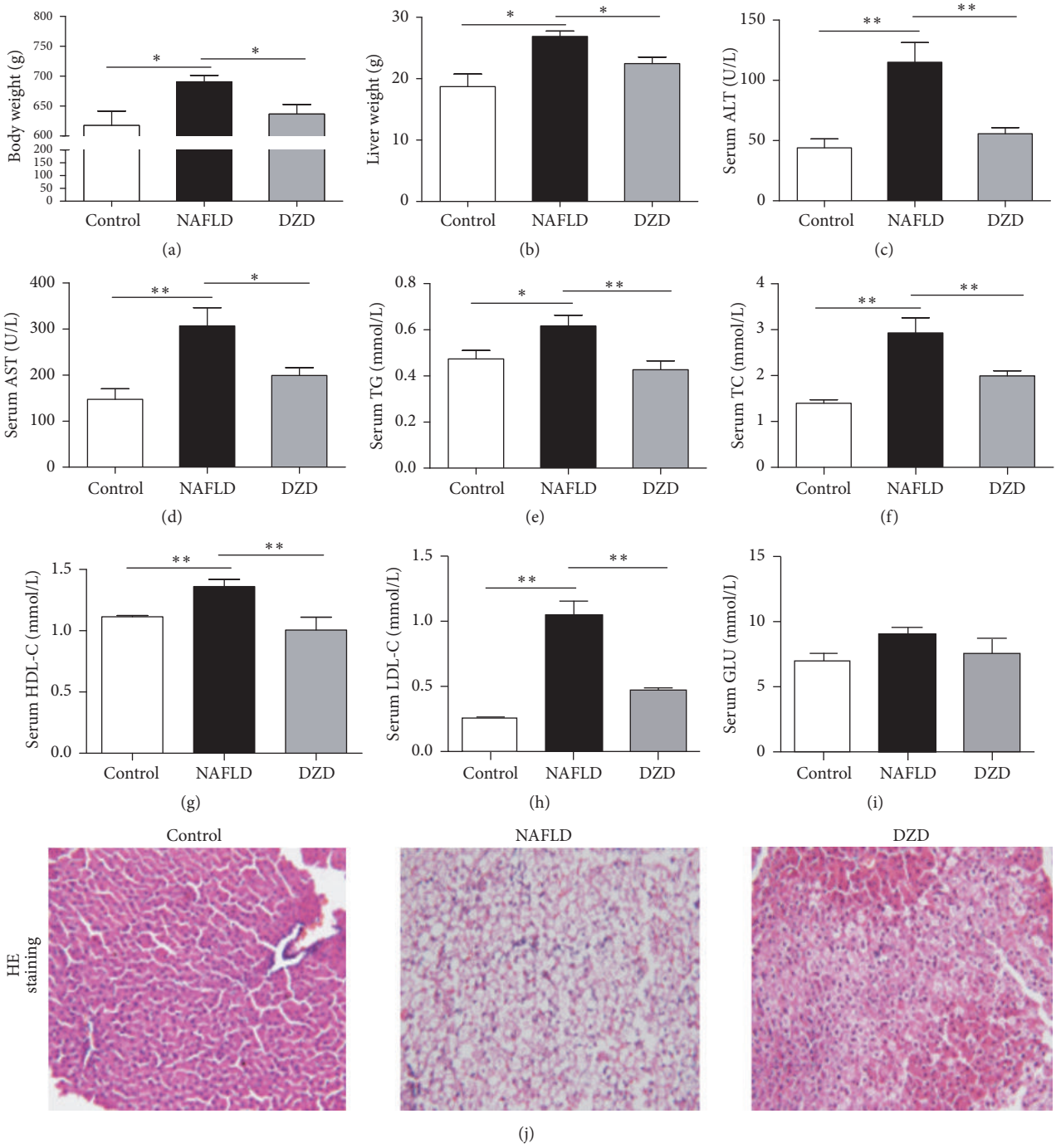

Figure 1: *Therapeutic effects of DZD on rat model of HFD-induced NAFLD*. Male SD rats (8 weeks old) were fed HFD for 16 weeks, followed by either 4-week DZD feeding or normal saline supplementation through gavage, while the rats fed normal diet were set as controls. The rats were sacrificed, from which the liver and serum were collected. Body weight (a), liver weight (b), serum ALT (c), serum AST (d), serum TG (e), serum TC (f), serum HDL-C (g), serum LDL-C (h), and serum GLU (i) levels were detected. Liver sections were stained with HE (j). The data are expressed as mean ± SEM. $N = 5$ to 8 for every group. $^{*}0.01 < P < 0.05$; $^{**}P < 0.01$. ALT: alanine aminotransferase; AST: aspartate transaminase; TG: triglyceride; TC: total cholesterol; HDL-C: high density lipoprotein-cholesterol; LDL-C: low density lipoprotein-cholesterol; GLU: glucose; HE: hematoxylin/eosin.

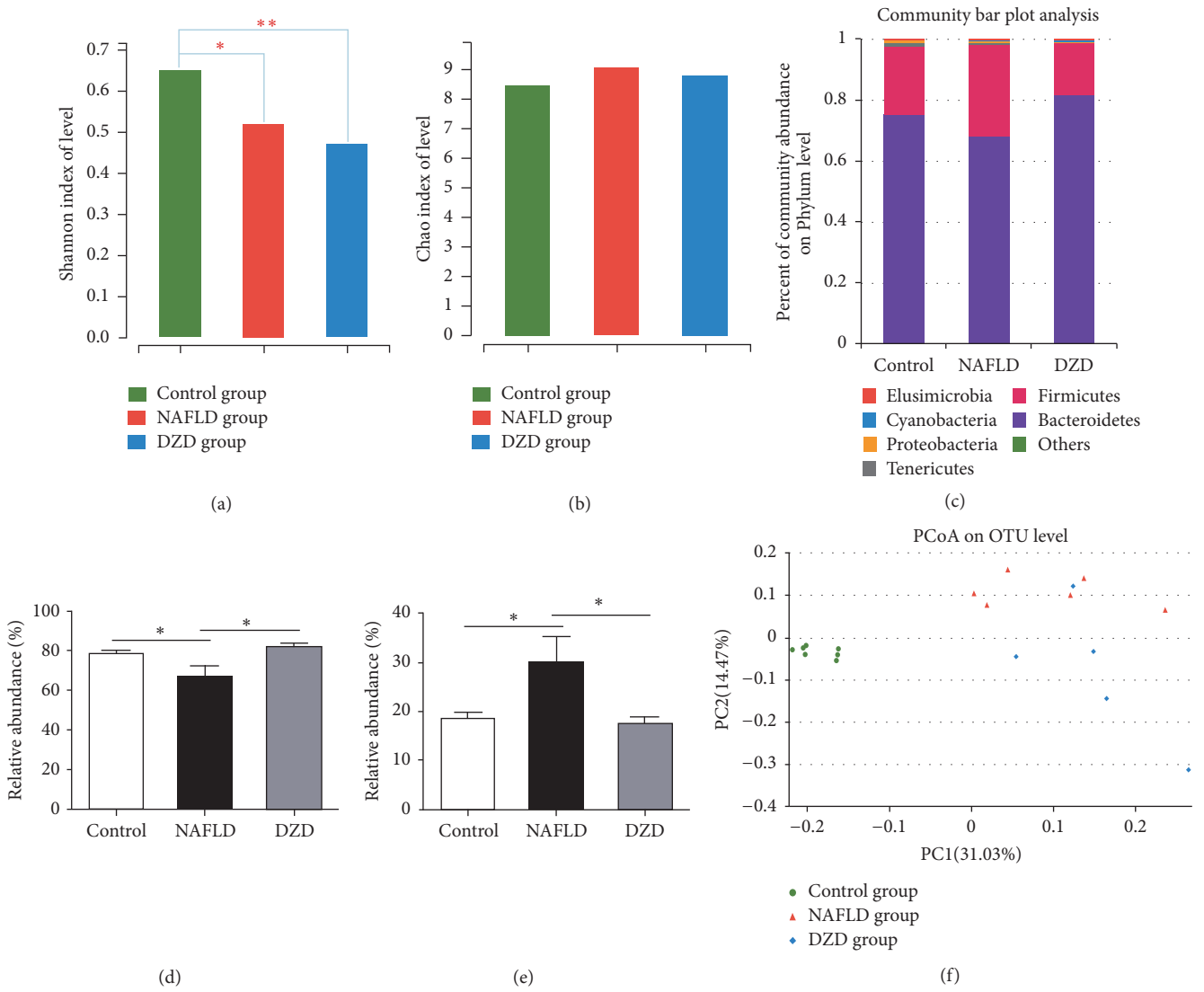

Figure 2: *Effects of DZD therapy on composition of gut microbiota*. Bacterial diversity is shown by the Shannon index (a). Bacterial richness is shown by the Chao index (b). Species on the phylum level (c), as well as alterations of Bacteroidetes (d) and Firmicutes (e) are indicated. PCoA score plot based on the unweighted significance test (f). The data are expressed as mean ± SEM. $N = 5$ to 8 for every group. $^{*}0.01 < P < 0.05$; $^{**}P < 0.01$.

group, which were reversed by DZD intervention (Figures 3(c) and 3(d)). Meanwhile, the relative abundances of *Bacteroides*, *Oscillibacter*, and *Butyricicoccus* were significantly lower in the NAFLD group, which were restored by DZD intervention (Figures 3(e)–3(g)). In short, DZD altered the intestinal microbiota composition of NAFLD rats.

(3) DZD Intervention Activated the TLR4 Signaling Pathway in the Ileum. Damage of the intestinal barrier may induce intestinal endotoxemia and subsequent TLR4 activation in the liver, which is implicated in the pathogenesis of NAFLD [15, 16]. Kim et al. reported that HFD-induced intestinal inflammatory response by activating the TLR4 signaling pathway [17]. To further investigate whether DZD regulated intestinal inflammation via this pathway, the expressions of TLR4 and mitogen-activated protein kinase (MAPK) members in the ileum were detected by Western blotting. The protein expression levels of TLR4 and MyD88 were upregulated in the ileum of the HFD group (Figures 4(a)–4(c)). After treatment with DZD, such levels were restored to normal (Figures 4(a)–4(c)). The phosphorylation levels of ERK and JNK in the HFD group exceeded those of the control group (Figures 4(d), 4(e), and 4(g)). However, the three groups had similar ERK and JNK levels (Figures 4(d), 4(f), and 4(h)). Similarly, DZD downregulated the phosphorylation levels of these proteins (Figures 4(d), 4(e), and 4(g)). Thus, activation of the TLR4 signaling pathway in the ileum was enhanced by HFD, whereas DZD reduced the activity of this pathway to normal.

(4) DZD Intervention Activated the TLR4 Signaling Pathway in the Colon. We also detected the protein expression levels of

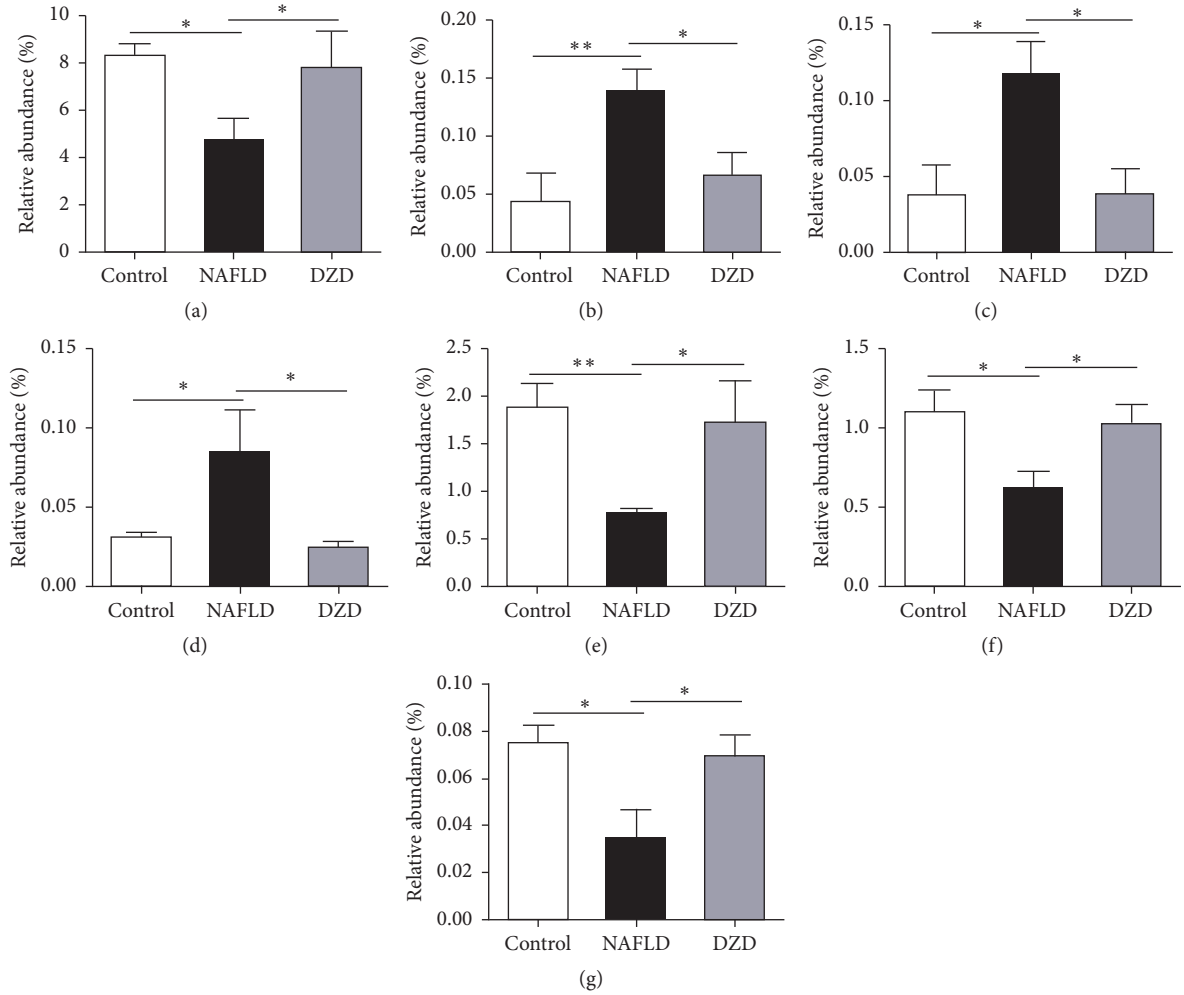

Figure 3: *Relative abundances of gut microbiota on different taxonomic levels among three groups*. On the family level, the alterations of Ruminococcaceae (a) and Desulfovibrionaceae (b) were indicated. At the genus level, the alterations of *Desulfovibrio* (c), *Escherichia*/*Shigella* (d), *Bacteroides* (e), *Oscillibacter* (f), and *Butyricicoccus* (g) were indicated. The data are expressed as mean ± SEM. $N = 5$ to 8 for every group. $^{*}0.01 < P < 0.05$; $^{**}P < 0.01$.

members in the TLR4 signaling pathway in the colon of different groups. HFD upregulated the expression levels of TLR4 and MyD88 in the colon (Figures 5(a)–5(c)). Compared to the HFD group, DZD intervention downregulated their protein expressions (Figures 5(a)–5(c)). Nevertheless, there was no significant difference between control and DZD groups. Identical to results in the ileum, the phosphorylation levels of ERK and JNK in the HFD group were higher than those in the control group, which were downregulated by DZD (Figures 5(d), 5(e), and 5(g)). Similarly, the total protein expression levels of ERK and JNK in the colon were not significantly different among the three groups (Figures 5(d), 5(f), and 5(h)). Taken together, HDF caused activation of the TLR4 signaling pathway in the colon, which was attenuated by DZD.

(5) DZD Intervention Relieved Loss of Intestinal Barrier Integrity in the NAFLD Model. TJ proteins of the intestinal mucosa, such as ZO-1 and occludin, are crucial to maintenance of the intestinal barrier [18]. Decrease in the expressions of ZO-1 and occludin can increase the intestinal permeability and play an important role in the pathophysiology of NAFLD [19]. To assess the effects of HFD and DZD on the intestinal barrier function, we used immunohistochemistry to detect the protein expression levels of ZO-1 and occludin in the gut. In accordance with previous studies, ZO-1 and occludin were highly expressed in both the ileum and colon of the control group, which were reduced by HFD intervention (Figures 6(a)–6(f)). After treatment with DZD, the protein expressions of ZO-1 and occludin in the gut were recovered compared with those of the HFD group (Figures 6(a)–6(f)). Therefore, the expressions of ZO-1 and occludin in the gut, which were reduced by HDF, were restored by DZD, thereby mitigating the loss of intestinal barrier integrity in the NAFLD model.

(6) Identification of Components of DZD. The components of DZD water extract were identified by HPLC-MS. Ten

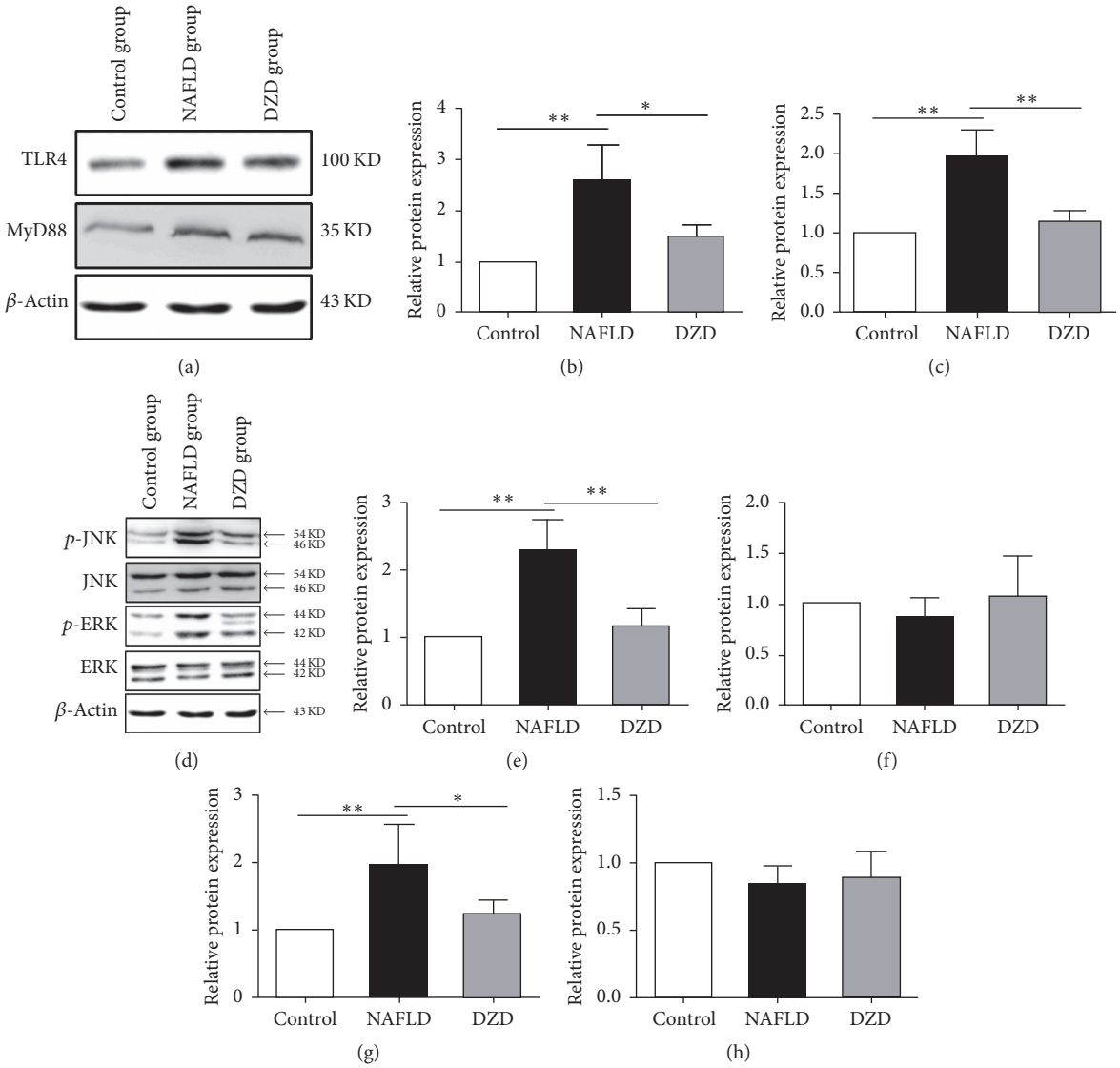

Figure 4: *DZD intervention activated the TLR4 signaling pathway of the ileum*. The ilea of rats were collected. TLR4, MyD88 (a), *p*-JNK, JNK, *p*-ERK, and ERK (d) protein expressions of ileum tissues were analyzed by Western blot. Bar graphs are the plots of TLR4 (b), MyD88 (c), *p*-JNK (e), JNK (f), *p*-ERK (g), and ERK (h). The data are expressed as mean ± SEM. $N = 5$ to 8 for every group. $^{*}0.01 < P < 0.05$; $^{**}P < 0.01$.

potential compounds, that is, gallic acid, chrysophanol, rhein, emodin, physcion, alisol C monoacetate, alisol B, atractylenolide I, atractylenolide II, and atractylenolide III, were identified (Figure 7, Table 1). The characterizations and sources of these compounds are listed in Table 1.

4. Discussion

NAFLD is the liver manifestation of metabolic syndrome, with a high incidence rate worldwide [20, 21]. At present, NAFLD has become the main cause for hepatocellular carcinoma in the United States [22, 23]. There are still no effective therapies for NAFLD patients in Western countries [24]. Contrarily, the therapeutic effects of traditional Chinese medical formulations on NAFLD have been well-documented. Our study firstly demonstrated that DZD mitigated HFD-induced NAFLD. Sixteen weeks of HFD feeding increased body weight, as well as disturbing liver function parameters and blood lipid levels (Figures 1(a)–1(h)). Liver histological examination revealed extensive macrosteatosis and hepatocyte ballooning (Figure 1(j)), being consistent with previous studies. We also demonstrated that DZD administration for 4 weeks reduced body weight and blood lipid levels, improved liver function parameters, and alleviated the liver pathological changes of NAFLD rats (Figures 1(a)–1(h) and 1(j)). Hence, DZD indeed relieved HFD-induced NAFLD.

In sequencing studies, the microbiota composition of NAFLD patients markedly changed after HFD feeding, so DZD may mitigate NAFLD by altering the gut microbiota following oral administration. Firstly, we assessed the effect of DZD on the gut microbiota by using multivariate analysis.

Table 1: Identification of potential components of DZD.

Number	Rt (min)	Molecular formula	Molecular weight (m/z)	Observed ion peaks (m/z)	Identification
(1)	1.05	C7H6O5	170.12	169[M−H]$^-$, 125	Gallic acid
(2)	13.56	C15H10O4	254.23	254[M+H]$^+$, 237	Chrysophanol
(3)	14.08	C15H8O6	284.22	283[M−H]$^-$, 239	Rhein
(4)	16.67	C15H10O5	270.24	269[M−H]$^-$, 240.9, 225, 180.9	Emodin
(5)	14.31	C16H12O5	284.27	283[M−H]$^-$, 268	Physcion
(6)	14.62	C32H48O6	528.728	529[M+H]$^+$, 511, 469, 451, 415	Alisol C monoacetate
(7)	18.31	C30H48O4	472.70	473[M+H]$^+$, 455, 437, 383, 365	Alisol B
(8)	15.46	C15H18O2	230.30	231[M+H]$^+$, 213, 203, 185, 157, 143	Atractylenolide I
(9)	17.79	C15H20O2	232.32	233[M+H]$^+$, 215, 197, 187, 159, 151	Atractylenolide II
(10)	15.47	C15H20O3	248.32	249[M+H]$^+$, 231, 203, 189, 163, 135.69	Atractylenolide III

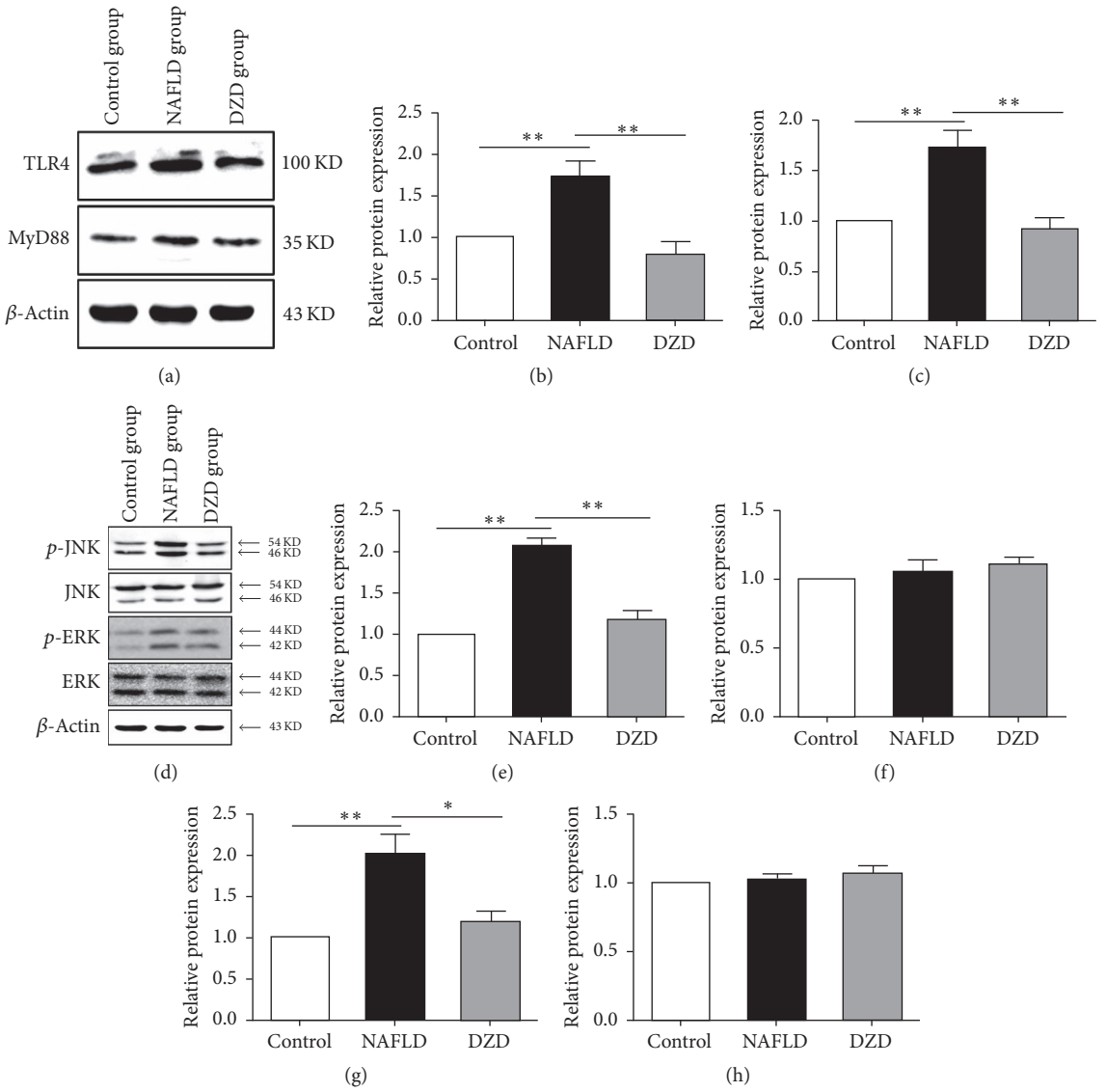

Figure 5: *DZD intervention activated the TLR4 signaling pathway of the colon*. The colons of rats were collected. TLR4, MyD88 (a), *p*-JNK, JNK, *p*-ERK, and ERK (d) protein expressions of colon tissues were analyzed by Western blot. Bar graphs are the plots of TLR4 (b), MyD88 (c), *p*-JNK (e), JNK (f), *p*-ERK (g), and ERK (h). The data are expressed as mean ± SEM. $N = 5$ to 8 for every group. $^*0.01 < P < 0.05$; $^{**}P < 0.01$.

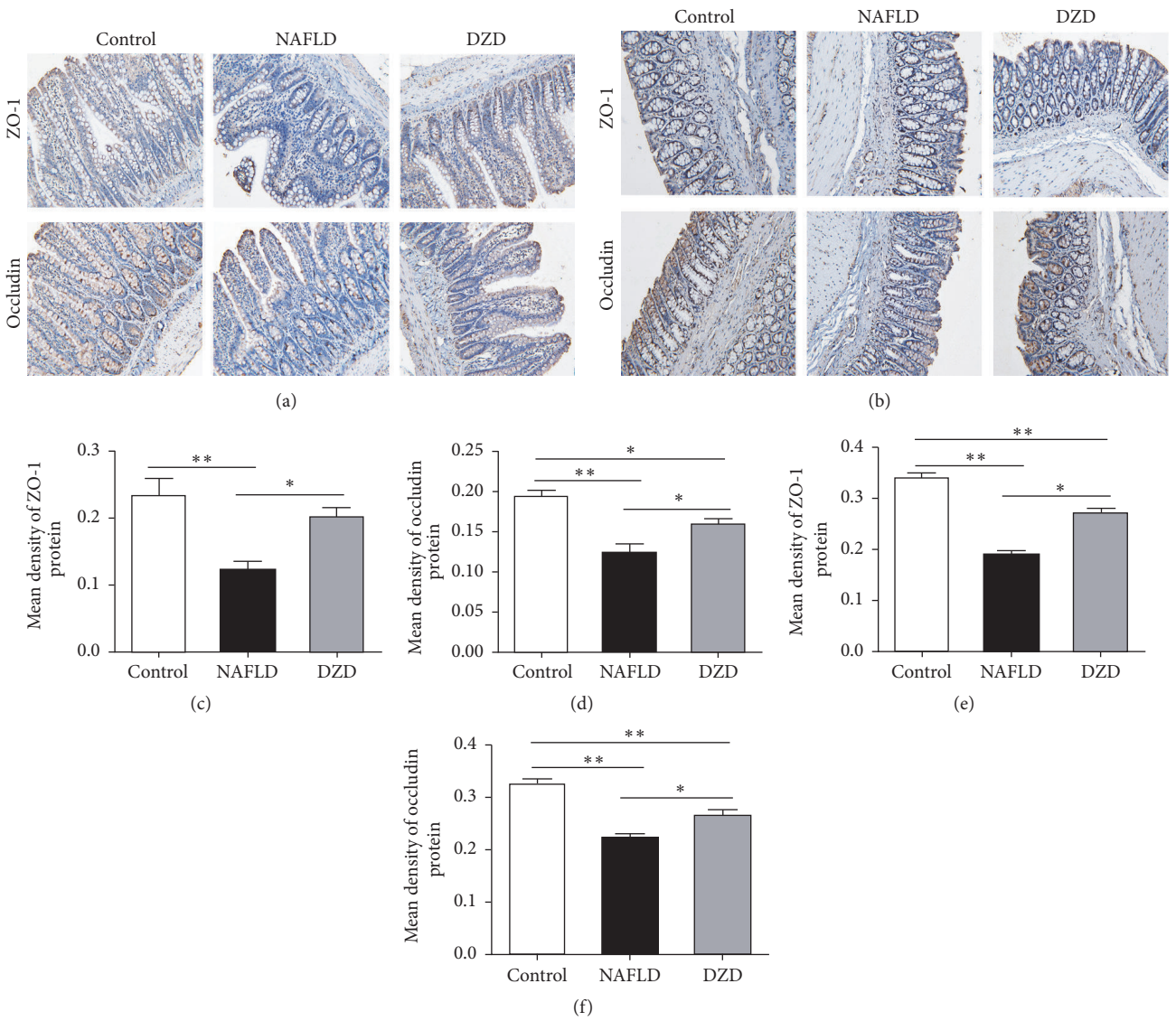

Figure 6: *DZD intervention alleviated loss of intestinal TJ proteins*. Immunohistochemical staining for ZO-1 and occludin in ileum (a) and colon (b) tissues. Bar graphs are the plots of ZO-1 (c) and occludin (d) in the ileum and ZO-1 (e) and occludin (f) in the colon. The data are expressed as mean ± SEM. $N = 5$ to 8 for every group. $^{*}0.01 < P < 0.05$; $^{**}P < 0.01$.

The Shannon index and Chao index represented the diversity and richness of gut microbiota in each sample, respectively. HFD and DZD both significantly reduced the diversity of gut microbiota compared with that of the control group (Figure 2(a)). However, the three groups had similar richness (Figure 2(b)). Subsequently, we detected the gut microbiotas in different groups on the phylum level. The NAFLD group had lower percentage of Bacteroidetes but higher percentage of Firmicutes (Figures 2(c)–2(e)), similar to previous studies [25–27]. Nevertheless, the results were restored by DZD treatment (Figures 2(c)–2(e)).

The serum levels of LPS, as a gut bacteria-derived product, are elevated in NAFLD patients. LPS is an important component of the outer membrane of Gram-negative bacteria of which Bacteroidetes is the main type. In our study, Bacteroidetes decreased in the NAFLD group, but damage of the intestinal barrier and increase of the gut permeability induced more gut-derived bacterial LPS to enter blood via the hepatic portal system [28]. The integrity of the intestinal barrier is closely related to gut bacteria-derived products, and LPS can increase the gut permeability by inducing intestinal inflammatory response. Therefore, we further tested the relative abundances of Gram-negative bacteria on family and genus levels. *Bacteroides*, a genus of Bacteroidetes, changed following the same trend. Interestingly, the fecal microbiome of the NAFLD group had increased Desulfovibrionaceae family, *Desulfovibrio* genus, and *Escherichia/Shigella* genus (Figures 3(b)–3(d)). The relative abundances of Desulfovibrionaceae, a family of sulfate-reducing bacteria (SRB), and *Desulfovibrio*, a genus of SRB, increased in the NAFLD group, which were reversed by DZD (Figures 3(b) and 3(c)). A previous study showed that diet increased SRB *in vitro* [29]. These gut

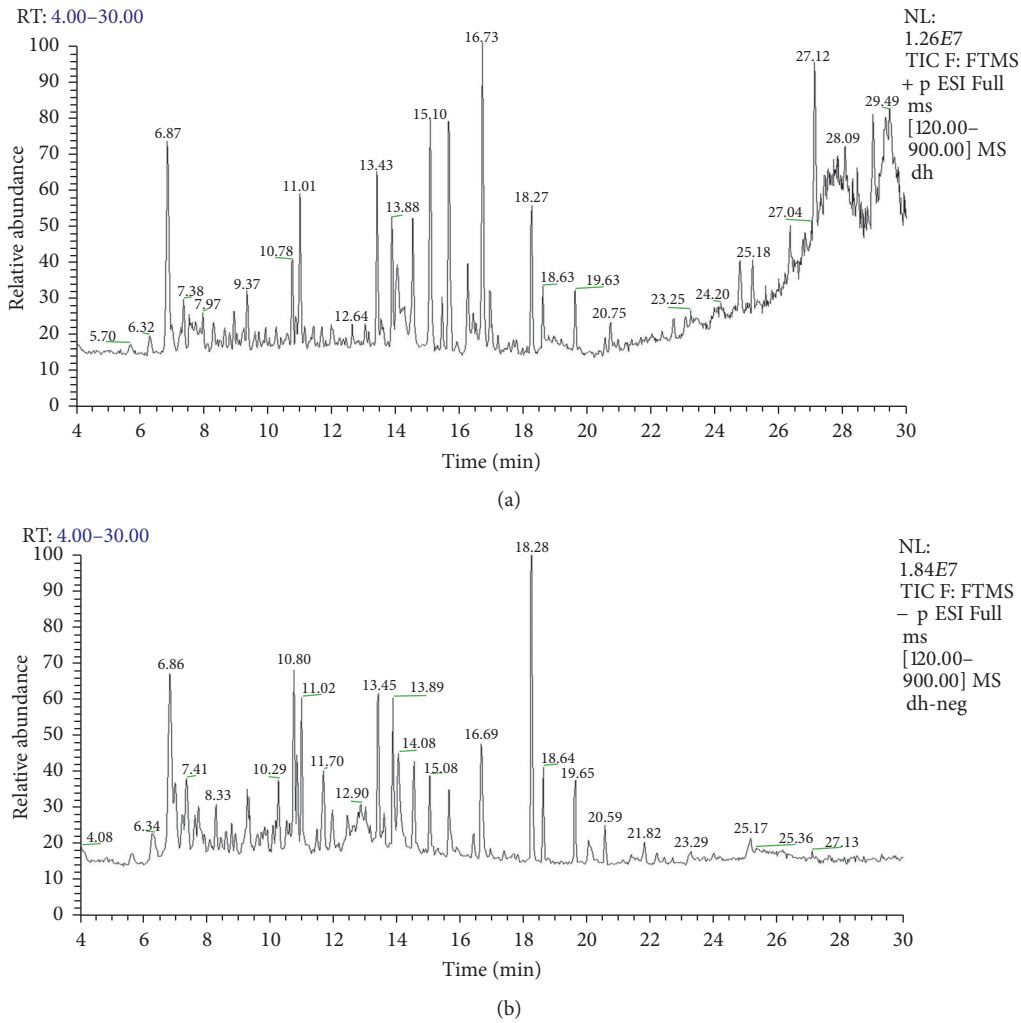

Figure 7: HPLC chromatogram of DZD. Total ions chromatograms of DZD in positive (a) and negative (b) ion modes. Identification of potential constituents of DZD (see Table 1).

bacteria can release hydrogen sulfide which is a genotoxic gas that affects epithelial intestinal cell integrity and causes barrier dysfunction [30]. Meanwhile, Lodowska et al. verified the high biological activity of LPS from *Desulfovibrio* [31]. Although these bacteria have low contents, LPS in them can evidently induce inflammation. Herein, *Escherichia/Shigella* genus was significantly enriched in the NAFLD group compared to that in the control group, which decreased to normal levels after DZD treatment (Figure 3(d)). Increase of *Escherichia/Shigella* can induce intestinal inflammation, causing intestinal barrier dysfunction [32, 33]. Therefore, even a small number of Gram-negative bacteria can still destroy the intestinal barrier through intense proinflammatory effects.

In our study, the fecal microbiome of the NAFLD group had decreased Ruminococcaceae family, *Oscillibacter* genus, and *Butyricicoccus* genus (Figures 3(a), 3(f), and 3(g)), but the results were restored by DZD treatment. Jiang et al. demonstrated that the Ruminococcaceae family and the *Oscillibacter* genus increased significantly in the healthy group compared to those in the NAFLD group [34]. Ruminococcaceae, *Oscillibacter*, and *Butyricicoccus* are short chain fatty acid- (SCFA-) producing bacteria which prevent metabolic endotoxemia by strengthening the gut barrier [35–37]. SCFAs can protect against gut inflammation and decrease intestinal permeability [38, 39]. Changes of these gut bacteria induce decrease of SCFAs, increasing the intestinal permeability. Nevertheless, we herein proved that DZD invention restored the changes of these gut bacteria induced by HFD.

In this study, we focused on the influence of gut microbiota-mediated inflammation activation on the intestinal barrier, so we detected the changes of inflammatory signaling pathway in the gut. LPS is a special pathogen-associated molecular pattern and one of microbial products, being able to activate inflammatory pathways by binding TLR4. As a result, intestinal inflammatory response then occurs [40]. Studies have suggested that TLR4-mediated signaling of the gut potently drove the progression of NAFLD [41, 42]. As the receptor of LPS, TLR4 is expressed on the membranes of hepatocytes, IECs, immune cells, and so on. MyD88 is a

downstream adaptor protein for all TLRs, except for TLR3 [43]. The TLR4-MyD88-MAPKs signaling cascade is crucial to inflammatory response and NAFLD progression. The MAPK signaling pathway is involved in a variety of physiological and pathological processes such as cell growth, inflammation, apoptosis, and proliferation [44–46]. ERK MAPK and JNK MAPK are two main components of the MAPK pathway. Activating TLR4 in the gut induces the inflammation of intestinal mucosa by mediating the phosphorylation of ERK and JNK. To further investigate whether DZD can regulate intestinal inflammation via the TLR4 signaling pathway, the expressions of members in the TLR4 signaling pathway of the ileum and colon were detected by Western blotting. The protein expression levels of TLR4 and MyD88 in the ileum were upregulated in the HFD group (Figures 4(a)–4(c)). After treatment with DZD, such levels were restored to normal (Figures 4(a)–4(c)). The total protein levels of ERK and JNK were similar among the three groups (Figures 4(d), 4(f), and 4(h)). However, the phosphorylation levels of these two proteins in the HFD group surpassed those of the control group (Figures 4(d), 4(e), and 4(g)). DZD downregulated the phosphorylation levels of ERK and JNK in NAFLD rats (Figures 4(d), 4(e), and 4(g)). These results confirmed that activation of the TLR4 signaling pathway in the ileum was upregulated by HFD. Meanwhile, DZD recovered the activity of the TLR4 signaling pathway to normal. Similar results were observed in the colon (Figures 5(a)–5(h)). Taken together, activation of TLR4 signaling in both the ileum and colon, which was induced by HDF, was downregulated by DZD.

Microbiota participates in liver diseases largely via the inflammatory pathway triggered by the interactions between intestinal bacteria and the intestinal barrier. The increased intestinal permeability in NAFLD patients has been attributed to intestinal microbiota [47]. Additionally, the gut microbiota influences the intestinal barrier function, while dysfunction of this barrier and LPS is closely related in human and animal models [48, 49]. A former research reported that LPS significantly induced the downregulation and redistribution of TJ proteins in Caco2 monolayers, as well as promoting the increase of intestinal epithelial permeability [50]. Damage of the intestinal barrier may result in translocation of intestinal bacteria and then entrance of gut-derived pathogens into portal circulation through the highly permeable intestinal barrier, triggering NAFLD eventually [51–53]. TJ proteins suppress the paracellular permeability and thus contribute essentially to the intestinal barrier, as a defense line, thereby impeding the entrance of intestinal pathogens into the liver. Intestinal permeability is regulated by TJ proteins of which transmembrane proteins ZO-1 and occludin have attracted wide attention. Given that ZO-1 and occludin are of great significance to the integrity of TJs, their downregulation is responsible for the disruption of TJ structure and the increase in paracellular permeability [54, 55]. In this study, immunohistochemistry revealed that HFD deceased the expressions of ZO-1 and occludin in both the ileum and colon (Figures 6(a)–6(f)). Accordingly, DZD upregulated such expressions (Figures 6(a)–6(f)) and then boosted the intestinal barrier function.

Furthermore, we analyzed the main components of DZD by using high-performance liquid chromatography coupled with mass spectrometry and successfully identified ten potential components of DZD, that is, gallic acid, chrysophanol, rhein, emodin, physcion, alisol C monoacetate, alisol B, atractylenolide I, atractylenolide II, and atractylenolide III (Figure 7, Table 1). Huang et al. demonstrated that gallic acid could improve high-fat diet- (HFD-) induced dyslipidaemia and hepatosteatosis [56]. Meng et al. reported that alisol B protected against nonalcoholic steatohepatitis in mice by activating farnesoid X receptor [57]. Rhein and emodin also can improve NAFLD induced by HFD [58, 59], and emodin can restore the increased intestinal permeability by inhibiting inflammation response [60]. Meanwhile, a former research revealed that alisol C monoacetate and alisol B could inhibit LPS-induced inflammatory reaction [61]. Although it is unclear whether atractylenolide can improve NAFLD, it has a definite anti-inflammatory and antiapoptosis effect [62, 63]. Due to complicated components of Chinese herbal medicine, we only identified ten of the main components of DZD. Further studies are still needed to clarify the main components of DZD and the potential mechanism for the therapeutic effects of DZD on NAFLD.

In conclusion, intestinal dysbacteriosis, activation of the TLR4 signaling pathway in the gut, and intestinal barrier dysfunction played important roles in NAFLD. Moreover, DZD changed intestinal bacterial communities, inhibited the intestinal TLR4 signaling pathway, restored the expressions of TJ proteins in the gut, and finally relieved HFD-induced NAFLD. Gallic acid, chrysophanol, rhein, emodin, physcion, alisol C monoacetate, alisol B, atractylenolide I, atractylenolide II, and atractylenolide III were ten main components of DZD. However, further studies are still needed to unravel the mechanism by which DZD treats NAFLD.

Conflicts of Interest

The authors declare that there are no conflicts of interest regarding the publication of this paper.

Acknowledgments

(1) This work was supported by grants from the National Natural Science Foundation of China (no. 81403376). (2) The authors gratefully acknowledge the valuable cooperation of Dr. Wen-bing Shang and the members of his laboratory in preparing this study.

References

[1] P. Almeda-Valdés, D. Cuevas-Ramos, and C. A. Aguilar-Salinas, "Metabolic syndrome and non-alcoholic fatty liver disease," *Annals of Hepatology*, vol. 8, no. 1, pp. S18–S24, 2009.

[2] J. C. Cohen, J. D. Horton, and H. H. Hobbs, "Human fatty liver disease: old questions and new insights," *Science*, vol. 332, no. 6037, pp. 1519–1523, 2011.

[3] S. Townsend and P. N. Newsome, "Non-alcoholic fatty liver disease in 2016," *British Medical Bulletin*, vol. 119, no. 1, pp. 143–156, 2016.

[4] S. Milić and D. Štimac, "Nonalcoholic fatty liver disease/steatohepatitis: epidemiology, pathogenesis, clinical presentation and treatment," *Digestive Diseases*, vol. 30, no. 2, pp. 158–162, 2012.

[5] C. D. Williams, J. Stengel, M. I. Asike et al., "Prevalence of nonalcoholic fatty liver disease and nonalcoholic steatohepatitis among a largely middle-aged population utilizing ultrasound and liver biopsy: a prospective study," *Gastroenterology*, vol. 140, no. 1, pp. 124–131, 2011.

[6] Z. M. Younossi, A. B. Koenig, D. Abdelatif, Y. Fazel, L. Henry, and M. Wymer, "Global epidemiology of nonalcoholic fatty liver disease—meta-analytic assessment of prevalence, incidence, and outcomes," *Hepatology*, vol. 64, no. 1, pp. 73–84, 2016.

[7] A. Wieland, D. N. Frank, B. Harnke, and K. Bambha, "Systematic review: microbial dysbiosis and nonalcoholic fatty liver disease," *Alimentary Pharmacology & Therapeutics*, vol. 42, no. 9, pp. 1051–1063, 2015.

[8] V. Tremaroli and F. Bäckhed, "Functional interactions between the gut microbiota and host metabolism," *Nature*, vol. 489, no. 7415, pp. 242–249, 2012.

[9] S. Guercio Nuzio, M. Di Stasi, L. Pierri et al., "Multiple gut-liver axis abnormalities in children with obesity with and without hepatic involvement," *Pediatric Obesity*, vol. 28, no. 6, pp. 1–7, 2016.

[10] G. Paolella and P. Vajro, "Childhood obesity, breastfeeding, intestinal microbiota, and early exposure to antibiotics: what is the link?" *JAMA Pediatrics*, vol. 170, no. 8, pp. 735–737, 2016.

[11] M. Mouzaki, E. M. Comelli, B. M. Arendt et al., "Intestinal microbiota in patients with nonalcoholic fatty liver disease," *Hepatology*, vol. 58, no. 1, pp. 120–127, 2013.

[12] M. Raman, I. Ahmed, P. M. Gillevet et al., "Fecal microbiome and volatile organic compound metabolome in obese humans with nonalcoholic fatty liver disease," *Clinical Gastroenterology and Hepatology*, vol. 11, no. 7, pp. 868–875.e3, 2013.

[13] A. M. Marchiando, W. V. Graham, and J. R. Turner, "Epithelial barriers in homeostasis and disease," *Annual Review of Pathology: Mechanisms of Disease*, vol. 5, pp. 119–144, 2010.

[14] G. Zhu, G. Zhang, and M. Wang, "Study on Hypolipidemic Effect of Zexie Decoction with Different Compatibility Proportions," *Chinese Archives of Traditional Chinese Medicine*, vol. 33, no. 1, pp. 189–191, 2015.

[15] L. Xue, J. He, N. Gao et al., "Probiotics may delay the progression of nonalcoholic fatty liver disease by restoring the gut microbiota structure and improving intestinal endotoxemia," *Scientific Reports*, vol. 7, Article ID 45176, 2017.

[16] L. Miele, V. Valenza, G. La Torre et al., "Increased intestinal permeability and tight junction alterations in nonalcoholic fatty liver disease," *Hepatology*, vol. 49, no. 6, pp. 1877–1887, 2009.

[17] K.-A. Kim, I.-A. Lee, W. Gu, S. R. Hyam, and D.-H. Kim, "β-Sitosterol attenuates high-fat diet-induced intestinal inflammation in mice by inhibiting the binding of lipopolysaccharide to toll-like receptor 4 in the NF-κB pathway," *Molecular Nutrition & Food Research*, vol. 58, no. 5, pp. 963–972, 2014.

[18] T. Suzuki, "Regulation of intestinal epithelial permeability by tight junctions," *Cellular and Molecular Life Sciences*, vol. 70, no. 4, pp. 631–659, 2013.

[19] A. R. Moschen, S. Kaser, and H. Tilg, "Non-alcoholic steatohepatitis: a microbiota-driven disease," *Trends in Endocrinology & Metabolism*, vol. 24, no. 11, pp. 537–545, 2013.

[20] N. Chalasani, Z. Younossi, and J. E. Lavine, "The diagnosis and management of non-alcoholic fatty liver disease: practice guideline by the American Association for the Study of Liver Diseases, American College of Gastroenterology, and the American Gastroenterological Association," *Hepatology*, vol. 55, no. 6, pp. 2005–2023, 2012.

[21] G. Vernon, A. Baranova, and Z. M. Younossi, "Systematic review: the epidemiology and natural history of non-alcoholic fatty liver disease and non-alcoholic steatohepatitis in adults," *Alimentary Pharmacology & Therapeutics*, vol. 34, no. 3, pp. 274–285, 2011.

[22] S. Mittal and H. B. El-Serag, "Epidemiology of hepatocellular carcinoma: consider the population," *Journal of Clinical Gastroenterology*, vol. 47, no. 1, pp. S2–S6, 2013.

[23] S. Mittal, H. B. El-Serag, Y. H. Sada et al., "Hepatocellular carcinoma in the absence of cirrhosis in united states veterans is associated with nonalcoholic fatty liver disease," *Clinical Gastroenterology and Hepatology*, vol. 14, no. 1, pp. 124–131.e1, 2016.

[24] T. Charytoniuk, K. Drygalski, K. Konstantynowicz-Nowicka, K. Berk, and A. Chabowski, "Alternative treatment methods attenuate the development of NAFLD: a review of resveratrol molecular mechanisms and clinical trials," *Nutrition Journal*, vol. 34, pp. 108–117, 2017.

[25] Q. Feng, W. Liu, S. S. Baker et al., "Multi-targeting therapeutic mechanisms of the Chinese herbal medicine QHD in the treatment of non-alcoholic fatty liver disease," *Oncotarget*, vol. 17, no. 8, pp. 27820–27838, 2017.

[26] C. Chang, C. Lu, C. Lin et al., "Antrodia cinnamomea reduces obesity and modulates the gut microbiota in high-fat diet-fed mice," *International Journal of Obesity*, vol. 6, pp. 1–45, 2017.

[27] S. Lim and D. Kim, "Bifidobacterium adolescentis IM38 ameliorates high-fat diet–induced colitis in mice by inhibiting NF-κB activation and lipopolysaccharide production by gut microbiota," *Nutrition Research*, vol. 41, pp. 86–96, 2017.

[28] T. Saito, H. Hayashida, and R. Furugen, "Metabolic endotoxemia initiates obesity and insulin resistance," *Diabetes*, vol. 56, no. 12, pp. 1761–1772, 2007.

[29] N. J. Kellow and M. T. Coughlan, "Effect of diet-derived advanced glycation end products on inflammation," *Nutrition Reviews*, vol. 73, no. 11, Article ID nuv030, pp. 737–759, 2015.

[30] F. Carbonero, A. C. Benefiel, A. H. Alizadeh-Ghamsari, and H. R. Gaskins, "Microbial pathways in colonic sulfur metabolism and links with health and disease," *Frontiers in Physiology*, vol. 3, article 448, 2012.

[31] J. Lodowska, D. Wolny, M. Jaworska-Kik, S. Kurkiewicz, Z. Dzierzewicz, and L. Węglarz, "The chemical composition of endotoxin isolated from intestinal strain of Desulfovibrio desulfuricans," *The Scientific World Journal*, vol. 2012, Article ID 647352, pp. 4–10, 2012.

[32] S. A. Bassett, W. Young, M. P. G. Barnett, A. L. Cookson, W. C. McNabb, and N. C. Roy, "Changes in composition of caecal microbiota associated with increased colon inflammation in interleukin-10 gene-deficient mice inoculated with Enterococcus species," *Nutrients*, vol. 7, no. 3, pp. 1798–1816, 2015.

[33] C. L. O'Brien, P. Pavli, D. M. Gordon, and G. E. Allison, "Detection of bacterial DNA in lymph nodes of Crohn's disease patients using high throughput sequencing," *Gut*, vol. 63, no. 10, pp. 1596–1606, 2014.

[34] W. Jiang, N. Wu, X. Wang et al., "Dysbiosis gut microbiota associated with inflammation and impaired mucosal immune function in intestine of humans with non-alcoholic fatty liver disease," *Scientific Reports*, vol. 5, no. 8, article 8096, 2015.

[35] D. Zhou, Q. Pan, F.-Z. Xin et al., "Sodium butyrate attenuates high-fat diet-induced steatohepatitis in mice by improving

gut microbiota and gastrointestinal barrier," *World Journal of Gastroenterology*, vol. 23, no. 1, pp. 60–75, 2017.

[36] P. Louis, K. P. Scott, S. H. Duncan, and H. J. Flint, "Understanding the effects of diet on bacterial metabolism in the large intestine," *Journal of Applied Microbiology*, vol. 102, no. 5, pp. 1197–1208, 2007.

[37] Z. Pataky, L. Genton, L. Spahr et al., "Impact of Hypocaloric Hyperproteic Diet on Gut Microbiota in Overweight or Obese Patients with Nonalcoholic Fatty Liver Disease: A Pilot Study," *Digestive Diseases and Sciences*, vol. 61, no. 9, pp. 2721–2731, 2016.

[38] K. A. Kles and E. B. Chang, "Short-chain fatty acids impact on intestinal adaptation, inflammation, carcinoma, and failuree," *Gastroenterology*, vol. 130, supplement 1, no. 2, pp. S100–S105, 2006.

[39] W. S. Wan Saudi and M. Sjöblom, "Short-chain fatty acids augment rat duodenal mucosal barrier function," *Experimental Physiology*, vol. 102, no. 7, pp. 791–803, 2017.

[40] K. Kim, W. Gu, I. Lee, E. Joh, and D. Kim, "High fat diet-induced gut microbiota exacerbates inflammation and obesity in mice via the TLR4 signaling pathway," *PLoS ONE*, vol. 7, no. 10, Article ID e47713, 2012.

[41] P. Jegatheesan, S. Beutheu, K. Freese et al., "Preventive effects of citrulline on Western diet-induced non-alcoholic fatty liver disease in rats," *British Journal of Nutrition*, vol. 116, no. 2, pp. 191–203, 2016.

[42] S. Kapil, A. Duseja, B. K. Sharma et al., "Small intestinal bacterial overgrowth and toll-like receptor signaling in patients with non-alcoholic fatty liver disease," *Journal of Gastroenterology and Hepatology*, vol. 31, no. 1, pp. 213–221, 2016.

[43] T. Hirotani, M. Yamamoto, Y. Kumagai et al., "Regulation of lipopolysaccharide-inducible genes by MyD88 and Toll/IL-1 domain containing adaptor inducing IFN-β," *Biochemical and Biophysical Research Communications*, vol. 328, no. 2, pp. 383–392, 2005.

[44] M. Das, D. S. Garlick, D. L. Greiner, and R. J. Davis, "The role of JNK in the development of hepatocellular carcinoma," *Genes & Development*, vol. 25, no. 6, pp. 634–645, 2011.

[45] Y.-J. Zhang, Z.-L. Tian, X.-Y. Yu, X.-X. Zhao, and L. Yao, "Activation of integrin β1-focal adhesion kinase-RasGTP pathway plays a critical role in TGF beta1-induced podocyte injury," *Cellular Signalling*, vol. 25, no. 12, pp. 2769–2779, 2013.

[46] J.-P. Tsai, P.-C. Hsiao, S.-F. Yang et al., "Licochalcone a suppresses migration and invasion of human hepatocellular carcinoma cells through downregulation of MKK4/JNK via NF-κB mediated urokinase plasminogen activator expression," *PLoS ONE*, vol. 9, no. 1, Article ID e86537, 2014.

[47] S. M. Ferolla, C. A. Couto, L. Costa-Silva et al., "Beneficial effect of synbiotic supplementation on hepatic steatosis and anthropometric parameters, but not on gut permeability in a population with nonalcoholic steatohepatitis," *Nutrients*, vol. 8, no. 7, article 397, 2016.

[48] X. D. Xu, Y. S. Sun, Q. S. Shao, J. F. Hu et al., "Effect of early enteral nutrition supplemented with glutamine on postoperative intestinalmucosal barrier function in patients with gastric carcinoma," *Zhonghua Wei Chang Wai Ke Za Zhi*, vol. 14, no. 6, pp. 436–439, 2011.

[49] A. B. Ribeiro, H. Giusti, A. P. Souza, C. R. Franci, and R. S. Saia, "Dexamethasone prevents lipopolysaccharide-induced epithelial barrier dysfunction in rat ileum," *Shock*, no. 6, pp. 1–16, 2017.

[50] S. Lei, T. Cheng, Y. Guo, C. Li, W. Zhang, and F. Zhi, "Somatostatin ameliorates lipopolysaccharide-induced tight junction damage via the ERK-MAPK pathway in Caco2 cells," *European Journal of Cell Biology*, vol. 93, no. 7, pp. 299–307, 2014.

[51] P. D. Cani, R. Bibiloni, C. Knauf et al., "Changes in gut microbiota control metabolic endotoxemia-induced inflammation in high-fat diet-induced obesity and diabetes in mice," *Diabetes*, vol. 57, no. 6, pp. 1470–1481, 2008.

[52] J. Du Plessis, H. Korf, J. Van Pelt et al., "Pro-inflammatory cytokines but not endotoxin-related parameters associate with disease severity in patients with NAFLD," *PLoS ONE*, vol. 11, no. 12, Article ID e0166048, 2016.

[53] A. Strier, D. Kravarusic, A. G. Coran et al., "The effect of elevated intra-abdominal pressure on TLR4 signaling in intestinal mucosa and on intestinal bacterial translocation in a rat," *Journal of Laparoendoscopic & Advanced Surgical Techniques*, vol. 27, no. 2, pp. 211–216, 2017.

[54] A. Bein, A. Zilbershtein, M. Golosovsky, D. Davidov, and B. Schwartz, "LPS induces hyper-permeability of intestinal epithelial cells," *Journal of Cellular Physiology*, vol. 232, no. 2, pp. 381–390, 2017.

[55] A. Bocsik, F. R. Walter, A. Gyebrovszki et al., "Reversible opening of intercellular junctions of intestinal epithelial and brain endothelial cells with tight junction modulator peptides," *Journal of Pharmaceutical Sciences*, vol. 105, no. 2, pp. 754–765, 2016.

[56] C.-Z. Huang, Y.-T. Tung, S.-M. Hsia, C.-H. Wu, and G.-C. Yen, "The hepatoprotective effect of Phyllanthus emblica L. fruit on high fat diet-induced non-alcoholic fatty liver disease (NAFLD) in SD rats," *Food & Function*, vol. 8, no. 2, pp. 842–850, 2017.

[57] Q. Meng, X.-P. Duan, C.-Y. Wang et al., "Alisol B 23-acetate protects against non-alcoholic steatohepatitis in mice via farnesoid X receptor activation," *Acta Pharmacologica Sinica*, vol. 38, no. 1, pp. 69–79, 2017.

[58] J. Wei, Y.-Z. Zhen, J. Cui et al., "Rhein lysinate decreases inflammation and adipose infiltration in KK/HlJ diabetic mice with non-alcoholic fatty liver disease," *Archives of Pharmacal Research*, vol. 39, no. 7, pp. 960–969, 2016.

[59] S. Wang, X. Li, H. Guo et al., "Emodin alleviates hepatic steatosis by inhibiting sterol regulatory element binding protein 1 activity by way of the calcium/calmodulin-dependent kinase kinase–AMP-activated protein kinase–mechanistic target of rapamycin–p70 ribosomal S6 kinase signaling pathway," *Hepatology Research*, vol. 47, no. 7, pp. 683–701, 2016.

[60] L. Qi, Q. Fu, C. Du et al., "Amelioration of hypoxia and LPS-induced intestinal epithelial barrier dysfunction by emodin through the suppression of the NF-κB and HIF-1α signaling pathways," *International Journal of Molecular Medicine*, vol. 34, no. 6, pp. 1629–1639, 2014.

[61] H. Matsuda, T. Kageura, I. Toguchida, T. Murakami, A. Kishi, and M. Yoshikawa, "Effects of sesquiterpenes and triterpenes from the rhizome of Alisma orientale on nitric oxide production in lipopolysaccharide-activated macrophages: Absolute stereostructures of alismaketones-B 23-acetate and -C 23-acetate," *Bioorganic & Medicinal Chemistry Letters*, vol. 9, no. 21, pp. 3081–3086, 1999.

[62] X. Tang, Z. Liao, Y. Huang, X. Lin, and L. Wu, "Atractylenolide I protects against lipopolysaccharide-induced disseminated intravascular coagulation by anti-inflammatory and anticoagulation effect," *Asian Pacific Journal of Tropical Medicine*, vol. 10, no. 6, pp. 582–587, 2017.

[63] M. S. Yoou, S. Y. Nam, M. H. Jin, S. Y. Lee et al., "Ameliorative effect of atractylenolide III in the mast cell proliferation induced by TSLP," *Food and Chemical Toxicology*, vol. 8, pp. 78–85, 2017.

Hindawi
Evidence-Based Complementary and Alternative Medicine
Volume 2017, Article ID 4390636, 9 pages
https://doi.org/10.1155/2017/4390636

Research Article

Artemisia iwayomogi plus *Curcuma longa* Synergistically Ameliorates Nonalcoholic Steatohepatitis in HepG2 Cells

Hyeong-Geug Kim,[1] Sung-Bae Lee,[1] Jin-Seok Lee,[1] Won-Young Kim,[1] Seung-Hoon Choi,[2] and Chang-Gue Son[1]

[1]*Liver and Immunology Research Center, Daejeon Oriental Hospital of Oriental Medical College of Daejeon University, 176-9 Daeheung-ro, Jung-gu, Daejeon 301-724, Republic of Korea*
[2]*Department of Medical Consilience, Dankook University, 152 Jukjeon-ro, Suji-gu, Yongin-si, Gyeonggi-do 16890, Republic of Korea*

Correspondence should be addressed to Chang-Gue Son; ckson@dju.ac.kr

Received 30 May 2017; Accepted 10 September 2017; Published 17 October 2017

Academic Editor: Jairo Kennup Bastos

The combination of *Artemisia iwayomogi* and *Curcuma longa* radix is frequently prescribed for liver diseases in TKM. However, the synergic effects of the two herbs on nonalcoholic steatohepatitis (NASH) have not yet been studied. Therefore, we investigated the anti-NASH effects of the water extract of *A. iwayomogi* (AI), *C. longa* radix (CL), and combination of the two herbs (ACE). Hepatic steatosis and NASH were induced in HepG2 cells by treatment with palmitic acid (PA, for 6 h) with/without pretreatment of ACE (25 or 50 μg/mL), AI (50 or 100 μg/mL), CL (50 or 100 μg/mL), curcumin (5 μg/mL), or scopoletin (5 μg/mL). The PA treatment (200 μM) drastically altered intracellular triglyceride levels, total cholesterol, and expression levels of genes related to lipid metabolism (CD36, SREBP1c, PPAR-γ, and PPAR-α), whereas pretreatment with ACE significantly attenuated these alterations. ACE also protected HepG2 cells from PA- (300 μM-) induced endoplasmic reticulum (ER) stress and apoptosis and attenuated the related key molecules including GRP78, eIF2, and CHOP, respectively. In conclusion, we found synergic effects of *A. iwayomogi* and *C. longa* on NASH, supporting the clinical potential for fatty liver disorders. In addition, modulation of ER stress-relative molecules would be involved in its underlying mechanism.

1. Introduction

Nonalcoholic fatty liver diseases (NAFLDs) include pathological conditions ranging from simple steatosis to nonalcoholic steatohepatitis (NASH). NAFLD is a major cause of chronic liver disorders, especially in developed countries, and the prevalence of NAFLD has been reported as 9% to 40% and 15% to 40% of the general populations of Asia and America, respectively [1]. Simple fat accumulation in the liver does not generally affect health; however, 10% of subjects with fatty liver progress to NASH, ultimately leading to liver cirrhosis and hepatocellular carcinoma [2, 3].

The details of NASH pathogenesis are not yet known, but the "multi-hit" theory is widely accepted [4]. With the consumption of a high-calorie and high-fat diet, obesity, hyperglycemia, hypertension, and diabetes, an increased flux of fatty acids into the liver results in hepatic steatosis. Severe hepatic steatosis induces multi-hit events, such as oxidative stress, lipid peroxidation, the influx of endotoxins from gastrointestinal tract, and mitochondrial dysfunction, which cause liver inflammation [5–7]. Therefore, fat accumulation and its related inflammatory responses are critical steps in NAFLD progression, and many studies have focused on these steps as therapeutic targets [8–10].

In traditional Korean medicine (TKM) theory, fat accumulation in the liver is defined as hepatic dysfunction by *"dampness and phlegm"* (濕痰) and *"blood stasis"* (瘀血) [11]. The herb *Artemisia iwayomogi* is frequently used to treat *"dampness and phlegm"* in TKM, and it also exerts effects against hyperlipidemia and obesity [12, 13]. *Curcuma longa* radix, the therapeutic and antihyperlipidemic properties of which are well-documented, has been used to cure pathological *"blood stasis"* [14, 15]. Also, their major active compounds, scopoletin in *Artemisia iwayomogi* or curcumin in *Curcuma*

longa, are also known partially or clinically to have the pharmaceutical actions on NASH or metabolic syndrome such as arteriosclerosis and hyperlipidemia [16–18].

The combination of *A. iwayomogi* and *C. longa* radix is frequently adapted in TKM clinical practices. However, the synergic effects of those two herbs on hepatic steatosis and NASH have not been studied until now. Herein, we evaluated the anti-NASH effects of a combination of *A. iwayomogi* and *C. longa* radix and investigated the corresponding mechanisms using an *in vitro* NAFLD and NASH model.

2. Materials and Methods

2.1. Preparation and Fingerprinting of ACE. *A. iwayomogi* and *C. longa* radix were purchased from Jeong-Seong traditional medicine company (Daejeon, South Korea). For extracts, 100 g samples of *A. iwayomogi* and *C. longa* radix were mixed separately in 1 L of 30% ethanol and shaken at 150 rpm overnight in a shaking incubator (Vision Scientific Co., Seoul, South Korea). The supernatant was centrifuged for 15 min at 150 ×g and filtered through filter paper (Dublin, CA, US). The filtered extract was lyophilized using a vacuum freeze-drying system and stored at −20°C. Finally, each 30% ethanol extract of *A. iwayomogi* (AI, the final yield of which was 10.22%) and *C. longa* (CL, the final yield of which was 4.89%) was obtained and stored at −20°C until use. An equal ratio of each extract (1.0 g of AI and 1.0 g of CL) was combined (ACE) for subsequent experiments. Before treatment with ACE, AI, and CL in HepG2 cells, these powders were dissolved in distilled water and filtered through a 0.45 μm syringe filter.

2.2. Fingerprinting of ACE. Fingerprinting analysis of ACE, AI, and CL was conducted using ultra-high-performance liquid chromatography-tandem mass spectrometry (UHPLC-MS/MS, Santa Clara, CA). A total of 5 mg of the ACE, AI, and CL samples was dissolved in 1 mL of 90% methanol, and the solution was filtered (0.45 μm). From each sample solution, 10 μL was subjected to UHPLC-MS/MS using an LTQ Orbitrap XL linear ion-trap MS Spectrometer (San Jose, CA). Separation was performed on an Accela UHPLC system using an Acquity BEH C18 column (1.7 μm, 100 × 2.1 mm; Waters, Milford, Connecticut). The column was eluted at a flow rate of 0.4 mL/min using water (in 0.1% formic acid) and acetonitrile (in 0.1% formic acid), which were used as mobile phases A and B, respectively. The following gradients were applied: 0-1 min, 0-1% B in A; 1–7 min, 1–100% B in A; 7–10 min, 100-1% B in A (linear gradient). Compositional analyses were conducted using a photodiode array at 200–600 nm. Full-scan mass spectra were acquired at 150–1500 m/z in positive and negative modes. An Orbit rap analyzer was used for high-resolution mass data acquisition with a mass resolving power of 30,000 FWHM at 400 m/z. Tandem mass (MS/MS) spectra were acquired in data-dependent mode by collision-induced dissociation. For quantitative analysis, four reference compounds (scopoletin for *A. iwayomogi* and bisdemethoxycurcumin, demethoxycurcumin, and curcumin for *C. longa* radix) were used (Figure 1).

2.3. Cell Culture. The HepG2 cell line (murine hepatocellular carcinoma cells) was obtained from the Korean Cell Line Bank (Seoul, South Korea). The cells were cultured in Dulbecco's Modified Eagle's Medium supplemented with 10% fetal bovine serum (FBS) and antibiotics (100 U/mL penicillin G and 100 μg/mL streptomycin). The cells were maintained under humidified conditions at 37°C in 5% CO_2.

2.4. In Vitro Model of NAFLD and NASH and Drug Treatment. In vitro model of NAFLD and NASH referred to in previous study; the models were modified to clinically access [19]. Palmitic acid (PA) was dissolved in a 10% solution of bovine serum albumin (BSA) and shaken overnight at 37°C. Finally, an 8 mM stock solution of PA was obtained. Then the PA was used to treat HepG2 cells (200 μM for the NAFLD model or 300 μM for the NASH model). Before PA treatment, the HepG2 cells were pretreated with AI (50 or 100 μg/mL), CL (50 or 100 μg/mL), ACE (25 or 50 μg/mL), or positive control (curcumin 5 μg/mL or scopoletin 5 μg/mL) for 4 h. The concentrations of ACE, AI, CL, scopoletin, and curcumin were based on a screening test using a cytotoxicity assay (Supplementary Figure 1 in Supplementary Material available online at https://doi.org/10.1155/2017/4390636).

2.5. Oil Red O Staining in HepG2 Cells. For Oil Red O staining, cells were cultured in a 24-well plate (5×10^4 per well) for 24 h. The cells were treated with 200 μM PA for 24 h, after pretreatment with AI (100 μg/mL), CL (100 μg/mL), ACE (25 or 50 μg/mL), curcumin (5 μg/mL), or scopoletin (5 μg/mL) for 4 h. All cells were fixed with 10% formalin and incubated for at least 1 h at room temperature. After washing the fixed cells, 60% isopropanol was added for 5 min at room temperature. After washing, cells were stained with Oil Red O working solution for 30 min and examined under an optical microscope (×100 magnifications).

2.6. Determination of Triglyceride and Total Cholesterol in HepG2 Cells. Intracellular triglyceride (TG) levels and total cholesterol (TC) were measured according to an enzymatic determination method as described in a previous study [20]. Cells were cultured in 100 mm culture dishes (1×10^6) for 24 h. The cells were treated with 200 μM PA for 24 h after pretreatment with AI (50 or 100 μg/mL), CL (50 or 100 μg/mL), ACE (25 or 50 μg/mL), curcumin (5 μg/mL), or scopoletin (5 μg/mL) for 4 h. All of cells were mixed in 10% Triton X-100, and TG and TC levels were determined using commercial kits (ASAN, Korea).

2.7. Cell Proliferation Assay in HepG2 Cells. Cell proliferation was measured with the CCK-8 kit using the WST-8 reagent according to the manufacturer's protocol (Dojindo, Kumamoto, Japan). Briefly, cells were cultured in a 96-well plate (2×10^3 per well) for 24 h. After pretreatment with AI (50 or 100 μg/mL), CL (50 or 100 μg/mL), ACE (25 or 50 μg/mL), curcumin (5 μg/mL), or scopoletin (5 μg/mL) for 4 h, the cells were treated with 300 μM PA for 24 h. For measurement of cell viability, 10% WST-8 reagent was added and incubated for 90 min, and absorbance at 450–600 nm the supernatants (150 μL total volume) was then measured using a Soft Max 5.1 plate Reader (Molecular Devices, Sunnyvale, CA, USA).

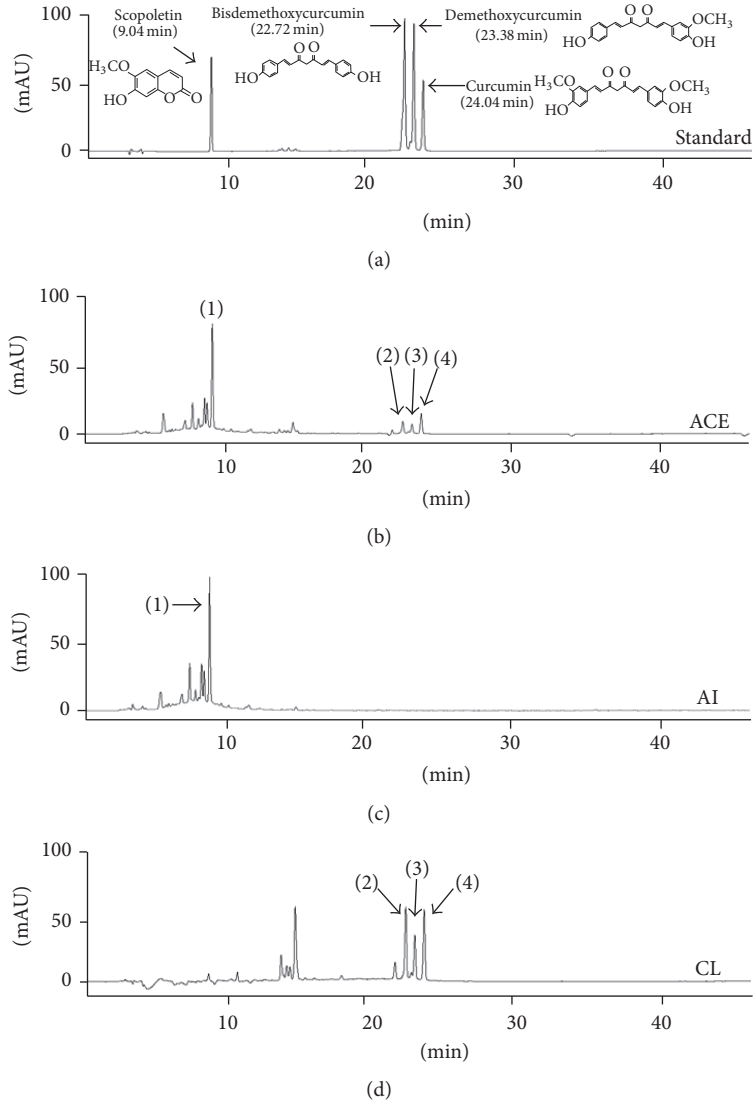

Figure 1: Fingerprint analysis of ACE using HPLC. (a) The four reference components, (b) ACE, (c) AI, and (d) CL were analyzed by HPLC. (1), (2), (3), and (4) are scopoletin, bisdemethoxycurcumin, demethoxycurcumin, and curcumin, respectively.

2.8. Apoptosis Analysis Using Flow Cytometry in HepG2 Cells. Cells were cultured in 100 mm culture dishes (1×10^6) for 24 h. The cells were treated with 300 μM PA for 6 h after being pretreated with AI (100 μg/mL), CL (100 μg/mL), ACE (25 or 50 μg/mL), curcumin (5 μg/mL), or scopoletin (5 μg/mL) for 4 h. All cells were harvested and washed twice with 0.1% FBS in ice-cold PBS. The cells were centrifuged (900 rpm for 5 min), then fixed in 5 mL cold 70% ethanol, and stored at 4°C until analysis. On the day of the analysis, the fixed cells were washed twice and resuspended in 1 mL FBS containing 0.1% PBS. A cell cycle analysis was conducted using the FACS system (BD Biosciences, San Jose, CA, USA) after incubation with RNase (100 μg/mL) for 15 min and staining with propidium iodide (PI, 50 μg/mL) at room temperature in the dark for at least 5 min. Histograms were generated, and the cell cycle analysis was carried out using Wind MDI 2.8 software (Joe Trotter, Scripps Research Institute, La Jolla, CA, USA).

2.9. Real-Time PCR for Gene Expression of Lipid Metabolism-Related Molecules in HepG2 Cells. Cells were cultured in 100 mm culture dishes (1×10^6) for 24 h. After being pretreated with AI (100 μg/mL), CL (100 μg/mL), ACE (25 or 50 μg/mL), curcumin (5 μg/mL), or scopoletin (5 μg/mL) for 4 h, the cells were treated with 200 μM PA for 6 h. Total RNA from cells was extracted using the QIAzol reagent (Germantown, MD). Complementary DNA (cDNA) synthesis from the RNA was performed using a High-Capacity cDNA Reverse Transcription Kit (Ambion, Austin, TX, USA). Real-time PCR was performed on 4 genes including β-actin using an iQ5 instrument (Bio-Rad, USA). The primer sequences were as follows: CD36: 5′-GCC AAG CTA TTG CGA CAT GAT-3′ and 3′-GAA AAG AAT CTC AAT GTC CGA GAG T-5′, SREBP1c: 5′-GAG CGA GCG TTG AAC TGT AT-3′ and 3′-ATG CTG GAG CTG ACA GAG AA-5′, PPAR-γ: 5′-AGG TGG AGA TGC AGG TTC TA-3′ and 3′-TGG GAG

ATT CTC CTG TTG AC-5′ and PPAR-α: 5′-TGG CAA AAG GCA AGG AGA AG-3′ and 3′-CCC TCT ACA TAG AAC TGC AAG GTT T-5′.

2.10. Western Blot Analysis for Apoptosis-Related Molecules in HepG2 Cells. Western blot detection of 5 proteins, including GRP78, peIF2α, eIF2α, CHOP, and β-actin as a reference protein, was conducted, and all primary antibodies were purchased from Abcam, CA, USA. Cells were cultured in 100 mm culture dishes (1×10^6) for 24 h. The cells were treated with 300 μM PA for 6 h, after being pretreated with AI (100 μg/mL), CL (100 μg/mL), ACE (25 or 50 μg/mL), curcumin (5 μg/mL), or scopoletin (5 μg/mL) for 4 h. The cells were lysed in RIPA buffer. Protein concentration was estimated using the Bio-Rad protein assay reagent (Hercules, CA, USA), and aliquots of cell lysates corresponding to 10 μg total protein were separated by 10% SDS-polyacrylamide gel electrophoresis and blotted onto a PVDF membrane. The membranes were blocked with 5% skim milk for 40 min and incubated with primary antibodies overnight and then washed with 0.1% PBST. The membranes were then incubated for 1 h with secondary antibody conjugated with peroxidase and washed with PBST. The signals were detected with a visually enhanced detector using a chemiluminescent detection system (MY ECL Imager, Thermo Scientific Co., San Jose, CA, USA).

2.11. Statistical Analysis. Data are expressed as the means ± SD. Differences between groups were assessed using one-way analysis of variance and Fisher's least-significant difference test. In all analyses, $P < 0.05$ or $P < 0.01$ was used as a threshold to indicate statistical significance.

3. Results

3.1. Compositional Analysis of ACE, AI, and CL. The compositional analyses for the main chemicals components of ACE, AI, and CL were performed using UHPLC-MS/MS. The histogram of ACE indicated that four types of flavonoid family chemicals were detected, including scopoletin, bisdemethoxycurcumin, demethoxycurcumin, and curcumin at 9.04, 22.72, 23.38, and 24.04 min of retention time, respectively. Quantitative analysis of the above chemicals was conducted using a UHPLC-MS/MS system, and their quantities were as follows: 0.635 (scopoletin), 0.039 (bisdemethoxycurcumin), 0.016 (demethoxycurcumin), and 0.037 (curcumin) μg/mg. ACE contained all the chemical components of both AI and CL (Figure 1 and Table 1).

3.2. Histological Analysis of Fat Accumulation. PA treatment (200 μM for 24 h) drastically increased fat accumulation in HepG2 cells compared with nontreated cells based on Oil Red O staining. The pretreatment with ACE (25 or 50 μg/mL) notably attenuated fat accumulation compared with PA treatment-only cells. This beneficial pattern was also observed in treatment with 100 μg/mL of AI or CL or with 5 μg/mL of curcumin or scopoletin (Figure 2(a)).

3.3. Effects on Total Cholesterol and Triglyceride Levels. PA treatment (200 μM for 24 h) dramatically elevated the quantity of TC (1.8-fold) and TG (4.9-fold) in hepG2 cells compared with the nontreated cells. Pretreatment with ACE significantly ameliorated the intracellular accumulation of both TG ($P < 0.01$ for both 25 μg/mL and 50 μg/mL) and TC ($P < 0.05$ for 25 μg/mL and $P < 0.01$ 50 μg/mL). These beneficial results were also observed in pretreatment with AI, CL, curcumin, or scopoletin, but ACE (50 μg/mL) was significantly superior to 50 μg/mL AI or CL ($P < 0.05$ for TG and TC, Figures 2(b) and 2(c)).

3.4. Effects on Cell Proliferation. PA treatment (300 μM for 24 h) completely inhibited proliferation of HepG2 cells. This lipotoxicity was significantly attenuated by pretreatments with ACE ($P < 0.01$ for 25 μg/mL and 50 μg/mL). The pretreatments with AI, CL, curcumin, or scopoletin also showed those protective effects, and then ACE (50 μg/mL) was significantly superior to 50 μg/mL of AI or CL ($P < 0.05$, Figure 3(a)).

3.5. Effects on Cell Apoptosis. PA treatment (300 μM for 6 h) drastically increased the apoptotic cell population by approximately 39% compared with the nontreated cells. The number of apoptotic cells was significantly attenuated by pretreatments with ACE ($P < 0.01$ for 25 μg/mL and 50 μg/mL). AI, CL, curcumin, or scopoletin also had significant effects against PA-induced apoptosis, but ACE (50 μg/mL) was significantly superior to 100 μg/mL AI or CL ($P < 0.05$, Figure 3(b)).

3.6. Effects on Gene Expressions Related to Lipid Metabolism. The PA treatment (200 μM for 6 h) markedly upregulated CD36 (2.5-fold), SREBP1c (1.8-fold), and PPAR-γ (1.9-fold) but downregulated PPAR-α (0.6-fold) compared with nontreated cells. The altered expression of these genes was significantly attenuated by the pretreatment with ACE ($P < 0.05$ or 0.01 for CD36, SREBP1c, PPAR-γ, and PPAR-α, Figure 4(a)). AI, CL, curcumin, or scopoletin also showed significant effects similar to ACE, but 50 μg/mL ACE was significantly superior to 100 μg/mL CL or the positive control compounds (curcumin and scopoletin).

3.7. Effects on Proapoptotic Proteins. The PA treatment (300 μM for 6 h) notably activated the endoplasmic reticulum (ER) stress-related proapoptotic proteins, including GRP78, peIF2α, and CHOP, in HepG2 cells compared with nontreated cells. Pretreatment with ACE (especially 50 μg/mL) considerably reduced the activation of those proteins. This pattern was observed in cells pretreated with curcumin or scopoletin, but not with AI or CL alone (Figure 4(b)).

4. Discussion

We adapted palmitic acid (PA) as an inducer of NAFLD and NASH models. PA is the major component of plasma free fatty acids (FFA), and serum concentration of PA is approximately 100 μM in healthy subjects and approximately 200 μM in obese patients [21]. To design an intracellular fat accumulation and lipotoxicity model, the present study used 200 and 300 μM PA. PA enters HepG2 cells through its

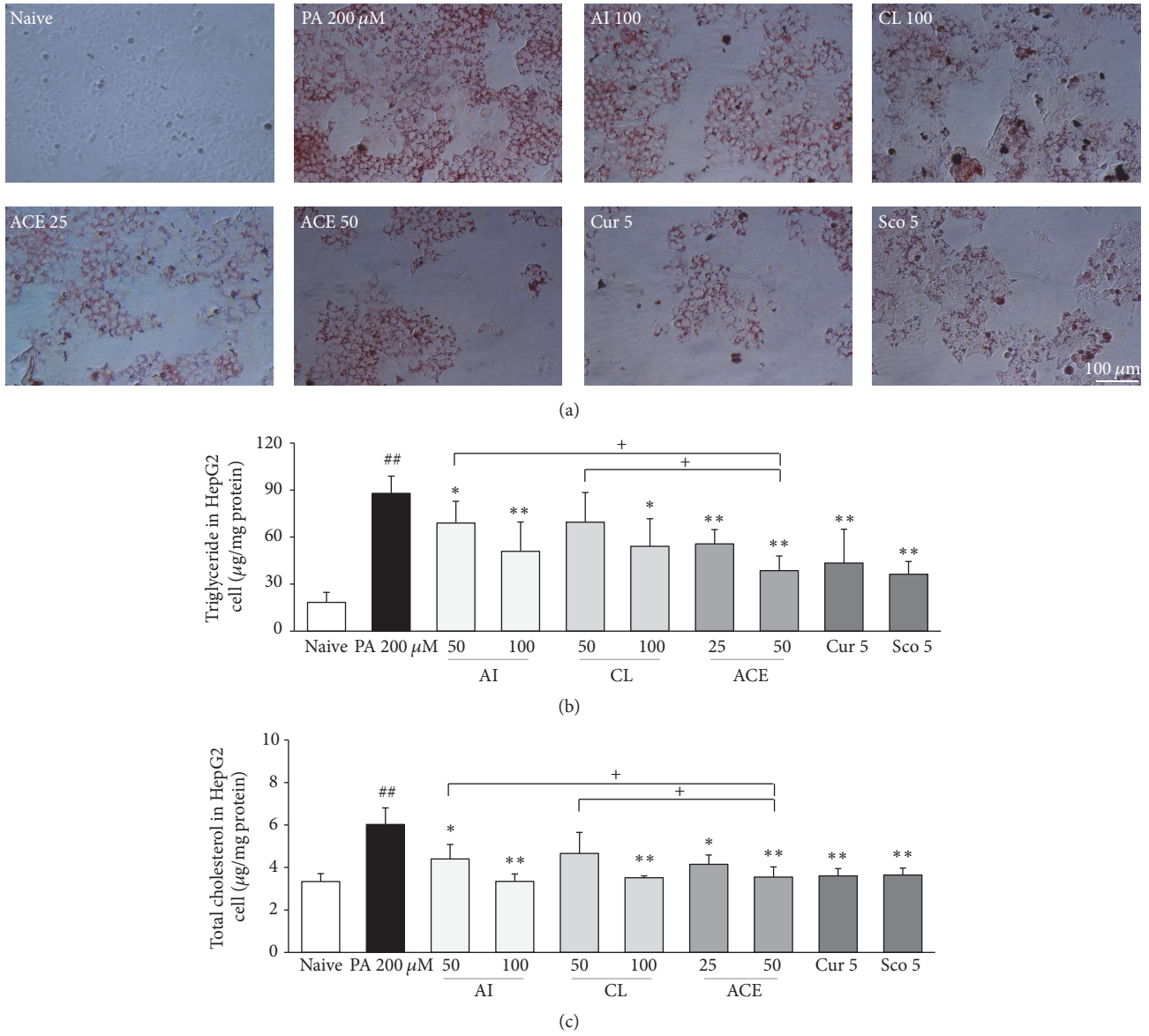

Figure 2: Oil Red O staining and lipid profiles in HepG2 cells. (a) HepG2 cells evaluated by Oil Red O staining. All images were obtained under 200x magnification. (b) Triglyceride and (c) total cholesterol were determined. The data are expressed as the mean ± SD ($n = 6$). $^{\#\#}P < 0.01$ compared with nontreatment cells; $^{*}P < 0.05$, $^{**}P < 0.01$ compared with PA-treated cells; $^{+}P < 0.05$ compared with ACE 50.

receptor (CD36), and excessive influx of PA both activates lipogenesis molecules such as SREBP1c and PPAR-γ and inactivates lipolysis molecules such as PPAR-α [22, 23]. As expected, treatment with PA (200 μM) resulted in the upregulation of the gene expression levels of CD36, SREBP1c, and PPAR-γ but the downregulation of PPAR-α (Figure 4(a)). These results were consistent with the dramatic accumulations of intracellular triglyceride (TG), total cholesterol (TC), and the degree of Oil Red O staining. Pretreatment with ACE significantly attenuated the gene expression alterations, as well as the intracellular levels of TC and TG (Figures 2 and 4(a)). These results are consistent with previous animal studies of hyperlipidemia and arteriosclerosis models [12, 24].

Overaccumulation of fat droplets is known to generate oxidative stressors such as reactive oxygen species and nitric oxide and to induce the inflammatory response in hepatic tissue [25]. In addition, endoplasmic reticulum (ER) stress and mitochondrial dysfunction ultimately lead to apoptosis of hepatic cells, which is known as NASH [26]. As shown in our results, treatment with 300 μM PA caused prominent apoptotic death of HepG2 cells, as had already been reported by others [27]. As expected, we found that ACE had statistically significant anti-NASH effects (Figure 3).

In addition to effects on key molecules in lipid metabolism, we further examined three molecules related to ER stress to explore the pharmaceutical action of ACE.

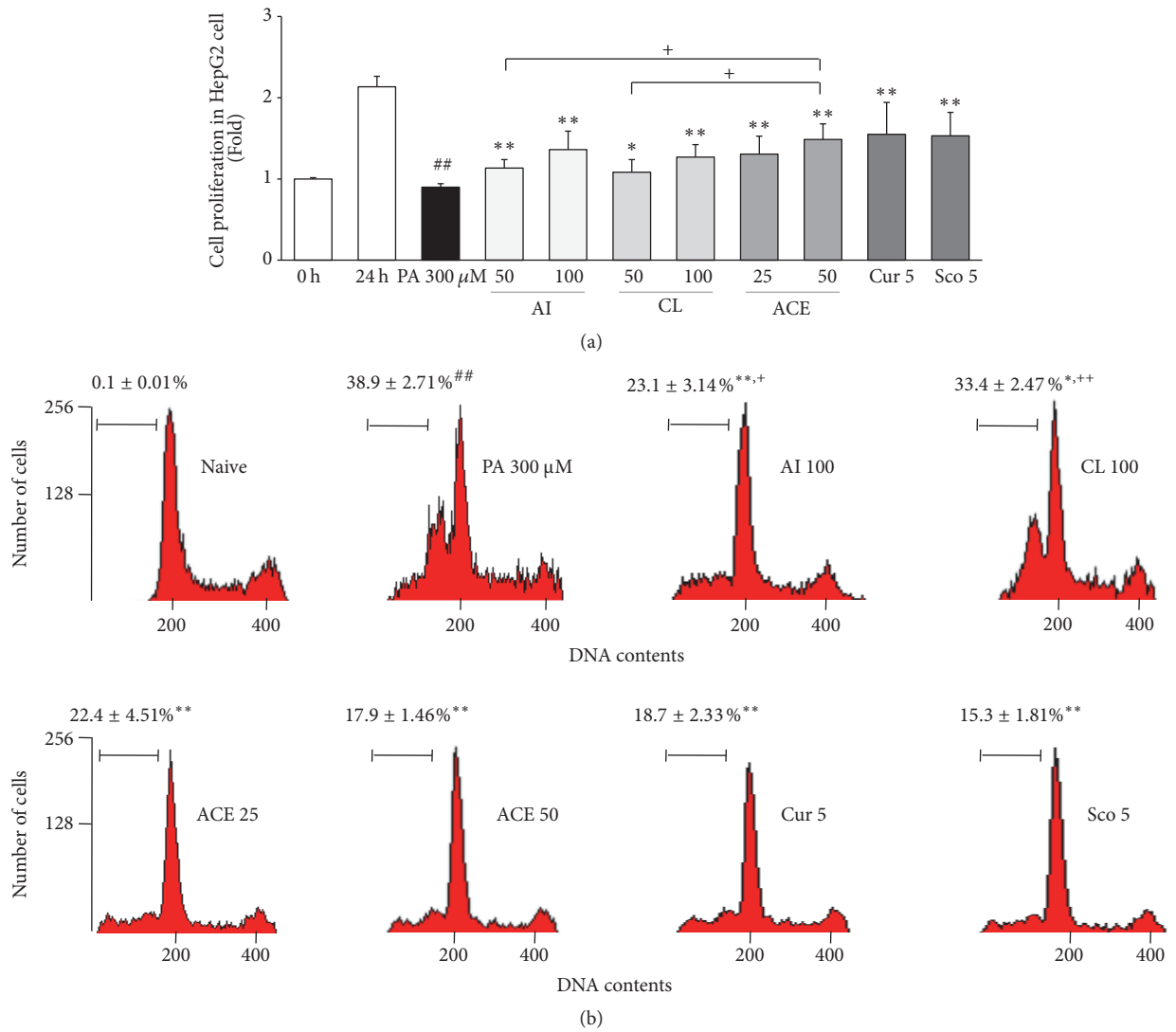

Figure 3: Cytotoxicity assay in HepG2 cells. (a) Cell proliferation and (b) cell cycle arrest assay were determined in HepG2 cells. The data are expressed as the mean ± SD ($n = 6$). $^{\#\#}P < 0.01$ compared with nontreatment cells; $^{*}P < 0.05$, $^{**}P < 0.01$ compared with PA-treated cells; $^{+}P < 0.05$, $^{++}P < 0.01$ compared with ACE 50.

Table 1: Retention time and contents of sample in ACE, AI, and CL.

Number	Compound	Retention time (min)	ACE		AI		CL	
			Mean	SD	Mean	SD	Mean	SD
			(μg/mg)		(μg/mg)		(μg/mg)	
(1)	Scopoletin	9.04	0.635	0.0047	0.730	0.0043	ND	ND
(2)	Bisdemethoxycurcumin	22.72	0.039	0.0026	ND	ND	0.047	0.0031
(3)	Demethoxycurcumin	23.38	0.016	0.0026	ND	ND	0.032	0.0021
(4)	Curcumin	24.04	0.037	0.0034	ND	ND	0.070	0.0028

The hepatic steatosis and ER stress have a bad influence on each other in pathological process, and ER stress is known to be a main mechanism in NASH [28]. Approximately 10% of subjects with NAFLD eventually develop of NASH [2]. Glucose-regulated protein 78 (GRP78) regulates several initiators of ER stress such as protein kinase RNA-like endoplasmic reticulum kinase (PERK), inositol requiring enzyme 1α (IRE1α), and eukaryotic initiation factor 2 (eIF2) [29, 30]. These molecules mediate the apoptosis of hepatocytes via the CCAAT-enhancer-binding protein

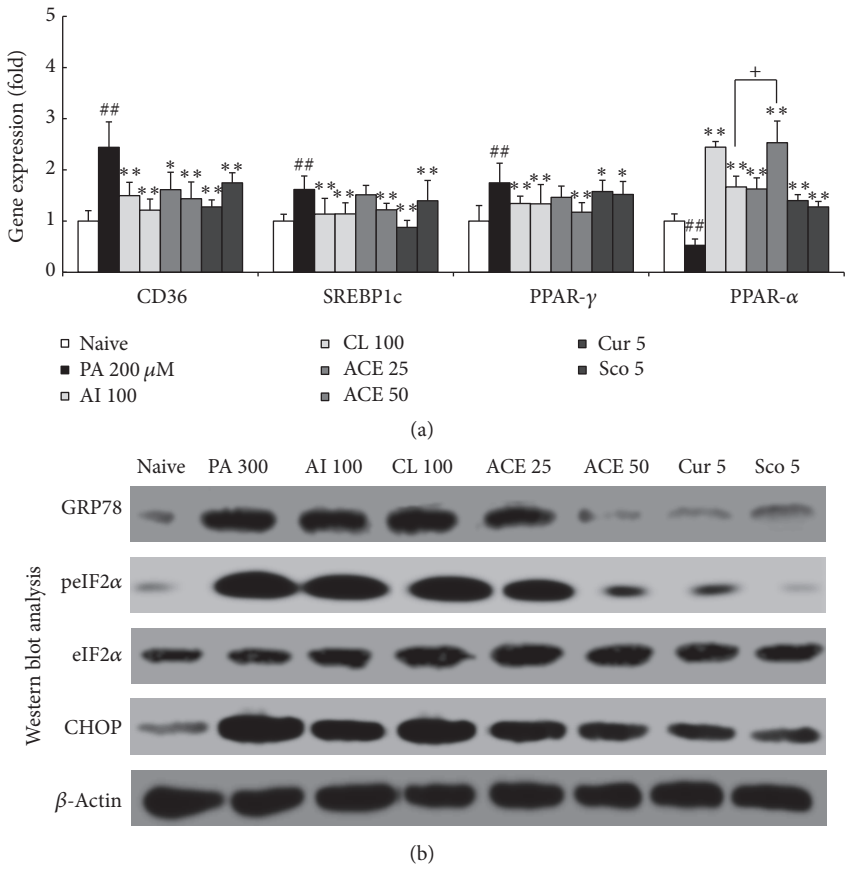

Figure 4: Gene expression and western blotting analyses of HepG2 cells. (a) mRNA expression levels of CD36, SREBP-1c, PPAR-γ, and PPAR-α were determined by quantitative real-time PCR. (b) Relative protein levels of GRP78, peIF2α, eIF2α, and CHOP were determined using western blotting. Data are expressed as the means ± SD (fold change relative to naïve group). $^{\#\#}P < 0.01$ compared with nontreatment cells; $^{*}P < 0.05$, $^{**}P < 0.01$ compared with PA-treated cells; $^{+}P < 0.05$ compared with ACE 50.

homologous protein (CHOP) pathway in NASH [31]. Our results showed that treatment with PA increased protein levels of GRP78, eIF2α, and CHOP, whereas pretreatment with ACE attenuated these alterations (Figure 4(b)).

From UHPLC-MS/MS analysis, we confirmed that the main compounds of ACE, AI, and CL were scopoletin, bisdemethoxycurcumin, demethoxycurcumin, and curcumin, respectively (Figure 1 and Table 1). We used scopoletin and curcumin as the positive controls, because these compounds have been reported to inactivate lipogenesis and to activate lipolysis [32, 33]. Accordingly, an anti-NAFLD or anti-NASH effect was expected. We consistently found the synergistic efficacy of ACE was greater compared with AI or CL alone. Regarding intracellular fat accumulation, 50 μg/mL ACE had significantly higher activity compared with the same dose (50 μg/mL) of AI or CL alone. Regarding hepatocyte apoptosis, 50 μg/mL ACE was far superior to AI or CL (100 μg/mL) as well as scopoletin and curcumin (5 μg/mL). The quantities of scopoletin and curcumin in 50 μg of ACE were approximately 31 ng and 1.9 ng, respectively. We can suppose that ACE contains other active compounds besides scopoletin and curcumin. In addition, the synergic action resulted from the combination of AI and CL, which are the representative herbs for treating *"dampness and phlegm"* (濕痰) and *"blood stasis"* (瘀血) in KTM, respectively.

We conclude that the combination of *A. iwayomogi* and *C. longa* radix has a synergic effect on NAFLD and NASH, and its corresponding mechanisms involve the regulations of lipid metabolism and ER stress molecules. Further studies are needed to identify the active compounds and the details of the molecular pathways mediating these responses.

Abbreviations

ACE: Combined extract of *Artemisia iwayomogi* and *Curcuma longa*
AI: *Artemisia iwayomogi* extract
CHOP: CCAAT-enhancer-binding protein homologous protein
CL: *Curcuma longa* extract
eIF2: Eukaryotic initiation factor 2
ER: Endoplasmic reticulum
GRP78: Glucose-regulated protein 78
IRE1α: Inositol requiring enzyme 1α
NAFLD: Nonalcoholic fatty liver diseases
NASH: Nonalcoholic steatohepatitis

PA:	Palmitic acid
PERK:	Protein kinase RNA-like endoplasmic reticulum kinase
PPAR-α:	Peroxisome proliferator-activated receptor alpha
PPAR-γ:	Peroxisome proliferator-activated receptor gamma
SREBP1c:	Sterol regulatory element-binding protein factor 1 type c
TC:	Total cholesterol
TG:	Triglyceride
TKM:	Traditional Korean medicine
UHPLC-MS/MS:	Ultra-high-performance liquid chromatography-tandem mass spectrometry.

Disclosure

Hyeong-Geug Kim and Sung-Bae Lee are co-first authors.

Conflicts of Interest

The authors declare that there are no conflicts of interest.

Authors' Contributions

Hyeong-Geug Kim and Chang-Gue Son participated in research design. Hyeong-Geug Kim conducted the experiments. Won-Yong Kim conducted fingerprinting analysis. Sung-Bae Lee and Jin-Seok Lee performed data analysis. Sung-Bae Lee and Chang-Gue Son wrote or contributed to the writing of the manuscript.

Acknowledgments

This study was supported by Daejeon University Research Grant (2013), Republic of Korea.

References

[1] D. Amarapurkar, P. Kamani, N. Patel et al., "Prevalence of non-alcoholic fatty liver disease: population based study," *Annals of Hepatology*, vol. 6, no. 3, pp. 161–163, 2007.

[2] A. Caligiuri, A. Gentilini, and F. Marra, "Molecular pathogenesis of NASH," *International Journal of Molecular Sciences*, vol. 17, no. 9, article no. 1575, 2016.

[3] L. Kikuchi, C. P. Oliveira, and F. J. Carrilho, "Nonalcoholic fatty liver disease and hepatocellular carcinoma," *BioMed Research International*, vol. 2014, Article ID 106247, 6 pages, 2014.

[4] C. P. Day and O. F. W. James, "Steatohepatitis: a tale of two "Hits"?" *Gastroenterology*, vol. 114, no. 4, pp. 842–845, 1998.

[5] J. C. Cohen, J. D. Horton, and H. H. Hobbs, "Human fatty liver disease: old questions and new insights," *Science*, vol. 332, no. 6037, pp. 1519–1523, 2011.

[6] T. Caballero, A. Gila, G. Sánchez-Salgado et al., "Histological and immunohistochemical assessment of liver biopsies in morbidly obese patients," *Histology and Histopathology*, vol. 27, no. 4, pp. 459–466, 2012.

[7] F. Caballero, A. Fernández, A. M. De Lacy, J. C. Fernández-Checa, J. Caballería, and C. García-Ruiz, "Enhanced free cholesterol, SREBP-2 and StAR expression in human NASH," *Journal of Hepatology*, vol. 50, no. 4, pp. 789–796, 2009.

[8] A. M. Oseini and A. J. Sanyal, "Therapies in non-alcoholic steatohepatitis (NASH)," *Liver International*, vol. 37, pp. 97–103, 2017.

[9] C. Labenz and J. M. Schattenberg, "Prime time for medical therapy in NASH?" *Zeitschrift fur Gastroenterologie*, vol. 55, no. 1, pp. 83-84, 2017.

[10] T. Charytoniuk, K. Drygalski, K. Konstantynowicz-Nowicka, K. Berk, and A. Chabowski, "Alternative treatment methods attenuate the development of NAFLD: A review of resveratrol molecular mechanisms and clinical trials," *Nutrition*, vol. 34, pp. 108–117, 2017.

[11] W. Xie, Y. Zhao, and L. Du, "Emerging approaches of traditional Chinese medicine formulas for the treatment of hyperlipidemia," *Journal of Ethnopharmacology*, vol. 140, no. 2, pp. 345–367, 2012.

[12] J.-M. Han, J.-S. Lee, H.-G. Kim et al., "Synergistic effects of Artemisia iwayomogi and Curcuma longa radix on high-fat diet-induced hyperlipidemia in a mouse model," *Journal of Ethnopharmacology*, vol. 173, article no. 9636, pp. 217–224, 2015.

[13] Y. Choi, Y. Yanagawa, S. Kim, W. K. Whang, and T. Park, "Artemisia iwayomogi extract attenuates high-fat diet-induced obesity by decreasing the expression of genes associated with adipogenesis in mice," *Evidence-based Complementary and Alternative Medicine*, vol. 2013, Article ID 915953, 2013.

[14] W.-F. Yiu, P.-L. Kwan, C.-Y. Wong et al., "Attenuation of fatty liver and prevention of hypercholesterolemia by extract of *Curcuma longa* through regulating the expression of CYP7A1, LDL-receptor, HO-1, and HMG-CoA reductase," *Journal of Food Science*, vol. 76, no. 3, pp. H80–H89, 2011.

[15] E.-M. Jang, M.-S. Choi, U. J. Jung et al., "Beneficial effects of curcumin on hyperlipidemia and insulin resistance in high-fat—fed hamsters," *Metabolism*, vol. 57, no. 11, pp. 1576–1583, 2008.

[16] N. Maithilikarpagaselvi, M. G. Sridhar, R. P. Swaminathan, R. Sripradha, and B. Badhe, "Curcumin inhibits hyperlipidemia and hepatic fat accumulation in high-fructose-fed male Wistar rats," *Pharmaceutical Biology*, vol. 54, no. 12, pp. 2857–2863, 2016.

[17] S. H. Park, Y. Sung, K. j. Nho, D. S. Kim, and H. K. Kim, "Effects of *Viola mandshurica* on Atherosclerosis and Hepatic Steatosis in ApoE$^{-/-}$ via the AMPK Pathway," *The American Journal of Chinese Medicine*, vol. 45, no. 04, pp. 757–772, 2017.

[18] S. Rahmani, S. Asgary, G. Askari et al., "Treatment of non-alcoholic fatty liver disease with curcumin: a randomized placebo-controlled trial," *Phytotherapy Research*, vol. 30, no. 9, pp. 1540–1548, 2016.

[19] M. Ricchi, M. R. Odoardi, L. Carulli et al., "Differential effect of oleic and palmitic acid on lipid accumulation and apoptosis in cultured hepatocytes," *Journal of Gastroenterology and Hepatology*, vol. 24, no. 5, pp. 830–840, 2009.

[20] T. P. Carr, C. J. Andresen, and L. L. Rudel, "Enzymatic determination of triglyceride, free cholesterol, and total cholesterol in tissue lipid extracts," *Clinical Biochemistry*, vol. 26, no. 1, pp. 39–42, 1993.

[21] J. N. Clore, J. Allred, D. White, J. Li, and J. Stillman, "The role of plasma fatty acid composition in endogenous glucose production in patients with type 2 diabetes mellitus.," *Metabolism: Clinical and Experimental*, vol. 51, no. 11, pp. 1471–1477, 2002.

[22] E. Berger, S. Héraud, A. Mojallal et al., "Pathways commonly dysregulated in mouse and human obese adipose tissue: FAT/CD36 modulates differentiation and lipogenesis," *Adipocyte*, vol. 4, no. 3, pp. 161–180, 2014.

[23] O. Ziouzenkova, S. Perrey, L. Asatryan et al., "Lipolysis of triglyceride-rich lipoproteins generates PPAR ligands: Evidence for an antiinflammatory role for lipoprotein lipase," *Proceedings of the National Academy of Sciences of the United States of America*, vol. 100, no. 5, pp. 2730–2735, 2003.

[24] H.-S. Shin, J.-M. Han, H.-G. Kim et al., "Anti-Atherosclerosis and hyperlipidemia effects of herbal mixture, *Artemisia iwayomogi* Kitamura and *Curcuma longa* Linne, in apolipoprotein E-deficient mice," *Journal of Ethnopharmacology*, vol. 153, no. 1, pp. 145–150, 2014.

[25] Y. Wei, D. Wang, F. Topczewski, and M. J. Pagliassotti, "Saturated fatty acids induce endoplasmic reticulum stress and apoptosis independently of ceramide in liver cells," *American Journal of Physiology—Endocrinology and Metabolism*, vol. 291, no. 2, pp. E275–E281, 2006.

[26] I.-P. Chou, Y. Y. Lin, S.-T. Ding, and C.-Y. Chen, "Adiponectin receptor 1 enhances fatty acid metabolism and cell survival in palmitate-treated HepG2 cells through the PI3 K/AKT pathway," *European Journal of Nutrition*, vol. 53, no. 3, pp. 907–917, 2014.

[27] I. Takahara, Y. Akazawa, M. Tabuchi et al., "Toyocamycin attenuates free fatty acidinduced hepatic steatosis and apoptosis in cultured hepatocytes and ameliorates nonalcoholic fatty liver disease in mice," *PLoS ONE*, vol. 12, no. 3, Article ID e0170591, 2017.

[28] S. Kojima, T. F. Kuo, H. Tatsukawa, and S. Hirose, "Induction of cross-linking and silencing of Sp1 by transglutaminase during liver injury in ASH and NASH via different ER stress pathways," *Digestive Diseases*, vol. 28, no. 6, pp. 715–721, 2010.

[29] D. Ron and P. Walter, "Signal integration in the endoplasmic reticulum unfolded protein response," *Nature Reviews Molecular Cell Biology*, vol. 8, no. 7, pp. 519–529, 2007.

[30] S. Hummasti and G. S. Hotamisligil, "Endoplasmic reticulum stress and inflammation in obesity and diabetes," *Circulation Research*, vol. 107, no. 5, pp. 579–591, 2010.

[31] C. Ji, "Dissection of endoplasmic reticulum stress signaling in alcoholic and non-alcoholic liver injury," *Journal of Gastroenterology and Hepatology (Australia)*, vol. 23, no. 1, pp. S16–S24, 2008.

[32] H.-I. Lee, K. W. Yun, K.-I. Seo, M.-J. Kim, and M.-K. Lee, "Scopoletin prevents alcohol-induced hepatic lipid accumulation by modulating the AMPK-SREBP pathway in diet-induced obese mice," *Metabolism*, vol. 63, no. 4, pp. 593–601, 2014.

[33] L. Ding, J. Li, B. Song et al., "Curcumin rescues high fat diet-induced obesity and insulin sensitivity in mice through regulating SREBP pathway," *Toxicology and Applied Pharmacology*, vol. 304, pp. 99–109, 2016.

Hindawi
Evidence-Based Complementary and Alternative Medicine
Volume 2017, Article ID 9058956, 9 pages
https://doi.org/10.1155/2017/9058956

Research Article

Euphorbia kansui Attenuates Insulin Resistance in Obese Human Subjects and High-Fat Diet-Induced Obese Mice

Seung-Wook Lee,[1] Hyun-Young Na,[1] Mi Hyeon Seol,[1] Mia Kim,[2] and Byung-Cheol Lee[1]

[1]*Department of Clinical Korean Medicine, Graduate School, Kyung Hee University, 26 Kyungheedae-ro, Dongdaemun-gu, Seoul 02447, Republic of Korea*
[2]*Department of Cardiovascular and Neurologic Disease (Stroke Center), College of Korean Medicine, Kyung Hee University, 23 Kyungheedae-ro, Dongdaemun-gu, Seoul 02447, Republic of Korea*

Correspondence should be addressed to Byung-Cheol Lee; hydrolee@khu.ac.kr

Received 13 May 2017; Revised 20 July 2017; Accepted 27 August 2017; Published 4 October 2017

Academic Editor: Elzbieta Janda

Background. Obesity is a main cause of insulin resistance (IR), metabolic syndrome, and fatty liver diseases. This study evaluated *Euphorbia kansui* radix (*Euphorbia*) as a potential treatment option for obesity and obesity-induced IR in obese human and high-fat diet- (HFD-) induced obese mice. *Methods*. In the human study, we analyzed the body weight change of 14 patients who took a single dose of 6 g of *Euphorbia* powder. In the animal study, male mice were divided into three groups: normal chow, HFD, and *Euphorbia* (high-fat diet and 100 mg/Kg *Euphorbia* once per week). Body weight, epididymal fat pad weight, fasting blood glucose, fasting insulin, HOMA-IR, and oral glucose tolerance test were measured. Also, macrophage infiltration and expression of CD68, tumor necrosis factor- (TNF-) α, interferon- (IFN-) γ, and interleukin- (IL-) 6 genes in the liver and adipose tissue were analyzed. *Results*. The human study showed that *Euphorbia* has a potential effect on body weight loss. In the in vivo study, body weight, epididymal fat weight, glucose level, IR, expression of CD68, TNF-α, IFN-r, and IL-6 genes, and macrophages in liver and adipose tissue were significantly reduced by *Euphorbia*. *Conclusions*. These results suggest that *Euphorbia* attenuates obesity and insulin resistance via anti-inflammatory effects.

1. Introduction

Obesity is rapidly increasing worldwide [1]. Increased visceral adipose tissue confers a proinflammatory milieu and insulin resistance (IR) [2], which is directly or indirectly related to various health problems including type 2 diabetes mellitus (T2DM), hypertension, dyslipidemia, and fatty liver diseases, resulting in an annual cost of about 150 billion dollars [3].

Many efforts, including lifestyle changes and antiobesity drugs, have been applied for obesity treatment. However, lifestyle change is not ensured to maintain weight loss for more than a few years, and the use of drugs has been limited by side effects such as negative mood changes, suicidal thoughts, and gastrointestinal or cardiovascular complications [4, 5]. Therefore, new efforts, including herbal medicines, can provide an alternative therapy for this medical challenge.

The root of *Euphorbia kansui* Liou *(Euphorbia)* is an herb that has been commonly used in China for thousands of years. It is in the cathartic (resolving water retention through stool) category of the Chinese medical literature [6]. In clinics, it is often used to treat ascites caused by hepatocirrhosis [7], pancreatitis [8, 9], and intestinal obstruction [10]. In recent years, there have been reports of its antitumor [11] and antiviral role [12, 13] as well as its ability to regulate the immune system [14]. Moreover, recent studies have revealed that *Euphorbia* has anti-inflammatory [15], antidiabetic [16], and antiobesity effects [17].

In this study, we evaluated the effects of *Euphorbia* on obesity, glycemic control, and IR. In addition, we addressed the safety issue of *Euphorbia* and investigated its mechanisms of action, especially with respect to the inflammatory reaction and macrophage infiltration in liver and adipose tissue.

2. Materials and Methods

2.1. Preparation of Euphorbia. *Euphorbia* was purchased from the Department of Pharmaceutical Preparation of Kyung Hee University Oriental Medical Hospital (Seoul, South Korea). The original source of the *Euphorbia* was Kyung Hee Herb Pharm (WonJu, South Korea). Drug quality was tested based on the standards of the Korea Food and Drug Administration and the standards of the hospital. Extractions were prepared from dried *Euphorbia*. *Euphorbia* (100 g) was added to 1,500 ml 80% ethanol and boiled for 2 hours using a heating mantle. The sieve-filtered solution was filtered into a 500 ml flask and concentrated with a rotary evaporator (model NE-1, EYELA Co., Tokyo, Japan). The solution was freeze-dried, and the *Euphorbia* extract was stored at room temperature. The final collection yield was 9.6%.

2.2. Human Study. The inclusion criteria were as follows: BMI over 23, age between 19 and 65 years, ability to provide informed consent, and stable health according to the opinion of the investigator. The exclusion criteria included pregnant or lactating women, participants who had undergone another obesity treatment in the previous 3 months, participants of clinical trials within the previous 3 months, clinically significant new illness in the 1 month before screening, or not being suitable for participating in the study in the opinion of the investigator including an existing physical or mental condition, significant change in smoking habits within the previous 3 months, and diseases including epilepsy, uncontrolled hypertension, or hypotension, cerebrovascular diseases, and clinically significant abnormal hepatic (e.g., AST or ALT greater than 2.5 × ULN or total bilirubin greater than 1.5 × ULN) or renal function lab tests (e.g., creatinine greater than 1.25 × ULN), suggestive of hepatic or renal impairment.

Eligible patients recruited from January 2014 to October 2014 were given a single 6 g dose of raw *Euphorbia* powder with simple dietary consultations at the Korean Medicine Hospital of Kyung Hee University, Seoul, South Korea. The consultations include taking 3 meals a day regularly and prohibiting confections. Patients were analyzed for body weight (BW), height, waist-hip ratio, body fat percentage, aspartic aminotransferase (AST), alanine aminotransferase (ALT), gamma glutamyltranspeptidase (GGT), blood urea nitrogen (BUN), and creatinine before and one month after treatment. Body mass index (BMI) and CockCroft-Gault estimated glomerular filtration rate (eGFR) were calculated from the above data. Furthermore, other side effects were noted after *Euphorbia* administration. BW, BMI, waist-hip ratio, and body fat percentage of patients were estimated using a body composition analyzer (Inbody Co., Seoul, Korea). This study was approved by the International Review Board of Kyung Hee Hospital (KOMCIRB-2014-06).

2.3. Animals and Diets. The animals used in this study were 19–21 g, 5-week-old, male C57BL/6 mice (Central LabAnimals, Inc., Korea). To determine the optimal dose of *Euphorbia*, thirty-five mice fed normal chow (NC) with 10% fat were randomized to be treated with the following dose levels of *Euphorbia* with five mice per dose level: no treatment, 20 mg/kg, 50 mg/kg, 100 mg/kg, 200 mg/kg, 500 mg/kg, and 1000 mg/kg of *Euphorbia* were orally administered once weekly for 28 days. Upon completion of the study, all mice were weighed and sacrificed, and the liver, spleen, and kidney were harvested and weighed. After 28 days of treatment, an 18.2% reduction of body weight was achieved with the 100 mg/kg dose level compared to the no treatment control group. No differences of liver, spleen, and kidney weight were observed with 100 mg/kg dose *Euphorbia*, finally, the 100 mg/Kg of *Euphorbia* was selected for main experiment. With free access to water and food, the mice were fed a high-fat diet (HFD) with 60% fat for 13 weeks in order to induce obesity, except in the group NC with 10% fat. After 8 weeks of the HFD diet, the HFD groups showed significant body weight differences compared to the NC-fed group (28.98 ± 1.40 g and 41.26 ± 1.14 g, resp., $p < 0.001$). The HFD-fed mice were randomly assigned to two groups: HFD and *Euphorbia* groups ($n = 5$ in each). For the remaining 5 weeks of the experiment, the *Euphorbia* group was fed *Euphorbia* (100 mg/kg) extract once a week, while the NC and HFD groups were administered normal saline. All experiments were carried out in accordance with guidelines of the Korean National Institute of Health Animal Facility. The Animal Care Committee at Kyung Hee University approved all protocols used in this study (KHMC-IACUC 14-025).

2.4. Body and Epididymal Weight Measurement. Body weight (BW) was recorded at the beginning and end of the experiment using an electronic scale (CAS 2.5D, Seoul, Korea) and was measured at the same time in the morning every day. The mice were killed at 13 weeks after blood collection by heart puncture. The epididymides and livers were removed rapidly and weighed.

2.5. Insulin Concentration and Insulin Resistance Measurement. At the 11th week of the experimental period, we withdrew blood from the tail vein of mice after 6 hours of fasting. Serum insulin concentration was measured using an ultrasensitive mouse insulin ELISA kit (Crystal Chem Inc., USA). Insulin resistance was calculated using the following equation: HOMA-IR = fasting blood glucose (mg/dl) × fasting blood insulin (mg/ml) × 0.0717225161669606.

2.6. Oral Glucose Tolerance Test (OGTT). At the 12th week, an oral glucose tolerance test was performed after the mice had undergone 14 hours of fasting. The fasting (baseline) blood glucose measurement was performed by applying a drop of tail blood to a strip-operated blood glucose sensor (ACCU-CHECK Performa, Australia). Glucose (2 g/kg body weight) was administered orally to each animal. Tail vein blood samples were withdrawn at 30, 60, and 120 minutes after glucose administration.

2.7. Stromal Vascular Cell (SVC) Segregation. Epididymal fat pad tissue, obtained at week 13 of the experimental period, was mixed with a solution of phosphate-buffered saline (PBS, Gibco, USA) and 2% bovine serum albumin (BSA, Gibco, USA). After cutting the fat pad into 1~2 mm sized round

shapes with scissors, collagenase (Sigma, USA) and DNase I (Roche, USA) were added. A 100 μm cell strainer (BD Biosciences, USA) was used to remove extraneous tissue.

2.8. Fluorescence Activated Cell Sorting (FACS) Analysis of Adipose Tissue Macrophages (ATMs). The number of SVCs obtained from the adipose tissue was counted by cellometer (Nexcelom Bioscience LLC, USA), and every sample was set at a concentration of 10^6 cells. FcBlock (BD Pharmingen, USA) was mixed with the sample at a ratio of 1 : 100, and the reaction was performed for 10 minutes. Fluorophore-conjugated antibodies were added to the shaded state and reacted for 20 minutes. The following antibodies were used: CD45-APC Cy7 (Biolegend, USA), CD68-APC (Biolegend, USA), CD11c-phycoerythrin (CD11b-PE, Biolegend, USA), and CD206-FITC (Biolegend, USA). The samples were analyzed by FACSCalibur (BD Biosciences, USA). A FlowJo (Tree Star, Inc., USA) was used to analyze the percentage of macrophages.

2.9. Immunofluorescence Staining of Stromal Vascular Cells. SVCs were plated onto glass coverslips for 2 hours, and nonadherent cells were removed by washing in PBS. The cells were fixed in 10% formalin for 20 minutes and then blocked in 2% BSA in PBS. Lipid staining was performed by incubation of fixed cells in 1 ug/ml Bodipy (Sigma-Aldrich) in PBS for 5 minutes. Coverslips were mounted on slides with Vectashield (Vector Laboratories, Burlingame, CA) and imaged under fluorescence microscopy (Olympus BX51, Olympus, Japan).

2.10. Immunohistochemistry. Immunohistochemistry was performed on 10% buffered formalin-fixed, paraffin-embedded liver tissues using antibodies against F4/80 (1 : 100, Genetex, Irvine, CA), followed by incubating in biotinylated anti-mouse/rabbit/goat IgG (H + L), made in horse (Vector Laboratories, Inc.). Liver tissue sections were consecutively stained with avidin-biotin horseradish peroxidase complex (Vectastain ABC ELITE kit; Vector Laboratories, Burlingame, CA) for 15 min before a substrate solution of 3,3′-diaminobenzidine tetrahydrochloride (DAB; Sigma Chemical, St. Louis, MO) was added. The sections were photographed under an Olympus photomicroscope (Olympus BX-50, Olympus Optical, Tokyo, Japan). The percentage of F4/80-positive area in liver tissues was analyzed using the ImageJ software (NIH, USA).

2.11. RNA Extraction and Real-Time Reverse Transcriptase-Polymerase Chain Reaction. Mini RNA Isolation IITM (ZYMO RESEARCH, CA, USA) was used for separation of RNA from liver and epididymal fat pads. To evaluate the gene expression of CD68 (macrophage marker), tumor necrosis factor-α (TNF-α), interferon-γ (IFN-γ), and interleukin-6 (IL-6) in adipose tissue, we performed quantitative reverse transcriptase-polymerase chain reaction (qRT-PCR). Primers for the analysis were designed as follows: CD68, 5′-TTCTGCTGTGGAAATGCAAG and 5′-AGAGGGGCT-GGTAGGTTGAT; TNF-α, 5′-TTCTGTCTACTGAAC-TTCGGGGTGATCGGTCC and 5′-GTATGAGATAGC-AAATCGGCTGACGGTGTGGG; IFN-γ, 5′-ACTGGC-AAAAGGATGGTGAC and 5′-TGAGCTCATTGAATG-CTTGG; IL-6, 5′-AACGATGATGCACTTGCAGA and 5′-GAGCATTGGAAATTGGGGTA; GAPDH, which was used as a housekeeping gene, 5′-AGTCCATGCCATCAC-TGCCACC and 5′-CCAGTGAGCTTCCCGTTCAGC. The threshold cycle (TC) of each gene expression, determined by SDS Software 2.4 (Applied Biosystems®, USA), was converted into Relative Quantitation (RQ) based on GAPDH, and the calculated fold change value was used for gene expression analysis. The fold change value of the experimental group was converted based on the NC group value, which was considered to be one.

2.12. Statistical Analysis. All calculations were performed using GraphPad PRISM 5 (GraphPad Software, Inc., San Diego, CA, USA). All values are expressed as mean ± SE. The significance of differences between groups was determined using one-way analysis of variance (ANOVA), followed by Tuckey's post hoc test. All p values were two-tailed, and significance was set at $p < 0.05$.

3. Results

3.1. Effects of Euphorbia in Overweight or Obese Human Patients. The BW changes of 14 patients were obtained at one month after one-time treatment with 6 g *Euphorbia*. There was significant decrease in BW and BMI after *Euphorbia* powder administration (65.37 ± 3.53 kg versus 64.10 ± 3.49 kg for BW and 24.93 ± 0.65 versus 24.28 ± 0.58 for BMI, $p < 0.05$) (Table 1). There was no significant difference in BUN, creatinine, eGFR, AST, ALT, GGT, protein, albumin, fasting glucose, and HbA1c before and after administration with *Euphorbia* (Table 1). As *Euphorbia* is traditionally classified as a cathartic herb, patients underwent an average of 0.92 ± 0.27 cases of vomiting and 8.08 ± 1.24 cases of diarrhea. There were several mild side effects including 1 report of mild abdominal pain and 6 cases of abdominal discomfort, which diminished after a few days.

3.2. Effects of Euphorbia on BW and Epididymal Fat Weight Changes in Mice. The fasting body weight (FBW) of the HFD group increased significantly compared to that of the NC group ($p < 0.05$), and *Euphorbia* group showed a decrease in BW compared to the HFD group ($p < 0.05$) (Figure 1(a)). The weight of epididymal fat also was significantly increased in the HFD group compared to the NC and was decreased by *Euphorbia* ($p < 0.001$) (Figure 1(a)).

3.3. Effects on Blood Glucose and Insulin Resistance in Mice. Fasting blood glucose (FBG) was significantly higher in the HFD group than NC group ($p < 0.001$), and it was significantly lower in the *Euphorbia* group than HFD group ($p < 0.01$). Fasting insulin concentration (FI) was significantly higher in the HFD group compared to the NC group ($p <$

Table 1: Comparison of outcome measures in an obese human study.

	Before	After	p value
BW (kg)	65.37 ± 3.53	64.10 ± 3.49	0.02
BMI	24.93 ± 0.65	24.28 ± 0.58	0.047
Waist-hip ratio	0.90 ± 0.01	0.90 ± 0.01	0.79
Percent body fat (%)	29.71 ± 1.44	29.56 ± 1.39	0.58
BUN (mg/dl)	15.28 ± 1.32	14.52 ± 1.14	0.44
Creatinine (mg/dl)	0.72 ± 0.39	0.72 ± 0.42	0.75
eGFR	97.38 ± 6.71	93.58 ± 4.94	0.36
AST (U/L)	32.42 ± 6.96	27.04 ± 2.53	0.51
ALT (U/L)	35.25 ± 13.56	25.96 ± 5.40	0.28
GGT (U/L)	44.91 ± 13.53	43.04 ± 13.49	0.77
Protein (g/dl)	6.98 ± 0.53	6.79 ± 0.55	0.21
Albumin (g/dl)	3.99 ± 0.32	3.98 ± 0.48	0.97
Fasting glucose (mg/dl)	94.5 ± 5.6	88.3 ± 9.99	0.12
HbA1c (%)	6.11 ± 0.58	5.97 ± 0.56	0.28

"Before" and "after" indicate before *Euphorbia* administration and after *Euphorbia* administration, respectively. Data are presented as mean ± SE. For p value, the results are from paired t-test to examine within-group effects. BW: body weight; BMI: body mass index; BUN: blood urea nitrogen; eGFR: CockCroft-Gault estimated glomerular filtration rate; AST: aspartic aminotransferase; ALT: alanine aminotransferase; GGT: gamma glutamyltranspeptidase.

0.001) and was significantly lower in the *Euphorbia* group compared to the HFD group ($p < 0.05$). Insulin resistance calculated by HOMA-IR was significantly higher in the HFD group than NC group ($p < 0.05$), while the HOMA-IR of the *Euphorbia* group was significantly lower than that HFD group ($p < 0.01$) (Figure 1(a)).

OGTT, conducted at 12 weeks after initiation of the study, showed the highest blood glucose concentration at 30 minutes in every group and decreased gradually. The 30-, 60-, and 120-minute glucose levels of the HFD group were elevated significantly compared to those of the NC group ($p < 0.05$) and were significantly lower in the *Euphorbia* group than in the HFD group ($p < 0.05$). The area under the curve (AUC) also showed similar tendencies, with the AUC of the HFD group being higher than that of the NC group, while that of the *Euphorbia* group was significantly lower than that of the HFD group ($p < 0.01$) (Figure 1(b)).

3.4. Effects on Expression of CD68, TNF-α, IFN-γ, and IL-6 Genes. The gene expression of CD68 in liver was significantly higher in the HFD group than NC group ($p < 0.001$) and was significantly lower in the *Euphorbia* group compared to the HFD group ($p < 0.01$). And TNF-α in liver and epididymal fat was significantly higher in the HFD group than NC group ($p < 0.001$), and *Euphorbia* significantly lowers TNF-α gene expression compared to the HFD group ($p < 0.001$). IL-6 expression in epididymal fat was also higher in the HFD group than in the NC group and decreased significantly in the *Euphorbia* group compared to the HFD group ($p < 0.05$). The IFN-γ in epididymal fat expression was significantly increased in the HFD group compared to the NC and *Euphorbia* groups ($p < 0.05$) (Figure 1(c)).

3.5. Effects on Macrophages in Liver and Adipose Tissue. The F4/80 positive Kupffer cells and fat deposits were markedly increased in HFD (F4/80-stained surface of 4.61 ± 0.64% in HFD versus 0.89 ± 0.18% in NC, $p < 0.01$), and the number of Kupffer cells and lipid accumulation were decreased in *Euphorbia* group (2.20 ± 0.22% in *Euphorbia* versus HFD, $p < 0.05$) (Figure 3). The RT-PCR analysis confirmed the markedly reduced the expression of CD68 mRNA in liver (Figure 1(c)). CD68 positive ATMs infiltration rate was significantly higher in the HFD group compared to the NC group ($p < 0.001$), and *Euphorbia* showed significant decrease in ATMs percentage ($p < 0.05$) (Figure 2(a)). The percentage of CD11c+ ATMs was significantly higher in the HFD group compared to the NC group ($p < 0.05$) and lower in the *Euphorbia* group compared to the HFD group, but the difference was not significant. In contrast, the CD206+ ATMs percentage was significantly lower in the HFD group than the NC group ($p < 0.01$) and significantly higher in the *Euphorbia* group than the HFD group ($p < 0.01$) (Figure 2(b)).

3.6. Immunofluorescence Staining of SVCs. Compared to the NC group, the HFD group showed an increase in the number of stained macrophages and lipid accumulation. For the *Euphorbia* group, the number of macrophages and lipid accumulation were decreased (Figure 3).

4. Discussion

In this study, we evaluated *Euphorbia* as a potential therapy for obesity and insulin resistance. We were able to obtain data on efficacy and safety of *Euphorbia* from human studies, since *Euphorbia* has already been approved for use as herbal medicine in the Republic of Korea when used by a professional physician [18]. Additionally, we conducted an *in vivo* study to estimate the efficacy, safety, and mechanism of *Euphorbia*, especially with respect to the anti-inflammatory effect.

In a study of 14 obese patients, we found that a 1-day prescription of 6 g *Euphorbia* caused significant decrease in BW and BMI. Because *Euphorbia* is a cathartic herbal medicine, the short-term effect of *Euphorbia* might mostly result from dehydration. However, in our human study, the weight loss effects persisted for one month, which allowed enough time to recover from dehydration. This result implies that the effect of *Euphorbia* depends on more than simple dehydration induced by diarrhea.

It was reported that administration of *Euphorbia* with herbal decoction to obese rats induced weight loss [17]. In agreement, administration of *Euphorbia* in the present study induced significant decrease in BW and epididymal fat weight, which is equivalent to visceral fat in humans. A decrease in epididymal fat weight after a five-week administration of *Euphorbia* in mice demonstrated the antiobesity effect of *Euphorbia*. In a previous study [16] of ethanol

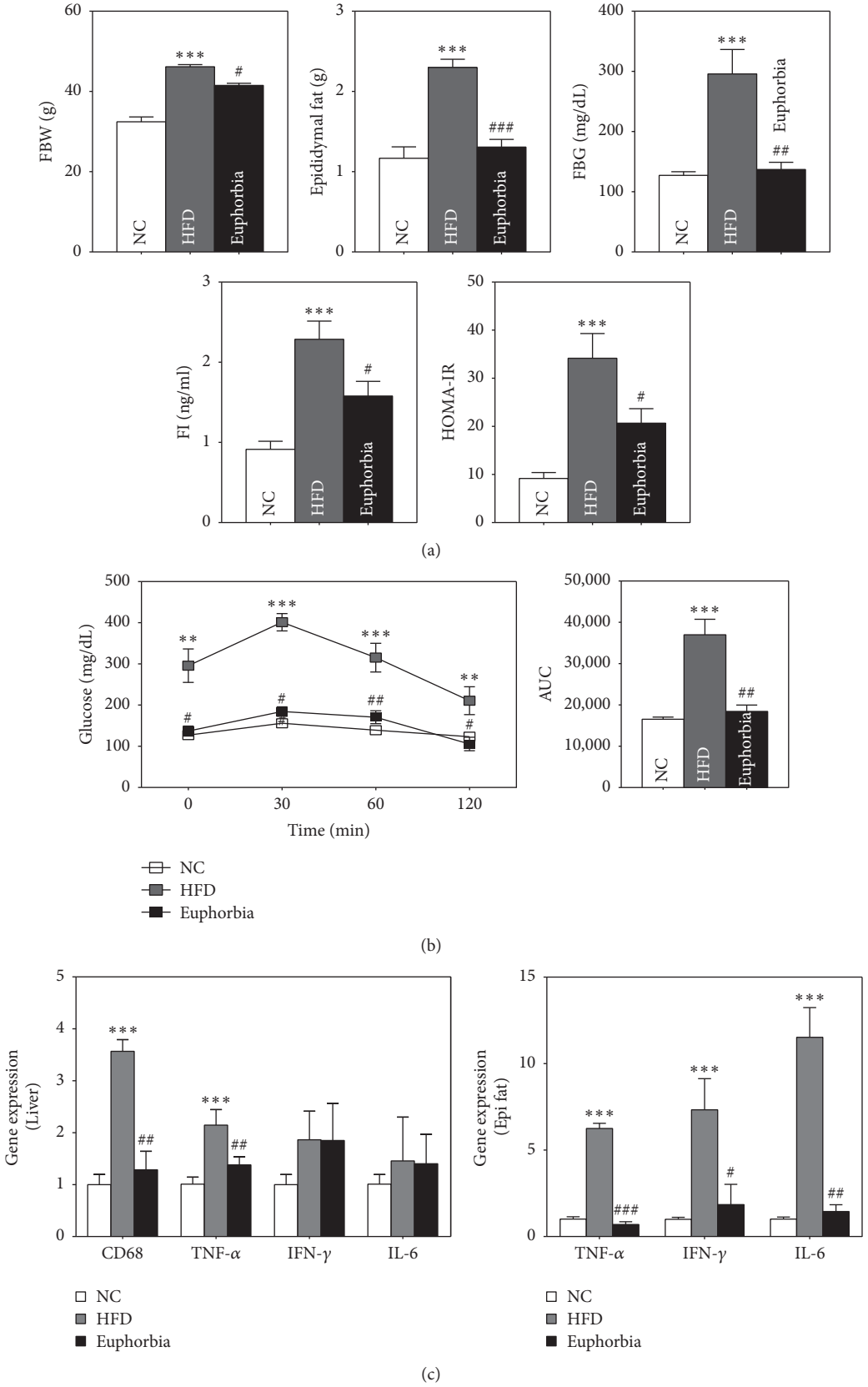

Figure 1: Main results of the *in vivo* study. (a) Fasting body weight (FBW), epididymal fat weight, fasting blood glucose (FBG), fasting insulin (FI), HOMA-IR of normal chow NC, HFD, and *Euphorbia* groups. (b) Oral glucose tolerance test (OGTT) and area under curve (AUC) of the three groups. (c) Expression of CD68, TNF-α, IFN-γ, and IL-6 genes in the three groups. $^{**}p < 0.01$ and $^{***}p < 0.001$, HFD compared with NC; $^{\#}p < 0.05$, $^{\#\#}p < 0.01$, and $^{\#\#\#}p < 0.001$, *Euphorbia* compared with HFD. NC: NC group; HFD: HFD group; *Euphorbia*: *Euphorbia* group.

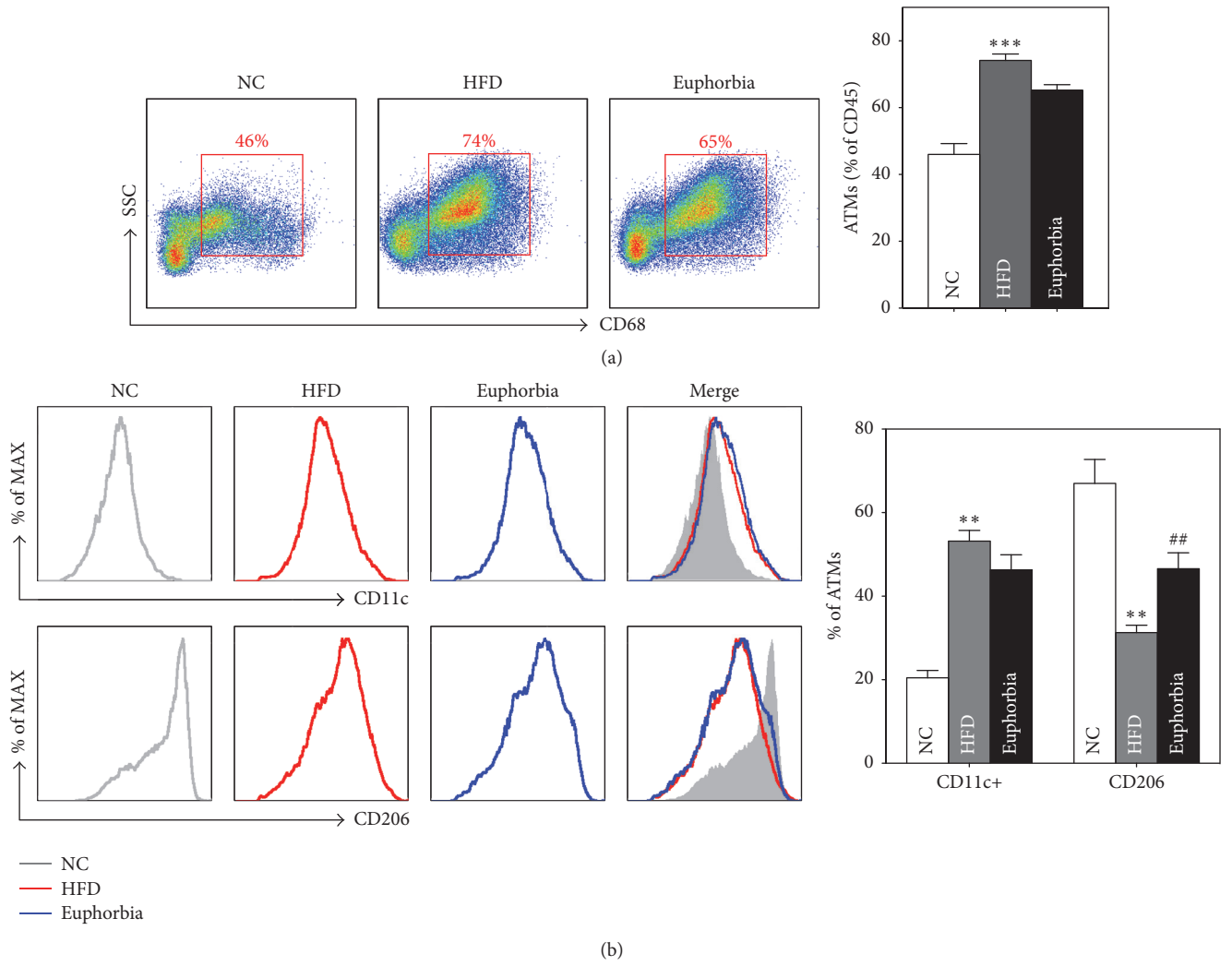

Figure 2: (a) ATM infiltration rate; (b) CD206- and CD11c-positive ATMs. NC: NC group; HFD: HFD group; *Euphorbia*: *Euphorbia* group. $^{**}p < 0.01$; $^{***}p < 0.001$ versus NC group. $^{\#\#}p < 0.01$ versus HFD group.

extracts of *Euphorbia*, a new tetracyclic triterpenoid of *Euphorbia* and five known triterpenoids with euphane skeletons were shown to be potentially useful in the clinical treatment of diabetes. In this study, *Euphorbia* showed anti-hyperglycemic effects on FBG and OGTT of obese mice. In addition, changes in FI and HOMA-IR indicate that *Euphorbia* improves IR.

It has been shown that high-fat diet increases Kupffer cells number and induces their proinflammatory status, and cytokine and chemokine production by activated Kupffer cells is involved in the pathogenesis of liver damage [19]. Moreover, visceral adipose tissue is an endocrine organ that releases adipokines and cytokines, which have a role in fat metabolism and insulin sensitivity [20]. Particularly, macrophage accumulation with increased cytokines was observed in adipose tissue, which implies the chronic inflammatory features of obesity [21, 22]. In this study, *Euphorbia* administration was related to a significant decrease in gene expression of cytokines TNF-α, IFN-γ, and IL-6. TNF-α is known to reduce insulin sensitivity by impairing insulin signal transduction [23]. Also, an increase in the expression of IFN-γ and IL-6 was also associated with insulin resistance [24, 25].

The rate of Kupffer cells in liver and ATM infiltration into adipose tissue was also decreased in the *Euphorbia*-treated group. Particularly, the percentage of CD206+ ATMs, which indicates the anti-inflammatory activity of ATMs in adipose tissue, was significantly increased in the *Euphorbia*-treated group in comparison to the HFD group [26]. This result suggests that improvement of hyperglycemia and IR in the *Euphorbia* group is correlated with the anti-inflammatory effects of *Euphorbia* on liver and visceral adipose tissue.

In obesity, adipocyte-hypertrophy leads to hypoxia, endoplasmic reticulum stress, and lipotoxicity, which result in increased macrophage infiltration accompanied by elevated concentrations of inflammatory markers. The accumulation of macrophages in adipose tissue leads to a specific feature called crown-like structure, which is the

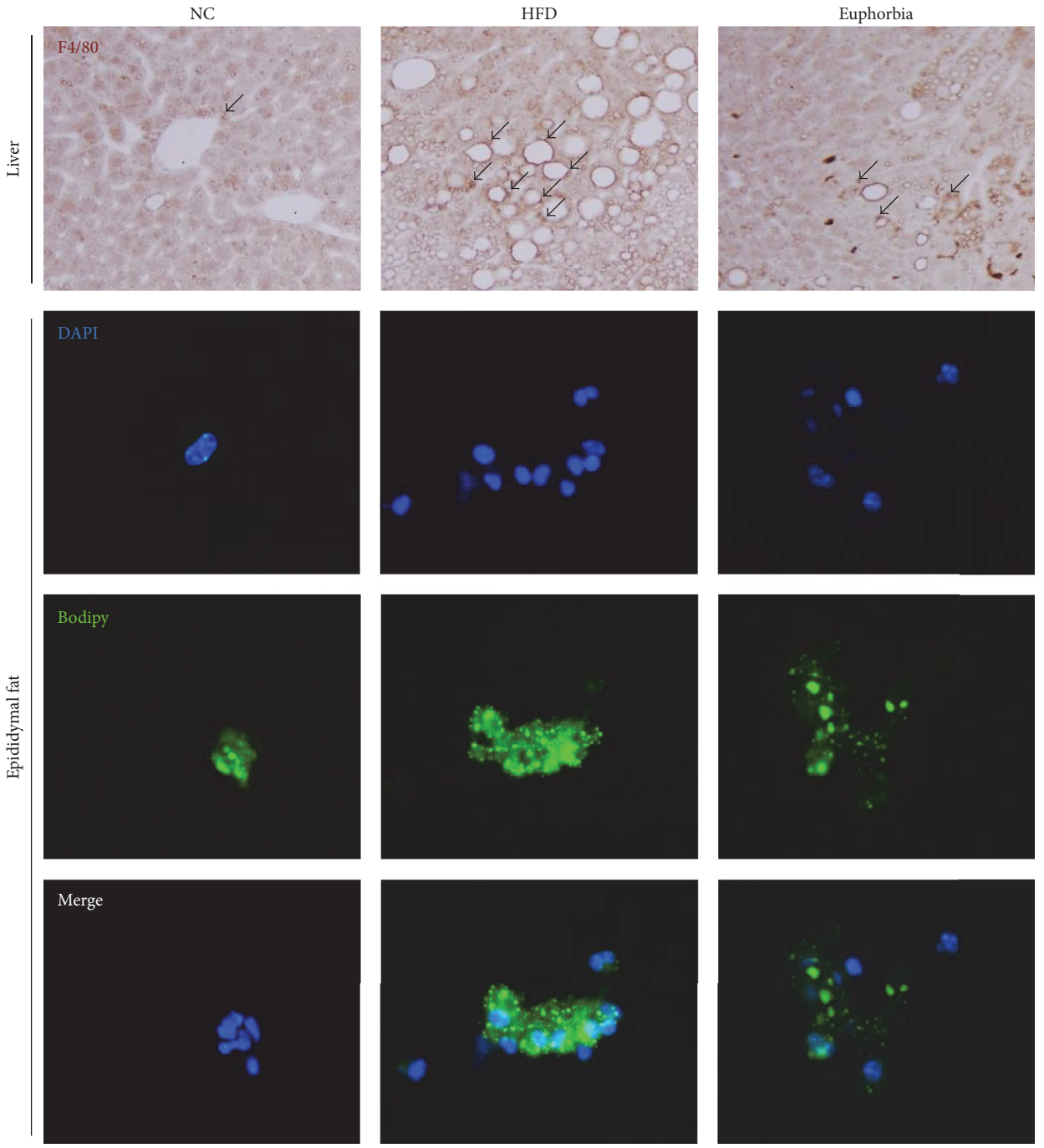

Figure 3: Immunohistochemical staining (F4/80) of liver and immunofluorescence staining of stromal vascular cells. Arrow indicates F4/80 positive Kupffer cells. NC: NC group; HFD: HFD group; *Euphorbia*: *Euphorbia* group.

cluster of macrophages around dead adipocytes [27]. We obtained SVCs from the epididymal fat pad and analyzed them using immunofluorescence microscopy. The SVCs from the *Euphorbia* group showed a decreased number of macrophages with a smaller amount of lipid accumulation compared to those in the HFD group.

Taken together, the degree of lipid accumulation in liver and visceral fat, Kupffer cells, ATM infiltration rate, which produces proinflammatory cytokines in liver and adipose tissue, and gene expression of cytokines are important for evaluating antiobesity, anti-inflammatory, and anti-IR effects. In this study, the BW decrease caused by *Euphorbia* treatment persisted for 1 month in humans, and the *in vivo* studies showed epididymal fat weight decrease, decline in Kupffer cells and ATM percentage, and decreased expression of TNF-α, IFN-γ, and IL-6 genes. These results indicate that *Euphorbia* has an antiobesity effect, which consequently induces an anti-inflammatory effect that improves IR.

5. Conclusion

In conclusion, our study showed that *Euphorbia* improves body weight and insulin resistance in human and *in vivo* study. A possible mechanism to explain this result is the reduction in the inflammatory reaction due to decreased Kupffer cells and adipose tissue macrophage infiltration. The cathartic effects of *Euphorbia* necessitate further research to assess issues with diarrhea that might affect long-term use, even though the results suggest that *Euphorbia* can be used to effectively improve obesity-related IR.

Disclosure

The authors are responsible for the writing and content of the paper.

Conflicts of Interest

The authors have no conflicts of interest.

Authors' Contributions

Seung-Wook Lee and Hyun-Young Na contributed equally to this work.

Acknowledgments

This study was supported by the Traditional Korean Medicine Research and Development Program funded by the Ministry of Health and Welfare through Korea Health Industry Development Institute (Grant no. HI13C0700).

References

[1] C. L. Ogden, M. D. Carroll, and K. M. Flegal, "Prevalence of obesity in the United States: Reply," *JAMA - Journal of the American Medical Association*, vol. 312, no. 2, pp. 189-190, 2014.

[2] A. R. Aroor, S. McKarns, V. G. Demarco, G. Jia, and J. R. Sowers, "Maladaptive immune and inflammatory pathways lead to cardiovascular insulin resistance," *Metabolism: Clinical and Experimental*, vol. 62, no. 11, pp. 1543–1552, 2013.

[3] Z. Yang and N. Zhang, "The burden of overweight and obesity on long-term care and medicaid financing," *Medical Care*, vol. 52, no. 7, pp. 658–663, 2014.

[4] H. R. Wyatt, "Update on treatment strategies for obesity," *Journal of Clinical Endocrinology and Metabolism*, vol. 98, no. 4, pp. 1299–1306, 2013.

[5] R. Padwal, S. K. Li, and D. C. Lau, "Long-term pharmacotherapy for obesity and overweight.," *Cochrane database of systematic reviews (Online)*, no. 3, p. CD004094, 2004.

[6] T. M. Ehrman, D. J. Barlow, and P. J. Hylands, "Phytochemical informatics of traditional Chinese medicine and therapeutic relevance," *Journal of Chemical Information and Modeling*, vol. 47, no. 6, pp. 2316–2334, 2007.

[7] C. G. Zhao ZX, S. Xie, XL. Zhou, and XL. Hu, "Dressing navel with Euphorbia kansui in combination with taken DuShenTang orally to cure ascites caused by hepatocirrhosis in clinic," *Journal of Emergency in Traditional Chinese Medicine*, vol. 19, pp. 388-389.

[8] Y. Zhang, X. S. Lv, Y. X. Li, H. H. Tang, X. R. Li, and F. Y. Wu, "Therapeutic effect of kansui root on patients with severe acute pancreatitis," *Chinese Journal of General Surgery*, vol. 13, pp. 401–404, 2004.

[9] D. M. Ouyang JB and YM. Ouyang, "Therapeutic effect on adjuvant treatment of severe acute pancreatitis with Euphorbia kansui Lious," *China Journal of Modern Medicine*, vol. 14, 2004.

[10] Y. C. D. Fan, X. X. Gu, G. Y. Wang, and Ma J., "Treatment of intestinal obstruction with a large dose of kansui," *Journal of Emergency in Traditional Chinese Medicine*, vol. 14, pp. 278-279, 2005.

[11] L. C. Whelan and M. F. Ryan, "Ethanolic extracts of *Euphorbia* and other ethnobotanical species as inhibitors of human tumour cell growth," *Phytomedicine*, vol. 10, no. 1, pp. 53–58, 2003.

[12] Z. WF, "Study on in vivo antiviral activity of four diterpenoids from ethanol extracts of Euphorbia kansui," *Chinese Traditional Herbal Drugs*, vol. 35, pp. 65–68, 2004.

[13] W. F. Zheng, Z. Cui, and Q. Zhu, "Cytotoxicity and antiviral activity of the compounds from Euphorbia kansui," *Planta Medica*, vol. 64, no. 8, pp. 754–756, 1998.

[14] S. Nunomura, S. Kitanaka, and C. Ra, "3-O-(2,3-dimethylbutanoyl)-13-odecanoylingenol from Euphorbia kansui suppresses IgE-mediated mast cell activation," *Biological and Pharmaceutical Bulletin*, vol. 29, no. 2, pp. 286–290, 2006.

[15] R. C. Dutra, P. R. De Cezaro De Souza, A. F. Bento et al., "Euphol prevents experimental autoimmune encephalomyelitis in mice: Evidence for the underlying mechanisms," *Biochemical Pharmacology*, vol. 83, no. 4, pp. 531–542, 2012.

[16] J. Guo, L.-Y. Zhou, H.-P. He, Y. Leng, Z. Yang, and X.-J. Hao, "Inhibition of 11β-HSD1 by tetracyclic triterpenoids from euphorbia kansui," *Molecules*, vol. 17, no. 10, pp. 11826–11838, 2012.

[17] J.-W. Kim and E.-Y. Kim, "The effect of Hyungbangdojucksan-Gami and Kamsuchunilhwan on the obesity in the Rats," *Journal of Sasang Constitutional Medicine*, vol. 12, pp. 184–194, 2000.

[18] Ministry of Food and Drug Safety, *The Korean Herbal Pharmacopoeia*, Shinil Books, Seoul, South Korea, 2011.

[19] M. Sharma, S. Mitnala, R. K. Vishnubhotla, R. Mukherjee, D. N. Reddy, and P. N. Rao, "The riddle of nonalcoholic fatty liver disease: progression from nonalcoholic fatty liver to nonalcoholic steatohepatitis," *Journal of Clinical and Experimental Hepatology*, vol. 5, no. 2, pp. 147–158, 2015.

[20] P. E. Scherer, "Adipose tissue: from lipid storage compartment to endocrine organ," *Diabetes*, vol. 55, no. 6, pp. 1537–1545, 2006.

[21] S. P. Weisberg, D. McCann, M. Desai, M. Rosenbaum, R. L. Leibel, and A. W. Ferrante Jr., "Obesity is associated with macrophage accumulation in adipose tissue," *Journal of Clinical Investigation*, vol. 112, no. 12, pp. 1796–1808, 2003.

[22] H. Xu, G. T. Barnes, Q. Yang et al., "Chronic inflammation in fat plays a crucial role in the development of obesity-related insulin resistance," *The Journal of Clinical Investigation*, vol. 112, no. 12, pp. 1821–1830, 2003.

[23] G. Kollias and P. Sfikakis, *TNF Pathophysiology*, vol. 11, KARGER, Basel, 2010.

[24] N. Paquot, M. J. Castillo, P. J. Lefèbvre, and A. J. Scheen, "No increased insulin sensitivity after a single intravenous administration of a recombinant human tumor necrosis factor receptor: fc fusion protein in obese insulin-resistant patients," *The Journal of Clinical Endocrinology & Metabolism*, vol. 85, no. 3, pp. 1316–1319, 2000.

[25] R. W. O'Rourke, M. D. Metcalf, A. E. White et al., "Depot-specific differences in inflammatory mediators and a role for NK cells and IFN-γ in inflammation in human adipose tissue," *International Journal of Obesity*, vol. 33, no. 9, pp. 978–990, 2009.

[26] B.-C. Lee and J. Lee, "Cellular and molecular players in adipose tissue inflammation in the development of obesity-induced insulin resistance," *Biochimica et Biophysica Acta—Molecular Basis of Disease*, vol. 1842, no. 3, pp. 446–462, 2014.

[27] J. L. Schultze, A. Schmieder, and S. Goerdt, "Macrophage activation in human diseases," *Seminars in Immunology*, vol. 27, no. 4, pp. 249–256, 2015.

Hindawi
Evidence-Based Complementary and Alternative Medicine
Volume 2017, Article ID 4658543, 8 pages
https://doi.org/10.1155/2017/4658543

Research Article

Effect of Seyoeum on Obesity, Insulin Resistance, and Nonalcoholic Fatty Liver Disease of High-Fat Diet-Fed C57BL/6 Mice

Hyun-Young Na,[1] Mi Hyeon Seol,[1] Mia Kim,[2] and Byung-Cheol Lee[1]

[1]*Department of Clinical Korean Medicine, Graduate School, Kyung Hee University, 26 Kyungheedae-ro, Dongdaemun-gu, Seoul 02447, Republic of Korea*
[2]*Department of Cardiovascular and Neurologic Disease (Stroke Center), College of Korean Medicine, Kyung Hee University, 23 Kyungheedae-ro, Dongdaemun-gu, Seoul 02447, Republic of Korea*

Correspondence should be addressed to Byung-Cheol Lee; hydrolee@khu.ac.kr

Received 13 May 2017; Revised 20 July 2017; Accepted 3 August 2017; Published 11 September 2017

Academic Editor: Chang G. Son

Background. This study was performed to evaluate the effect of Seyoeum (SYE), a novel herbal meal replacement, on insulin resistance and nonalcoholic fatty liver disease (NAFLD) in obese mice fed with a high-fat diet (HFD). *Methods*. SYE contained six kinds of herbal powder such as *Coix lacryma-jobi*, *Oryza sativa*, *Sesamum indicum*, *Glycine max*, *Liriope platyphylla,* and *Dioscorea batatas*. Male C57BL/6 mice were divided into four groups: normal chow (NC), HFD, SYE, and HFD plus SYE (HFD + SYE). The mice in groups other than NC were fed HFD for 9 weeks to induce obesity and then were fed each diet for 6 weeks. Clinical markers related to obesity, diabetes, and NAFLD were examined and gene expressions related to inflammation and insulin receptor were determined. *Results*. Compared with HFD group, body weight, serum glucose, serum insulin, HOMA-IR, total cholesterol, triglyceride, epididymal fat pad weight, liver weight, and inflammatory gene expression were significantly reduced in SYE group. Insulin receptor gene expression increased in SYE group. *Conclusions*. Based on these results, we conclude that SYE improved obesity and insulin resistance in high-fat fed obese mice. Our findings suggest that SYE could be a beneficial meal replacement through these antiobesity and anti-insulin resistance effects.

1. Introduction

Obesity is a major risk factor for many chronic diseases including insulin resistance, type 2 diabetes, atherosclerosis, and nonalcoholic fatty liver disease (NAFLD) [1]. Insulin resistance is a common pathogenic event that links obesity with metabolic syndrome and NAFLD [2]. High insulin concentration in insulin resistance stimulates lipogenesis through the activation of sterol regulatory element-binding protein 1 (SREBP-1c) [3], which inhibits insulin receptor substrate 2 (IRS-2) mediated insulin signaling [4]. NAFLD activates gluconeogenesis leading to hepatic insulin resistance [5]. The excess accumulation of lipid in adipose tissue and liver accompanies a chronic, subacute state of inflammation, which can be seen in the involved tissues and systemically, in terms of elevated circulating levels of inflammatory markers [1].

A number of strategies including exercise, a structured dietary plan, cognitive behavioral therapy, pharmacotherapy, and bariatric surgery are available [6]. Yet, it is hard to make a significant and sustainable difference by lifestyle interventions, and pharmacologic or surgical interventions should be considered only in certain patients [7].

Meal replacement is commonly used as adjunctive therapy in the diet of various treatments for obesity. Meal replacement is convenient and has a low risk of side effect, providing a fixed amount of calorie, dose, and nutritional content [8]. Some studies suggest it for an effective option for long-term compliance or improvement in metabolic risk factors of outpatients [9–13]. Clinical studies showed that partial meal replacement therapy had better weight loss and long-term effects compared to conventional calorie restriction [14]; however, most of the studies about meal replacement have

targeted weight loss effects for humans. Besides, there are few studies about effects of using meal replacements only, and there are very few mechanism studies about effects of meal replacements on metabolic risk factors. So in this study, we investigated the effect of Seyoeum (SYE), a new meal replacement which consisted of six kinds of herbs, on obesity and insulin resistance, on high-fat diet (HFD) fed C57BL/6 mice.

2. Materials and Methods

2.1. Preparation of Seyoeum. The herbs were obtained from the Department of Pharmaceutical Preparation of Korean Medicine, Korean Medical Hospital, Kyung Hee University, Seoul, Korea. SYE is a combination of herbal powder (i.e., *Coix lacryma-jobi* Linné var. *ma-yuen* Stapf, *Oryza sativa* Linné, *Sesamum indicum* Linné, *Glycine max* Merrill, *Liriope platyphylla* F. T. Wang & Tang, and *Dioscorea batatas* Decne.) at a ratio of 1 : 1 : 2 : 2: 2 : 1.5. Five kinds of herbs except *Liriope platyphylla* were roasted to develop flavors. They were dried and grounded to form a powder. The powder was kneaded in water, dried in feed form, and fed. Some SYE powder was kneaded with the same weight of HFD and dried in feed form.

2.2. Measurements of Calorie and Nutritional Component of Seyoeum. SYE was requested for analysis of nutritional components by the Korea Advanced Food Research Institute. Twelve components including calorie, carbohydrate, crude protein, crude fat, sodium, sugars, saturated fat, trans fat, cholesterol, dietary fiber, iron, and calcium were analyzed.

2.3. Animal Model and Treatment. Six-week-old male C57BL/6J mice were purchased from the Central Lab. Animal Inc. (Seoul, Korea). They were in a moisture controlled room (40–70%) with a 12-hour light-dark cycle and allowed access to water and diet ad libitum. After 1-week period of acclimation, every mouse except normal chow (NC) diet group were fed a HFD (60% energy by fat) known for causing obesity for a 9-week period. The mice were divided into four groups according to diet: NC group ($n = 6$), HFD group ($n = 6$), SYE group ($n = 5$), and HFD plus SYE group (HFD + SYE, $n = 5$). Then the mice were fed one of the HFD, SYE, or HFD plus SYE for 6 weeks. HFD plus SYE were mixed at 1 : 1 ratio. The body weight of each mouse was measured at the beginning and before the final sampling. The total amount of food consumption was recorded every day. To assess the food intake, the total consumption of food during a day was measured in every cage. Then the 1-day consumption of each mouse was calculated by dividing into the number of the mice in each cage. At week 16, the mice were sacrificed and the weights of livers and the epididymal fat pads were measured. This study was approved by the Institutional Animal Care and Use Committee of Kyung Hee University, Seoul.

2.4. Oral Glucose Tolerance Test (OGTT). At week 14, mice were fasted for 14 hours and glucose (2 g/kg body weight) dissolved in water was administered to all the mice orally. Blood samples were taken from tail vein at 0, 30, 60, and 120 minutes after glucose administration. Glucose was measured using a strip-operated blood glucose sensor (ACCU-CHEK Performa. Castle Hill, NSW, Australia). The area under the curve (AUC) of glucose in the OGTT was calculated from measurements taken before (0 minutes) and after (up to 120 minutes) glucose administration on the basis of the trapezoidal rule, which is a method used to approximate a definite integral by evaluating the integrand at two points.

2.5. Biochemical Assays. At week 14, blood was collected from the tail vein of each mouse. Plasma insulin concentration was quantified using an ultrasensitive mouse insulin ELISA kit (Crystal Chem INC., Chicago, IL, USA). Glucose and insulin levels were measured and insulin resistance was assessed by a homeostatic model assessment of insulin resistance (HOMA-IR). HOMA-IR was calculated using the following formula: HOMA-IR = Fasting blood glucose (mg/dl) × Fasting insulin (ng/ml) × 0.0717225161669606. At week 16, blood was collected from the hearts, while the mice were under anesthesia with diethyl ether. Aspartate transaminase (AST), alanine transaminase (ALT), total cholesterol, high density lipoprotein (HDL) cholesterol, and triglyceride levels were measured.

2.6. Morphological Analysis of Liver. The liver samples were immersion-fixed in 10% buffered formalin and embedded in paraffin for study by light microscopy. Two sections per animal, 5 μm thick (at an interval of 100 μm), were stained with periodic acid-Schiff (PAS) reagent. The sections were photographed under a photomicroscope (Olympus BX-50; Olympus Optical, Tokyo, Japan).

2.7. RNA Isolation and Quantitative Real-Time Polymerase Chain Reaction Analysis. At week 16, the mice were sacrificed and the epididymal fat pads were dissected. RNA extraction was performed using a Mini RNA Isolation IITM (Zymo Research, Orange, CA, USA). RNA from liver tissue was extracted using Trizol reagent. To evaluate the gene expression levels, we performed quantitative real-time polymerase chain reaction (qRT-PCR). The complementary DNA (cDNA) was synthesized using an Advantage RT for PCR Kit (Clontech, Palo Alto, CA, USA). The sequences of primes used in this study are shown in Table 1. PCR was carried out in a 7900HT Fast Real-Time PCR System (Applied Biosystems®, Foster City, CA, USA). For gene expression analysis, threshold cycle (Ct) of each gene was calculated by SDS Software 2.4 (Applied Biosystems, Foster City, CA, USA); then relative quantitation (RQ) was performed relative to glyceraldehyde-3-phosphate dehydrogenase (GAPDH, housekeeping gene). The fold change was calculated according to NC group which was considered as 1.

2.8. Statistical Analysis. Statistical analyses were performed using GraphPad PRISM 6 (Graphpad software inc., San Diego, CA, USA). Statistical comparisons between the groups were performed with one-way analysis of variance (ANOVA), followed by Tukey's post hoc test. The data are presented as mean ± SE. A two-tailed P value of <0.05 was considered statistically significant.

Table 1: Primer sequences.

Target	Primer	Sequence (5′-3′)
TNF-α	F	TTCTGTCTACTGAACTTCGGGGTGATCGGTCC
	R	GTATGAGATAGCAAATCGGCTGACGGTGTGGG
IFN-γ	F	ACTGGCAAAAGGATGGTGAC
	R	TGAGCTCATTGAATGCTTGG
IL-6	F	AACGATGATGCACTTGCAGA
	R	GAGCATTGGAAATTGGGGTA
MCP-1	F	CCCACTCACCTGCTGCTACT
	R	TCTGGACCCATTCCTTCTTG
Cxcl3	F	AGGCTACAGGGGCTGTTGT
	R	GGGTTGAGGCAAACTTCTTG
IR	F	GAGATGGTCCACCTGAAGGA
	R	GGACAGACATCCCCACATTC
IRS-1	F	AAGCACCTGGTGGCTCTCTA
	R	TCAGGATAACCTGCCAGACC
IRS-2	F	ATACCGCCTATGCCTGTCTG
	R	TGGTCTCATGGATGTTCTGC
GAPDH	F	AGTCCATGCCATCACTGCCACC
	R	CCAGTGAGCTTCCCGTTCAGC

Table 2: Calorie and composition of Seyoeum.

Nutrition facts (per 100 g)	Amount
Calorie (kcal)	398.3
Carbohydrate (g)	61.7
Crude protein (g)	19.3
Crude fat (g)	12.7
Sodium (mg)	17.34
Sugars (g)	4.6
Saturated fat (g)	2.2
Trans fat (g)	0.39
Cholesterol (mg)	1.55
Dietary fiber (g)	20.0
Iron (mg)	10.72
Calcium (mg)	480.97

3. Results

3.1. Calorie and Composition of SYE. The calorie value of SYE was 398.3 kcal/100 g. The amounts of carbohydrate, crude protein, and crude fat per 100 g of SYE were 61.7 g, 19.3 g, and 12.7 g, respectively (Table 2).

3.2. SYE Reduced Body Weight, Epididymal Fat Weight, and Liver Weight in HFD Mice. The body weight of HFD mice significantly increased to 52.48 ± 0.56 g, while that of NC mice was 31.71 ± 0.90 ($P < 0.001$). SYE significantly lowered body weight compared to HFD group, as much as 43.8% in SYE group (29.48 ± 4.95, $P < 0.001$) and 16.7% in HFD + SYE group (43.72 ± 7.59, $P < 0.01$) (Figure 1(a)). The amount of food intake (data not shown) and calorie intake were also examined to determine if the weight loss was due to a decrease in the intake. Compared with the HFD group, there were significant decreases both in food intake and calorie intake in the SYE group ($P < 0.001$) but not in the HFD + SYE group (Figure 1(b)). Weight of epididymal fat pad significantly increased by HFD compared to NC group ($P < 0.001$) and SYE significantly reduced the epididymal fat as much as 65.9% in SYE group ($P < 0.001$) and 37.0% in HFD + SYE group ($P < 0.001$) (Figure 1(c)). Weight of liver significantly increased in HFD group compared to that in NC group ($P < 0.001$). In SYE group, weight of liver was significantly lower than HFD group ($P < 0.001$), but in HFD + SYE group the liver weight was lower without significance (Figure 1(d)).

3.3. SYE Improved Hyperglycemia and Insulin Resistance in HFD Mice. In HFD group, blood glucose levels were elevated compared to NC group at 0, 30, 60, and 120 minutes ($P < 0.05$ at 30 min and $P < 0.001$ at others). SYE significantly reduced fasting blood glucose levels as much as 64.3% in SYE group ($P < 0.001$) and 51.0% in HFD + SYE group ($P < 0.01$), compared to HFD group. At the other time points, SYE made significant reduce in both groups (Figures 1(e) and 1(f)). Fasting insulin level, HOMA-IR, and AUC were significantly increased in HFD group compared to NC group ($P < 0.001$) and were reduced significantly in SYE group and HFD + SYE group compared to HFD group (Figures 1(g), 1(h), and 1(i)).

3.4. Effects of SYE on Liver Enzyme, Lipid Levels in Serum, and Lipid Accumulation in Liver. In HFD group, both AST and ALT significantly increased ($P < 0.001$) compared to NC group but, however, significantly decreased in SYE group ($P < 0.01$ for AST and $P < 0.001$ for ALT) compared to HFD group (Figures 2(a) and 2(b)). HFD significantly raised total

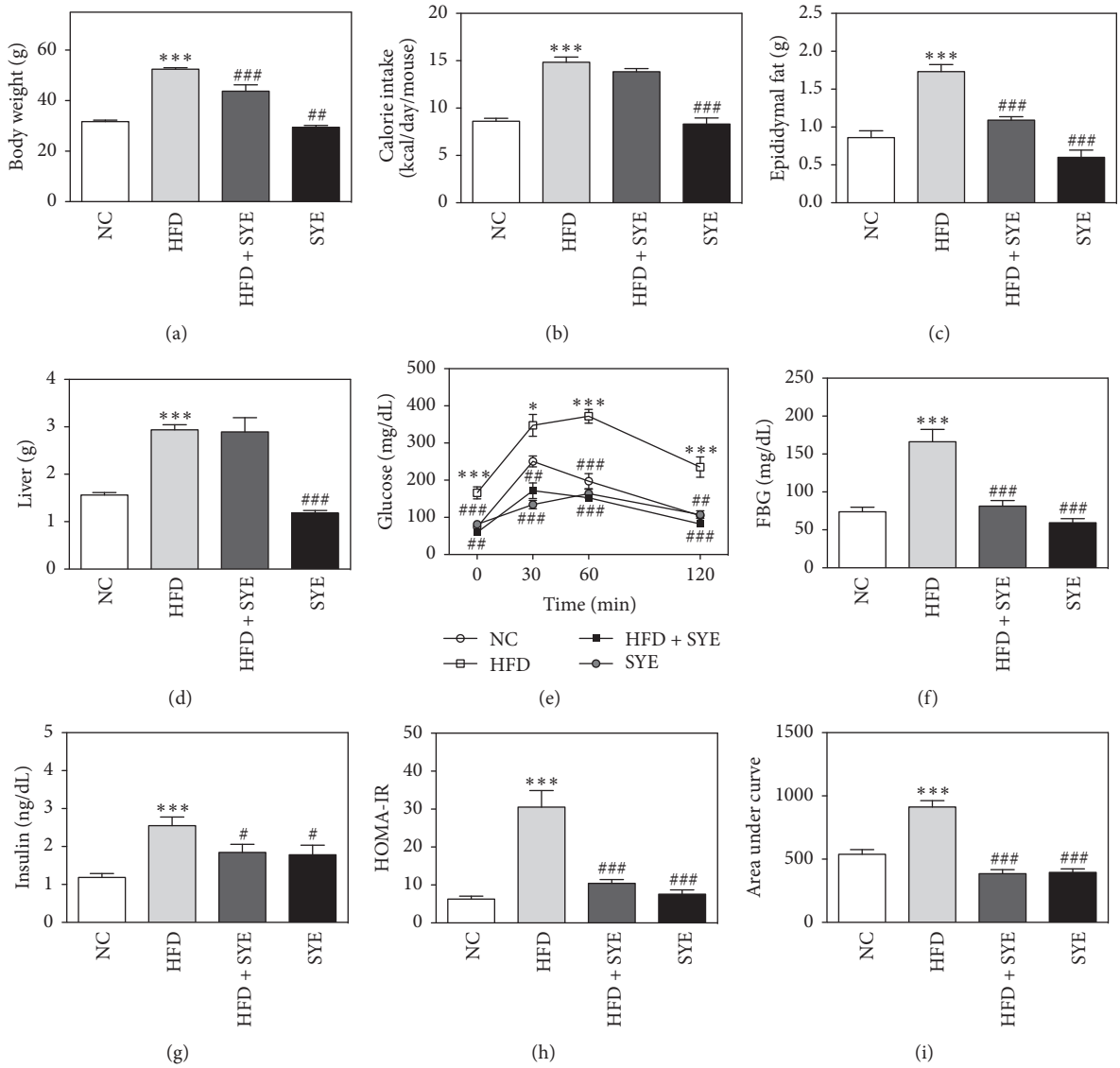

Figure 1: The changes by Seyoeum on body weight, calorie intake, epididymal fat, liver weight, calorie intake, OGTT, fasting blood glucose, insulin, HOMA-IR, and AUC. $N = 6$ in NC and HFD groups, and $N = 5$ in SYE and HFD + SYE groups. $^{***}P < 0.001$ versus NC group; $^{\#}P < 0.05$ and $^{\#\#\#}P < 0.001$ versus HFD group. ## means $P < 0.01$ versus HFD group. $*$ means $P < 0.05$ versus NC group.

cholesterol and triglyceride ($P < 0.001$ for total cholesterol and $P < 0.05$ for triglyceride) and decreased HDL cholesterol level without significance, compared to NC. SYE significantly lowered total cholesterol levels ($P < 0.001$) and lowered triglyceride level, compared to HFD. HFD + SYE mice decreased triglyceride level ($P < 0.01$), but did not show any differences among total cholesterol, HDL cholesterol (Figures 2(c), 2(d), and 2(e)). Since the liver TG level showed a tendency to be lowered by SYE treatment, histological analysis was performed by staining the liver with periodic acid-Schiff. Marked lipid accumulation was observed in hepatocytes in the HFD group, whereas there was little lipid accumulation in hepatocytes in the HFD + SYE and SYE groups (Figure 3).

3.5. SYE Suppressed the Inflammatory Gene Expression in Epididymal Adipose Tissue of HFD Mice. Because adipose tissue releases inflammatory cytokines which induce insulin resistance, we analyzed the inflammatory cytokine gene expression in epididymal fat. The genes examined were tumor necrosis factor alpha (TNF-α), interferon gamma (IFN-γ), and interleukin-6 (IL-6) for inflammatory cytokines and monocyte chemotactic protein-1 (MCP-1) and Chemokine (C-X-C motif) ligand 3 (Cxcl3) for chemokines. TNF-α and IFN-γ expressions in the HFD group significantly increased compared to NC group ($P < 0.001$). SYE significantly decreased TNF-α expression in both SYE and HFD + SYE groups ($P < 0.001$) and significantly lowered IFN-γ expression in SYE group only ($P < 0.05$). There were no significant differences in IL-6 expression between HFD and NC group, but also between HFD and SYE or HFD + SYE group (Figure 4(a)). HFD significantly increased both MCP-1 and Cxcl3 expressions compared to NC group ($P < 0.001$), and SYE significantly decreased the levels in both SYE ($P <$

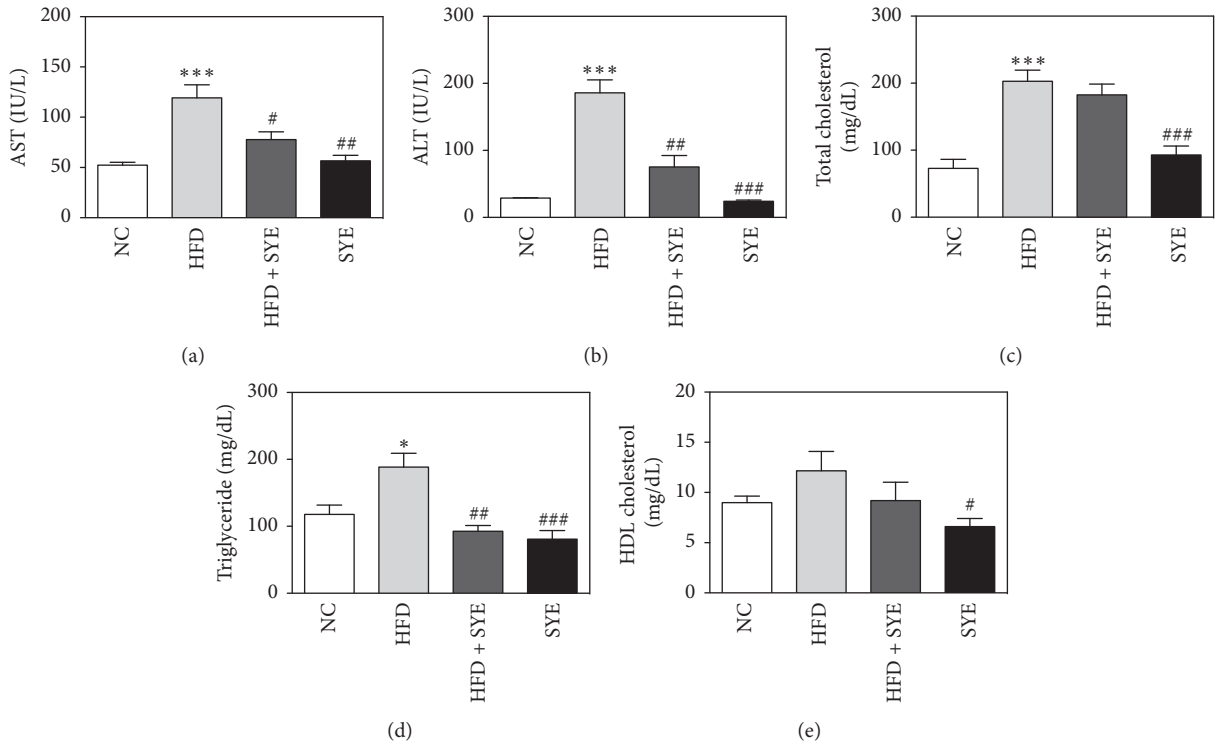

Figure 2: The changes of liver enzyme and lipid levels by Seyoeum. Blood samples were obtained at week 16. $N = 6$ in NC and HFD groups, and $N = 5$ in SYE and HFD + SYE groups. $^{*}P < 0.05$ and $^{***}P < 0.001$ versus NC group; $^{\#}P < 0.05$, $^{\#\#}P < 0.01$, and $^{\#\#\#}P < 0.001$ versus HFD group.

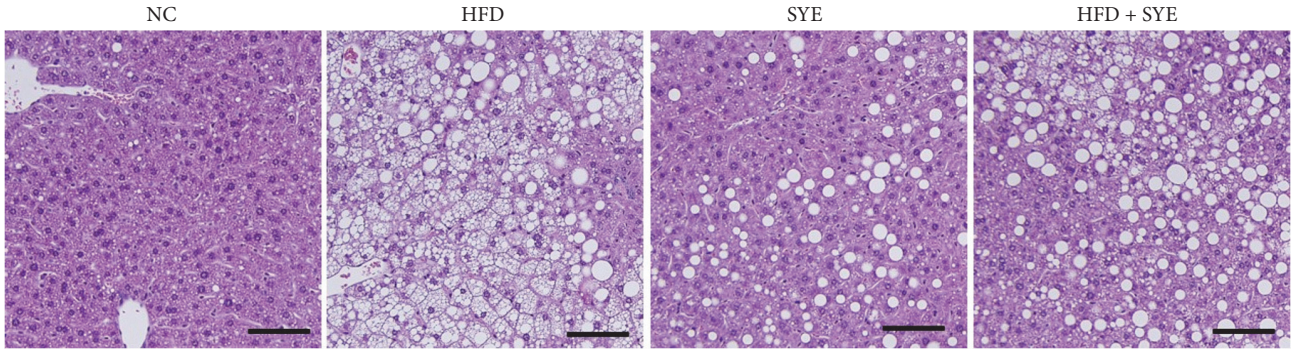

Figure 3: Effects of Seyoeum on liver in mice. Liver sections from representative mice of each group (periodic acid-Schiff, scale bar = 100 μm).

0.05) and HFD + SYE groups ($P < 0.05$ for MCP-1 and $P < 0.001$ for Cxcl3) (Figure 4(b)).

3.6. SYE Improved the Insulin Receptor Gene Expression in Liver Tissue of HFD Mice. Obesity changes the secretion of adipose tissue inflammatory cytokines, which modulate insulin signaling, so we analyzed the insulin signaling gene expression including insulin receptor (IR), insulin receptor substrate 1 (IRS-1), and IRS-2 in liver tissue. The IR and IRS-2 expression levels were significantly decreased in HFD group relative to the NC group ($P < 0.001$), and SYE significantly increase the levels compared to HFD group in both SYE ($P < 0.05$) and HFD + SYE groups ($P < 0.001$). In case of IRS-1 expression level, there were no significant differences among the groups (Figure 4(c)).

4. Discussion

In an obese state, excessive accumulation of lipids in adipose tissue activates inflammatory cytokines and chemokines secretion, which causes chronic low-level inflammation and insulin resistance. Therefore, obesity becomes a risk factor for many diseases, including metabolic syndrome, cardiovascular disease, and cancer [1, 15, 16]. If we can block the systemic inflammation and insulin resistance as well as the reduction of fat cells, it can be expected to lower the risk

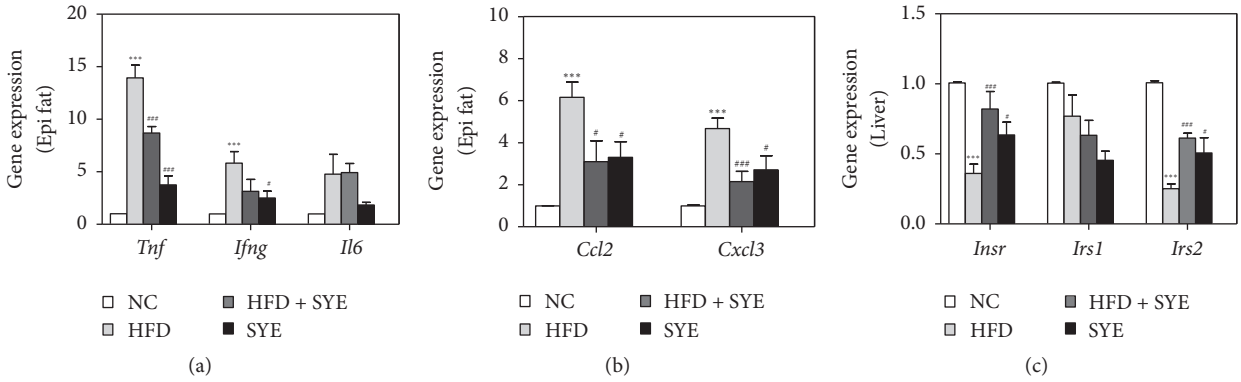

Figure 4: The changes by Seyoeum on inflammatory cytokine and chemokine gene expression in adipose tissue, and insulin receptor gene expression in liver tissue. Adipose and liver tissue was obtained at week 16 and quantitative RT-PCR was used for measuring gene expression. Gene expression was normalized to that of GAPDH. $N = 6$ in NC and HFD groups, and $N = 5$ in SYE and HFD + SYE groups. $^{*}P < 0.05$ and $^{***}P < 0.001$ versus NC group; $^{\#}P < 0.05$ and $^{\#\#\#}P < 0.001$ versus HFD group.

of complications due to obesity. In this study, we tried to evaluate the effects of a new meal replacement on obesity and metabolic syndrome in mice, using clinical markers including body weight, glucose level, insulin level, HOMA-IR, lipid level, epididymal fat pad weight, liver weight, and gene expressions related to inflammation and insulin receptor.

"Sunsik" is a substitute food in Korea that takes a variety of roasted grains, vegetables, nuts, and other foods into water or milk [17]. The authors developed a meal replacement based on the idea of Sunsik. We selected candidate herbs by screening for common kinds of whole grains used in Sunsik and herbs that have been clinically and experimentally proven to be effective against obesity, diabetes, or NAFLD. Then, some formulations with good flavor were developed to increase compliance, and blind tasting was given to 10 testers to confirm the highest preference.

For the six selected herbs, either themselves or the ingredients were reported to be effective in obesity, IR, dyslipidemia, or NAFLD. *Coix lacryma-jobi* has effects on obesity and hyperlipidemia through modulating TNF-alpha and leptin [18], and *Oryza sativa* decreases hepatic fat accumulation, hyperlipidemia [19], and hepatic steatosis [20]. Liriope platyphylla improves fat accumulation and glucose regulation [21] and stimulates insulin secretion and suppresses fatty liver formation [22]. *Dioscorea batatas* has beneficial activities against obesity through decreasing expression of inflammatory cytokines [23] and has an effect on insulin resistance [24]. Sesamol, a component of *Sesamum indicum*, has beneficial activities against hypercholesterolemia, insulin resistance, and hepatic steatosis [25]. The common name for Glycine max is soy, and soy beta- conglycinin improved metabolic abnormalities in a NAFLD rat [26] and improved hepatic insulin resistance [27]. SYE significantly decreased body weight, liver weight, and epididymal fat weight of HFD fed mice. HFD + SYE diet also reduced body weight and epididymal fat weight without significant calorie difference from HFD, so the weight loss effect might be resulted from not only reduced calorie intake but also pharmacological effect of SYE itself. High-fat diet induces weight gain of liver, through accumulation of cholesterol and triglyceride in the liver [28]. Liver fat is highly and linearly correlated with all components of the metabolic syndrome, independent of obesity [29]. Epididymal fat is equivalent to human visceral fat, and visceral fat secretes adipokines and cytokines related to fat metabolism and insulin sensitivity [15]. Visceral fat is known to be more related to metabolic syndrome than body mass index (BMI) [1].

In other similar experiments, lipid decrease was mainly observed [30, 31], but SYE showed significant changes in glucose metabolism. SYE remarkably improved all the indicators related to insulin resistance, including glucose level, serum insulin level, HOMA-IR, and AUC in both SYE and HFD + SYE groups. Through this, we have identified the potential effects of SYE on fat loss and metabolic syndrome. SYE mostly consists of whole grain and has large amounts of dietary fiber and phenolic compounds compared with refined cereal, which could be considered to protect against obesity complications such as cardiovascular disease, cancer, and diabetes [32].

The effect of SYE on the inflammatory gene expression in adipose tissue was prominent in TNF-α. TNF-α is one of the major local regulators in adipose tissue that contributes to insulin resistance and inflammation [33]. MCP-1 and Cxcl3 are chemokines that promote the adhesion of monocytes and induce low-inflammation, and SYE decreased the expression of MCP-1 and Cxcl3. Cxcl3, also known as the oncogene, interacts with the cell surface chemokine receptor MCP-1, to regulate the migration and adhesion of monocytes and regulate the effect on target cells [34, 35]. By inhibiting TNF-α, MCP-1, and Cxcl3 expression in adipocytes, SYE seems to inhibit local inflammatory responses.

IL-6 is a classical inflammatory cytokine considered to be a risk factor for the onset of diabetes [36]. Both TNF-α and IL-6 are involved in classical receptor mediated processes, including c-Jun aminoterminal kinase (JNK) and IκB kinase-β (IKK-β)/nuclear factor-κB (NF-κB), which upregulate inflammatory mediators [37]. SYE significantly inhibited the expression of TNF-α but not IL-6. TNF-α is mainly

produced by activated macrophages [38], whereas IL-6 can be produced in a number of immune cells including activated macrophages and lymphocytes [39]. This suggests that SYE is more effective in inhibiting macrophages than other immune cells. IFN-γ activates immune cells, including macrophages, secreted only by T cells and NK cells. The hypothesis that SYE specifically inhibits the action of macrophages could also explain the low effect of SYE on IFN-γ in the HFD + SYE group [34, 35]. From these results, we supposed that SYE inhibits immune cell adhesion and reduces insulin resistance and inflammation; activated macrophage especially was likely to be suppressed.

Inhibition of the insulin receptor signaling pathway by inflammation or stress is a key mechanism of insulin resistance. Defects in insulin receptor signaling pathway are observed in most of the systemic insulin resistance [40]. To evaluate insulin signaling, gene expression of IR, IRS-1, and IRS-2 in the liver was analyzed. IR and IRS-2 expressions were increased in the SYE and HFD + SYE groups compared to HFD group. The expression of IRS-1 in the liver appears to be relatively unaffected by obesity. The anti-inflammatory effect of SYE appears to improve the insulin signaling pathway in the liver.

5. Conclusions

Based on these results, we conclude that SYE improved obesity, insulin resistance, and NAFLD in high-fat diet-fed obese mice. Our findings suggest that these antiobesity, anti-insulin resistance effects of SYE could be mediated by the suppression of adipose tissue inflammatory cytokines and enhancing the insulin signaling pathway. Further studies related to other mechanisms on inflammatory response in adipose tissue, obesity, and insulin resistance should be taken for the clinical application of SYE.

Disclosure

The authors are responsible for the writing and contents of the paper.

Conflicts of Interest

The authors have no conflicts of interest.

Acknowledgments

This study was supported by the Traditional Korean Medicine Research and Development program funded by the Ministry of Health and Welfare through the Korea Health Industry Development Institute (Grant no. HI13C0700).

References

[1] S. E. Shoelson, L. Herrero, and A. Naaz, "Obesity, inflammation, and insulin resistance," *Gastroenterology*, vol. 132, no. 6, pp. 2169–2180, 2007.

[2] G. Marchesini, R. Marzocchi, F. Agostini, and E. Bugianesi, "Nonalcoholic fatty liver disease and the metabolic syndrome," *Current Opinion in Lipidology*, vol. 16, no. 4, pp. 421–427, 2005.

[3] I. Shimomura, Y. Bashmakov, S. Ikemoto, J. D. Horton, M. S. Brown, and J. L. Goldstein, "Insulin selectively increases SREBP-1C mRNA in the livers of rats with streptozotocin-induced diabetes," *Proceedings of the National Academy of Sciences of the United States of America*, vol. 96, no. 24, pp. 13656–13661, 1999.

[4] T. Ide, H. Shimano, N. Yahagi et al., "SREBPs suppress IRS-2-mediated insulin signalling in the liver," *Nature Cell Biology*, vol. 6, no. 4, pp. 351–357, 2004.

[5] V. T. Samuel, Z.-X. Liu, X. Qu et al., "Mechanism of hepatic insulin resistance in non-alcoholic fatty liver disease," *The Journal of Biological Chemistry*, vol. 279, no. 31, pp. 32345–32353, 2004.

[6] R. G. Reichert, R. A. Reimer, V. Kacinik, S. Pal, R. J. Gahler, and S. Wood, "Meal replacements and fibre supplement as a strategy for weight loss. Proprietary PGX® meal replacement and PGX® fibre supplement in addition to a calorie-restricted diet to achieve weight loss in a clinical setting," *Biotechnology and Genetic Engineering Reviews*, vol. 29, no. 2, pp. 221–229, 2013.

[7] W. A. Nuffer and J. M. Trujillo, "Liraglutide: A New Option for the Treatment of Obesity," *Pharmacotherapy*, vol. 35, no. 10, pp. 926–934, 2015.

[8] R. I. Berkowitz, T. A. Wadden, C. A. Gehrman et al., "Meal replacements in the treatment of adolescent obesity: A randomized controlled trial," *Obesity*, vol. 19, no. 6, pp. 1193–1199, 2011.

[9] J. M. Ashley, S. T. St. Jeor, J. P. Schrage et al., "Weight control in the physician's office," *Archives of Internal Medicine*, vol. 161, no. 13, pp. 1599–1604, 2001.

[10] M. Flechtner-Mors, H. H. Ditschuneit, T. D. Johnson, M. A. Suchard, and G. Adler, "Metabolic and weight loss effects of long-term dietary intervention in obese patients: Four-year results," *Obesity Research*, vol. 8, no. 5, pp. 399–402, 2000.

[11] D. Quinn Rothacker, "Five-year self-management of weight using meal replacements: Comparison with matched controls in rural Wisconsin," *Nutrition*, vol. 16, no. 5, pp. 344–348, 2000.

[12] H. H. Ditschuneit, M. Flechtner-Mors, T. D. Johnson, and G. Adler, "Metabolic and weight-loss effects of a long-term dietary intervention in obese patients," *American Journal of Clinical Nutrition*, vol. 69, no. 2, pp. 198–204, 1999.

[13] D. Heber, J. M. Ashley, H.-J. Wang, and R. M. Elashoff, "Clinical evaluation of a minimal intervention meal replacement regimen for weight reduction," *Journal of the American College of Nutrition*, vol. 13, no. 6, pp. 608–614, 1994.

[14] S. B. Heymsfield, C. A. J. Van Mierlo, H. C. M. Van Der Knaap, M. Heo, and H. I. Frier, "Weight management using a meal replacement strategy: Meta and pooling analysis from six studies," *International Journal of Obesity*, vol. 27, no. 5, pp. 537–549, 2003.

[15] P. E. Scherer, "Adipose tissue: from lipid storage compartment to endocrine organ," *Diabetes*, vol. 55, no. 6, pp. 1537–1545, 2006.

[16] S. K. Fried, D. A. Bunkin, and A. S. Greenberg, "Omental and subcutaneous adipose tissues of obese subjects release interleukin-6: depot difference and regulation by glucocorticoid," *Journal of Clinical Endocrinology and Metabolism*, vol. 83, no. 3, pp. 847–850, 1998.

[17] S.-S. Chung and Y.-S. Han, "Consumer's recognition, nutrient composition, and safety evaluation of commercial Sunsik and Saengsik," *Journal of The Korean Society of Dietary Culture*, vol. 18, no. 3, pp. 235–243.

[18] S. O. Kim, S.-J. Yun, B. Jung et al., "Hypolipidemic effects of crude extract of adlay seed (Coix lachrymajobi var. mayuen) in obesity rat fed high fat diet:Relations of TNF-α and leptin

mRNA expressions and serum lipid levels," *Life Sciences*, vol. 75, no. 11, pp. 1391–1404, 2004.

[19] W. H. Choi, M. Y. Um, J. Ahn, C. H. Jung, and T. Y. Ha, "Cooked rice inhibits hepatic fat accumulation by regulating lipid metabolism-related gene expression in mice fed a high-fat diet," *Journal of Medicinal Food*, vol. 17, no. 1, pp. 36–42, 2014.

[20] H.-H. Jang, M.-Y. Park, H.-W. Kim et al., "Black rice (Oryza sativa L.) extract attenuates hepatic steatosis in C57BL/6 J mice fed a high-fat diet via fatty acid oxidation," *Nutrition and Metabolism*, vol. 9, article no. 27, 2012.

[21] J. Kim, I. Hwang, S. Choi et al., " Aqueous extract of ," *Laboratory Animal Research*, vol. 28, no. 3, p. 181, 2012.

[22] H. R. Lee, J. E. Kim, J. S. Goo et al., "Red Liriope platyphylla contains a large amount of polyphenolic compounds which stimulate insulin secretion and suppress fatty liver formation through the regulation of fatty acid oxidation in OLETF rats," *International Journal of Molecular Medicine*, vol. 30, no. 4, pp. 905–913, 2012.

[23] H.-W. Gil, E.-Y. Lee, J.-H. Lee et al., "Dioscorea batatas extract attenuates high-fat diet-induced obesity in mice by decreasing expression of inflammatory cytokines," *Medical Science Monitor*, vol. 21, pp. 489–495, 2015.

[24] S. Kim, H. Jwa, Y. Yanagawa, and T. Park, "Extract from Dioscorea batatas ameliorates insulin resistance in mice fed a high-fat diet," *Journal of Medicinal Food*, vol. 15, no. 6, pp. 527–534, 2012.

[25] A. K. Sharma, S. Bharti, J. Bhatia et al., "Sesamol alleviates diet-induced cardiometabolic syndrome in rats via up-regulating PPARγ, PPARα and e-NOS," *Journal of Nutritional Biochemistry*, vol. 23, no. 11, pp. 1482–1489, 2012.

[26] S. Wanezaki, N. Tachibana, M. Nagata et al., "Soy β-conglycinin improves obesity-induced metabolic abnormalities in a rat model of nonalcoholic fatty liver disease," *Obesity Research and Clinical Practice*, vol. 9, no. 2, pp. 168–174, 2015.

[27] N. Tachibana, Y. Yamashita, M. Nagata et al., "Soy β-conglycinin improves glucose uptake in skeletal muscle and ameliorates hepatic insulin resistance in Goto-Kakizaki rats," *Nutrition Research*, vol. 34, no. 2, pp. 160–167, 2014.

[28] A. P. Jayasooriya, M. Sakono, C. Yukizaki, M. Kawano, K. Yamamoto, and N. Fukuda, "Effects of *Momordica charantia* powder on serum glucose levels and various lipid parameters in rats fed with cholesterol-free and cholesterol-enriched diets," *Journal of Ethnopharmacology*, vol. 72, no. 1-2, pp. 331–336, 2000.

[29] A. Kotronen and H. Yki-Järvinen, "Fatty liver: a novel component of the metabolic syndrome," *Arteriosclerosis, Thrombosis, and Vascular Biology*, vol. 28, no. 1, pp. 27–38, 2008.

[30] S.-S. Kim, K.-S. Seong, O.-H. Lee et al., "Effects of phytoplant diets on body weight, feces production, body fat, and serum lipid levels in high-fat diet-induced hyperlipidemic rats," *Korean Journal of Food Science and Technology*, vol. 46, no. 4, pp. 477–482, 2014.

[31] I. Shin, H. Choi, S. Ku, and M. Kim, "The Effect of Natural Mixture Supplementation on Histopathological and Histomorphometrical aspects in High Fat Diet-induced Obese Mice," *The Korea Journal of Herbology*, vol. 27, no. 4, pp. 53–58, 2012.

[32] J. Y. Kim, J. H. Shin, and S. S. Lee, "Cardioprotective effects of diet with different grains on lipid profiles and antioxidative system in obesity-induced rats," *International Journal for Vitamin and Nutrition Research*, vol. 82, no. 2, pp. 85–93, 2012.

[33] P. Trayhurn and I. S. Wood, "Adipokines: inflammation and the pleiotropic role of white adipose tissue," *British Journal of Nutrition*, vol. 92, no. 3, pp. 347–355, 2004.

[34] D. F. Smith, E. Galkina, K. Ley, and Y. Huo, "GRO family chemokines are specialized for monocyte arrest from flow," *American Journal of Physiology - Heart and Circulatory Physiology*, vol. 289, no. 5, pp. H1976–H1984, 2005.

[35] S. K. Ahtga and P. M. Murphy, "The CXC chemokines growth-regulated oncogene (GRO) α, GROβ, GROγ, neutrophil-activating peptide-2, and epithelial cell-derived neutrophil-activating peptide-78 are potent agonists for the type B, but Not the type A, human interleukin-8 receptor," *Journal of Biological Chemistry*, vol. 271, no. 34, pp. 20545–20550, 1996.

[36] B.-C. Lee and J. Lee, "Cellular and molecular players in adipose tissue inflammation in the development of obesity-induced insulin resistance," *Biochimica et Biophysica Acta—Molecular Basis of Disease*, vol. 1842, no. 3, pp. 446–462, 2014.

[37] S. E. Kahn, R. L. Hull, and K. M. Utzschneider, "Mechanisms linking obesity to insulin resistance and type 2 diabetes," *Nature*, vol. 444, no. 7121, pp. 840–846, 2006.

[38] N. Parameswaran and S. Patial, "Tumor necrosis factor-a signaling in macrophages," *Critical Reviews in Eukaryotic Gene Expression*, vol. 20, no. 2, pp. 87–103, 2010.

[39] J. S. Yudkin, M. Kumari, S. E. Humphries, and V. Mohamed-Ali, "Inflammation, obesity, stress and coronary heart disease: is interleukin-6 the link?" *Atherosclerosis*, vol. 148, no. 2, pp. 209–214, 2000.

[40] K. E. Wellen and G. S. Hotamisligil, "Inflammation, stress, and diabetes," *Journal of Clinical Investigation*, vol. 115, no. 5, pp. 1111–1119, 2005.

Hindawi
Evidence-Based Complementary and Alternative Medicine
Volume 2017, Article ID 6178358, 11 pages
https://doi.org/10.1155/2017/6178358

Research Article

Yinchen Linggui Zhugan Decoction Ameliorates Nonalcoholic Fatty Liver Disease in Rats by Regulating the Nrf2/ARE Signaling Pathway

Yi Guo,[1,2] Jun-xiang Li,[2] Yun-liang Wang,[2] Tang-you Mao,[1,2] Chen Chen,[1,2] Tian-hong Xie,[1,2] Ya-fei Han,[1,2] Xiang Tan,[1,2] and Hai-xiao Han[2]

[1]*Beijing University of Chinese Medicine, No. 11, North Third Ring East Road, Beijing 100029, China*
[2]*Gastroenterology Department, Dongfang Hospital, Beijing University of Chinese Medicine, No. 6, 1st Section, Fangxingyuan, Fangzhuang, Beijing 100078, China*

Correspondence should be addressed to Hai-xiao Han; hujiaofen@163.com

Received 17 May 2017; Revised 11 July 2017; Accepted 30 July 2017; Published 28 August 2017

Academic Editor: Jing-Hua Wang

Yinchen Linggui Zhugan Decoction (YCLGZGD) is the combination of Linggui Zhugan (LGZGD) and Yinchenhao (YCHD) decoctions, two famous traditional Chinese medicine prescriptions. In previous studies, we found that Yinchen Linggui Zhugan Decoction (YCLGZGD) could regulate lipid metabolism disorder and attenuate inflammation in pathological process of nonalcoholic fatty liver disease (NAFLD). However, the exact underlying mechanism remains unknown. The aim of this study was to explore the effect of Yinchen Linggui Zhugan Decoction on experimental NAFLD and its mechanism in rats with high-fat diet (HFD) which was established by 8-week administration of HFD. YCLGZGD, LGZGD, and YCHD were administered daily for 4 weeks, after which the rats were euthanized. The level of blood lipid, liver enzymes, H&E, and Oil Red O staining were determined to evaluate NAFLD severity. Western blotting and real-time polymerase chain reaction were, respectively, used to determine hepatic protein and gene expression of Keap1, Nrf2, NQO1, and HO-1. Oral YCLGZGD ameliorated HFD-induced NAFLD. Furthermore, YCLGZGD increased the protein and gene expression of Nrf2, NQO1, and HO-1 without changing Keap1. Overall, these results suggest that YCLGZGD ameliorates HFD-induced NAFLD in rats by upregulating the Nrf2/ARE signaling pathway.

1. Introduction

Nonalcoholic fatty liver disease (NAFLD) is a type of liver disease that includes simple hepatic steatosis, nonalcoholic steatohepatitis (NASH), and irreversible cirrhosis [1]. The prevalence of NAFLD has rapidly increased in parallel to dramatic rise in obesity, diabetes [2, 3], hypertension [4, 5], and dyslipidemia [6]. Currently, NAFLD is regarded as the liver manifestation of metabolic syndrome. The pathogenesis of NAFLD is not fully understood thus far and the reported therapeutic trails are still under investigation [7, 8]. Some researchers agree with the "2-hit" hypothesis for the NAFLD pathogenesis. Briefly, the "first hit" involves hepatic triglyceride accumulation or steatosis. The "second hit" represents the relationship between inflammatory cytokines and oxidative stress. The Nrf2/antioxidant response element (ARE) signaling pathway plays an important role in oxidative stress and can induce the expression of antioxidative genes to protect hepatocytes from apoptosis.

NAFLD management strategies often include lifestyle modifications and pharmaceutical interventions [9–12]. However, compliance with the long-term lifestyle modification is poor and most medicines have adverse effects, which limit their usage [13]. Thus, it is necessary to develop novel strategies with fewer side effects and high therapeutic efficiency.

Chinese herbal medicine (CHM) has been traditionally used in China and other Asian countries for thousands of years and its use is now spreading worldwide. A unique and basic feature of CHM is the use of a formula containing

several herbs (mixed as a cocktail) to ameliorate various abnormalities related to a certain disease. Herbal extracts contain multiple natural compounds that can target various pathological pathways underlying a disease, providing therapeutic effects via a range of mechanisms. Linggui Zhugan (LGZGD) and Yinchenhao (YCHD) decoctions are two well-known traditional CHM, from Treatise on Febrile Diseases, and consist of Fuling *(Poria cocos)*, Guizhi *(cassia twig)*, Baizhu *(Atractylodes macrocephala* Koidz*)*, Gancao *(licorice)*, Yinchen *(herba artemisiae scopariae)*, Zhizi *(Gardenia)*, and Dahuang *(rhubarb)*. They are widely used to treat obesity and diabetes. As for chemical composition of YCHD and LGZGD, some previous researches were conducted to discuss effective components partly in two formulas by HPLC fingerprints. Catechins, anthraquinones, iridoids, crocetin, and chlorogenic acid can be responsible for curative effect of YCHD mainly [14], and LGZGD had therapeutic effect because of almost twenty compounds such as cinnamic acid, glycyrrhizic acid, and dehydrotumulosic acid [15].

Owing to synergistic effect, their combination is also used to treat NASH in clinics. In previous studies, we found that Yinchen Linggui Zhugan Decoction (YCLGZGD) has an anti-inflammatory effect [16, 17], which could regulate lipid metabolism disorder and attenuate inflammation in pathological process of NAFLD. Therefore, it is necessary to explore the difference in therapeutic effect of combination of compounds/herbs versus that of a single herb/compound and its possible mechanism.

2. Materials and Methods

2.1. Preparation of LGZGD, YCHD, YCLGZGD, and Sulforaphane (SFN). LGZGD, YCHD, and YCLGZGD granules were provided by Pharmacy Department of Dongfang Hospital, Beijing University of Chinese Medicine (Beijing, China). All granules contain equal amounts of ingredients of the LGZGD decoction (Fuling 12 g, Guizhi 9 g, Baizhu 6 g, and Gancao 6 g) and YCHD decoction (Yinchen 18 g, Zhizi 9 g, and Dahuang 6 g). Yinchen Linggui Zhugan Decoction is a combination of these two decoctions. SFN was purchased from LKT Laboratories (St. Paul, Minnesota, USA).

2.2. Animals and Treatment. Male Sprague-Dawley (SD) rats (7-week-old) were supplied by SPF Biotechnology Co. Ltd. (Beijing, China). All experimental procedures were approved by the Animal Ethics Committee of Beijing University of Chinese Medicine (number 2015BZHYLL0201) and followed the Regulations for Laboratory Animal Management. SD rats were maintained on a 12 h light/dark cycle at 22 ± 2°C with ad libitum access to a standard chow diet ($n = 10$) or high-fat diet (HFD, 34% fat, 19% protein, and 47% carbohydrate by energy composition) ($n = 10$) for 8 weeks to induce NAFLD. The granules and SFN were dissolved in 100 mL of distilled water and kept at 2–8°C until used. The rats received LGZGD, YCHD, and YCLGZGD (3.465 g/kg/day, 3.465 g/kg/day, and 6.93 g/kg/day, p.o., $n = 10$, resp.), and SFN (0.5 mg/kg/day, p.o., $n = 10$) after 8 weeks of HFD feeding. The rats in control group (fed chow; $n = 10$) received saline (10 mL/kg/day, p.o., $n = 10$). All groups were administered the drugs or saline for 4 weeks.

2.3. Determination of Metabolic Parameters: Liver Enzymes and Blood Lipid Levels in Rats. At the end of treatment, animals were anesthetized using 4% chloral hydrate after 12 h overnight fasting and blood samples were collected from the abdominal aorta. Fasting serum triglycerides (TGs), high-density lipoprotein cholesterol (HDL-C), and low-density lipoprotein cholesterol (LDL-C) were analyzed using enzyme-linked immunosorbent assay (ELISA) (Bio Sino, Beijing, China). Fasting serum alanine aminotransferase (ALT) and aspartate aminotransferase (AST) were also determined by ELISA, as previously described [18].

2.4. Histological Analyses. A fresh liver tissue sample was fixed with 10% formaldehyde solution. Paraffin-embedded sections were used for hematoxylin and eosin (H&E) staining (Ze-ping, Beijing, China). Frozen sections were stained with Oil Red O (ORO; Sigma Aldrich, St. Louis, Missouri, USA). Both staining methods were used to investigate architecture of the liver and hepatic lipid droplets. H&E and ORO-stained slides were visualized under a microscope (BX40, Olympus, Beijing, China), and images were captured with the attached digital camera using NIS Element SF 4.00.06 software (Beijing, China). For each group, liver samples from 3 to 5 rats were prepared and stained.

2.5. Western Blotting. To detect Keap1, Nrf2, NADPH quinone-oxidoreductase-1 (NQO1), and heme-oxygenase (HO-1) proteins, the liver tissue homogenates were extracted using ice-cold tissue lysis buffer. Protein concentration was determined using a BCA protein assay kit. Samples were separated by 10% SDS-PAGE and transferred onto polyvinylidene difluoride membranes. The membranes were immunoblotted with primary antibodies for *Keap1* (1 : 1000), *Nrf2* (1 : 1000), *NQO1* (1 : 1000), *HO-1* (1 : 1000) (Abcam, USA), and *β-actin* (ZSGB-BIO, Beijing, China). Peroxidase-conjugated secondary antibodies and an ECL detection system were used according to routinely used methods as previously described [19]. The intensities of the protein bands were analyzed using Gel-Pro 3.2 software. β-Actin protein was used as the internal control to normalize the protein loading.

2.6. Real-Time Polymerase Chain Reaction for Keap1, Nrf2, NQO1, and HO-1 mRNA Expression. As previously described [20], reverse transcription was performed with 1 μg of total RNA per 12 μl reaction using a standard cDNA synthesis kit (Takara, Japan). The real-time PCR primer sequences for target genes were as follows: Keap1, forward 5′-TAACCGGCTTAACTCGGCAG-3′ and reverse 5′-GGAGGCTACGAAAGTCCAGG-3′; Nrf2, forward 5′-AGCAGGCTGAGACTACCACT-3′ and reverse 5′-TCCAGTGAGGGGATCGATGA-3′; NQO1, forward 5′-GATTGTATTGGCCCACGCAG-3′ and reverse 5′-GATTCGACCACCTCCCATCC-3′; HO, forward 5′-GGGTCCTCACACTCAGTTTC-3′ and reverse 5′-CCAGGCATCTCCTTCCATTC-3′; β-actin,

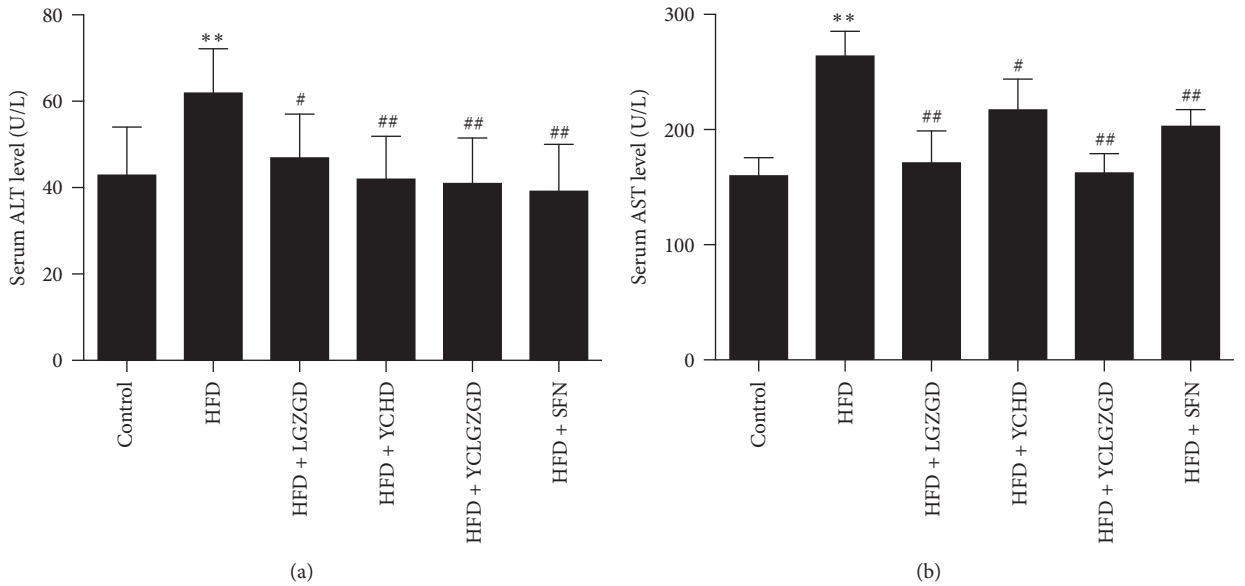

Figure 1: Effect of LGZGD, YCHD, and YCLGZGD on serum ALT and AST levels. (a) ALT levels in serum; (b) AST levels in serum. Data are means ± SD; $n = 10$/group; $^{**}P < 0.01$ versus control; $^{\#}P < 0.05$ and $^{\#\#}P < 0.01$ versus HFD.

forward 5′-CCCATCTATGAGGGTTACG-3′ and reverse 5′-TTTAATGTCACGCACGATTTC-3′ (CW-bio, Beijing, China). The PCR conditions were as follows: an initial activation step at 95°C for 5 min, 45 cycles of amplification, and a final melting curve (55–95°C). For comparison, the cDNA concentrations were normalized to β-actin PCR products. The data were analyzed by using the $2^{-\Delta\Delta Ct}$ method.

2.7. Data Analysis. All data are expressed as the mean ± SD, unless otherwise indicated. SPSS v20.0 (IBM Corp, Armonk, NY, USA) was used for statistical analyses. Data were analyzed by one-way ANOVA, followed by Student's t-tests. Differences were considered to be statistically significant at $P < 0.05$.

3. Results

3.1. Effect of LGZGD, YCHD, and YCLGZGD on Lipid Metabolism and Liver Enzymes in HFD-Fed Rats. All animals tolerated the experimental procedures well, and no deaths occurred during the study. Serum ALT (62.50 ± 9.66 U/L) and AST (266.00 ± 19.30 U/L) concentrations in HFD-fed rats were significantly higher than those in chow-fed rats [ALT (43.50 ± 10.50 U/L) and AST (162.14 ± 13.50 U/L); $P < 0.01$]. Treatment with LGZGD [ALT (47.52 ± 11.10 U/L), AST (173.33 ± 25.60 U/L)], YCHD [ALT (42.55 ± 9.35 U/L), AST (219.40 ± 24.56 U/L)], YCLGZGD [ALT (41.55 ± 9.96 U/L), AST (164.56 ± 14.60 U/L)], SFN [ALT (39.77 ± 10.24 U/L), and AST (205.00 ± 12.36 U/L)] significantly attenuated the elevated ALT and AST levels ($P < 0.05$, $P < 0.01$, Figure 1).

TG levels decreased in YCHD [0.67 ± 0.10 mmol/L] and YCLGZGD [0.54 ± 0.09 mmol/L] group compared to that in the HFD model group [0.85 ± 0.08 mmol/L, $P < 0.01$]. LGZGD also decreased TG concentration, but statistical significance was not achieved ($P > 0.05$). Furthermore, LGZGD [0.68 ± 0.19 mmol/L], YCLGZGD [0.61 ± 0.14 mmol/L], and SFN [0.50 ± 0.13 mmol/L, $P < 0.01$] decreased TC concentrations compared to that in the HFD model group [0.86 ± 0.18 mmol/L, $P < 0.01$]. However, YCHD did not decrease TC significantly ($P > 0.05$). LGZGD [0.35 ± 0.10 mmol/L], YCHD [0.30 ± 0.07 mmol/L], YCLGZGD [0.26 ± 0.06 mmol/L], and SFN [0.23 ± 0.05 mmol/L] treatments significantly attenuated the elevated LDL level [0.47 ± 0.09 mmol/L in HFD, $P < 0.05$, $P < 0.01$]. HDL-C levels increased in YCHD [0.57 ± 0.12 mmol/L], YCLGZGD [0.59 ± 0.13 mmol/L], and SFN [0.69 ± 0.12 mmol/L] groups compared to that in the HFD model group [0.32 ± 0.08 mmol/L, $P < 0.01$] (Figure 2). However, the effects of LGZGD were not significantly different compared to the HFD group ($P > 0.05$, Figure 2).

3.2. LGZGD, YCHD, and YCLGZGD Treatment Alleviated Hepatic Morphological Changes. Photomicrographs of the H&E-stained tissue sections showed that the majority of the hepatocytes of HFD-fed rats were distended owing to the presence of fat compared to that reported for the control group (Figures 3(a) and 3(b)), indicating that HFD feeding increased hepatic fat deposits. The H&E-stained sections also displayed steatosis, ballooning degeneration, and infiltration of inflammatory cells in the intercellular substance, which could have caused conspicuous swelling of cells and cytoplasmic vacuolation (Figure 3(b)). Treatment of HFD-fed rats with LGZGD, YCHD, YCLGZGD, and SFN reduced fat deposits in the liver (Figures 3(c), 3(d), 3(e), and 3(f)). Groups treated with LGZGD, YCHD, and YCLGZGD showed lower fat deposits than the HFD group did as shown in Figures 3(c), 3(d), and 3(e).

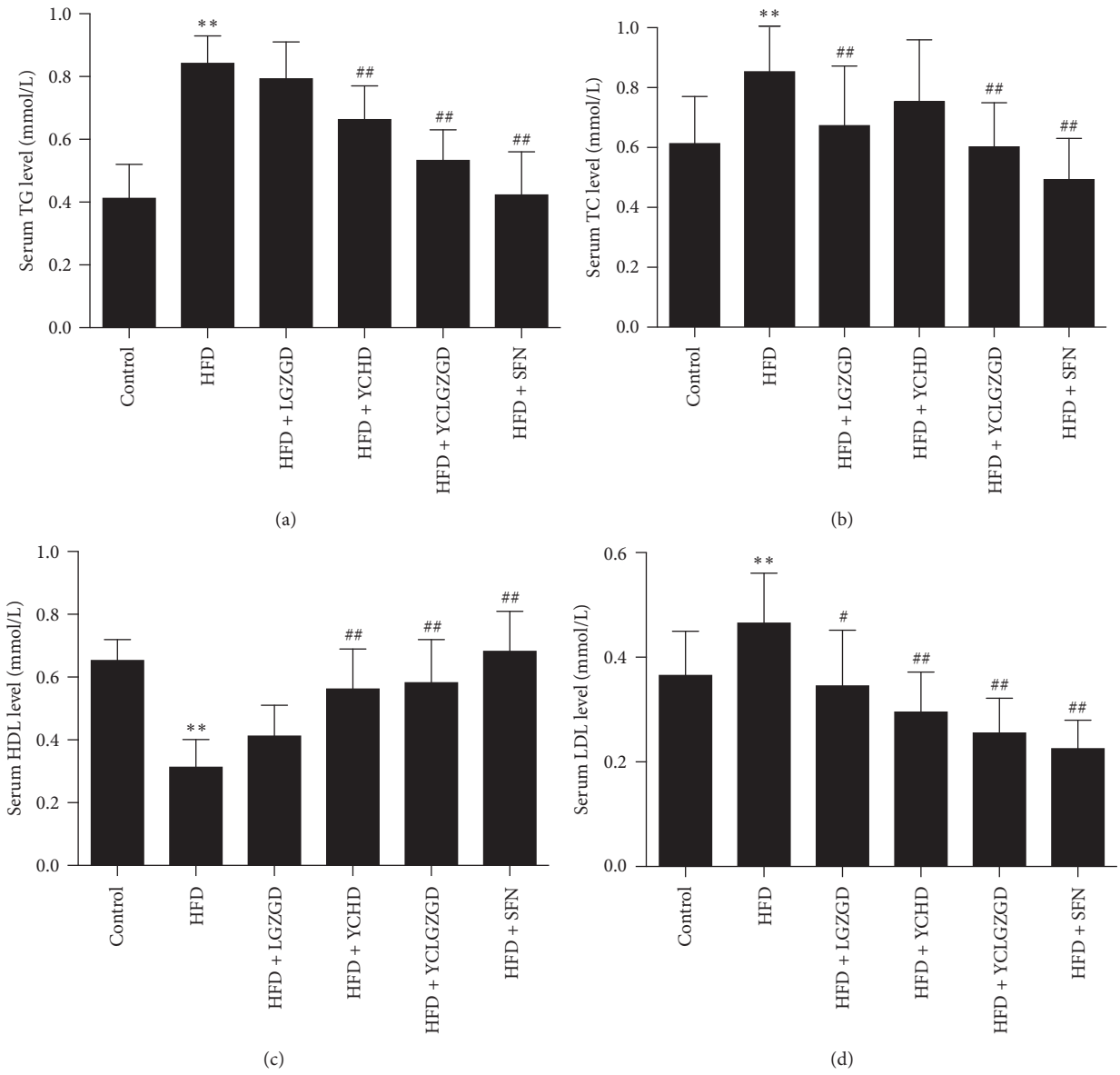

Figure 2: Effect of LGZGD, YCHD, and YCLGZGD on serum levels of TG, TC, HDL, and LDL. Serum levels of (a) TG; (b) TC; (c) HDL; (d) LDL are shown. Data are means ± SD $n = 10$ rats/group; $^{**}P < 0.01$ versus control; $^{\#}P < 0.05$ and $^{\#\#}P < 0.01$ versus HFD.

Only few lipid droplets were detected in the ORO-stained frozen liver sections from the control group (Figure 4(a)). Compared to the HFD-fed model rats (Figure 4(b)), treatment with LGZGD, YCHD, YCLGZGD, and SFN remarkably reduced lipid droplets deposited in the hepatocytes (Figures 4(c), 4(d), 4(e), and 4(f)).

3.3. LGZGD, YCHD, and YCLGZGD Regulated Hepatic Keap1 Protein and Keap1 mRNA Expression in HFD-Fed Rats. The HFD group showed a lower Keap1 expression than the control group did ($P < 0.05$). Similarly, LGZGD, YCHD, YCLGZGD, and SFN treatment groups had a lower Keap1 expression than the control group did ($P < 0.05$). However, there was no significant difference in Keap1 expression between all other groups and HFD group ($P > 0.05$, Figure 5). The expression of Keap1 gene was similar among all six groups.

3.4. LGZGD, YCHD, and YCLGZGD Increased Hepatic Nrf2 Protein and Nrf2 mRNA Expression in HFD-Fed Rats. We investigated whether LGZGD, YCHD, and YCLGZGD had a regulatory effect on Nrf2 expression in the liver. Nrf2 levels in the liver significantly increased in the HFD group ($P < 0.05$) compared to that in the control group. LGZGD, YCLGZGD, and SFN treatment showed a sharp increase in Nrf2 expression ($P < 0.01$) compared to that reported for the HFD group.

Next, Nrf2 gene expression was measured to confirm the effects of YCLGZGD on the liver. As shown in Figure 6,

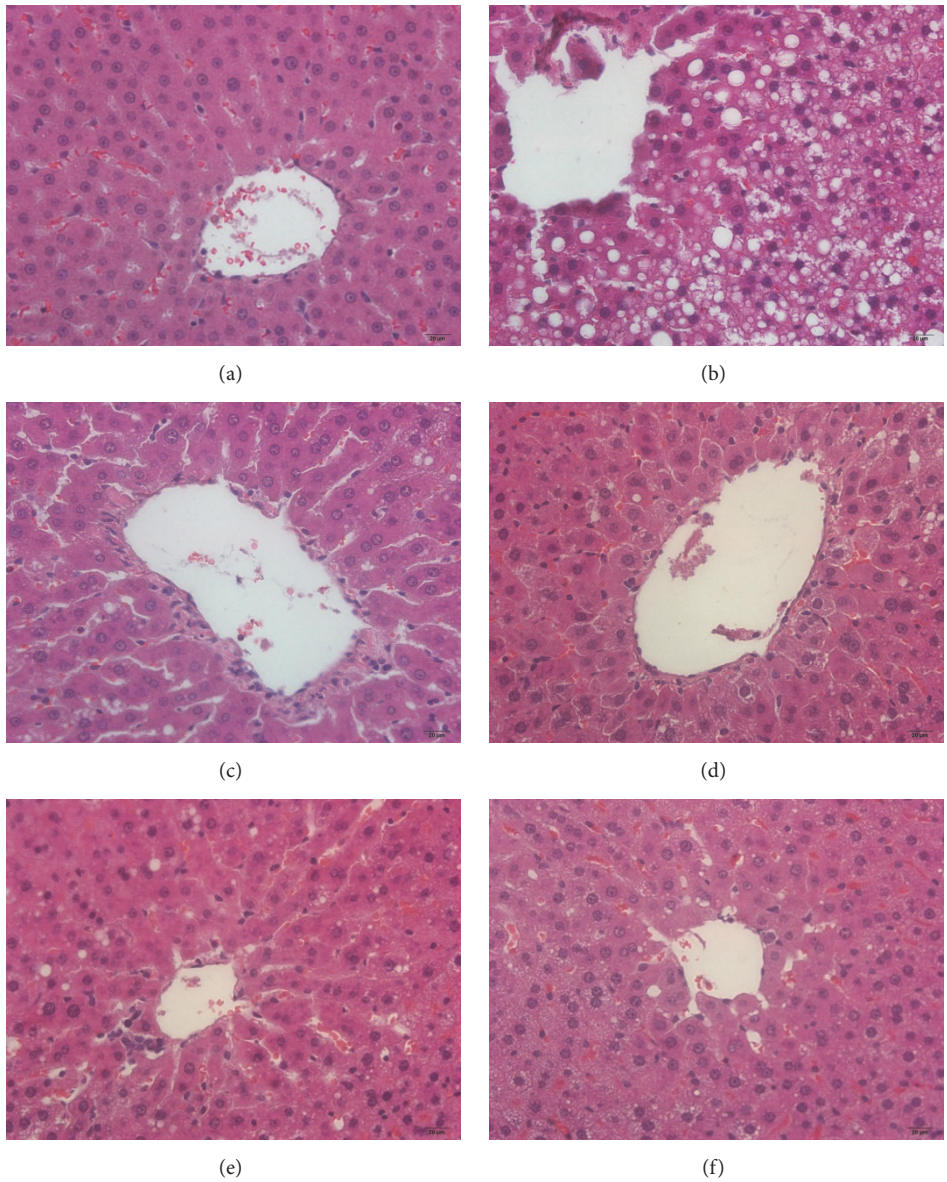

Figure 3: The results of H&E staining, ×200. (a) Control fed rat, (b) HFD model rats, (c) LGZGD treatment rats, (d) YCHD treatment rats, (e) YCLGZGD treatment rats, and (f) SFN treatment rats.

HFD group had a significantly elevated hepatic Nrf2 gene expression compared to that reported for the control group ($P < 0.05$). Treatment with LGZGD, YCLGZGD, and SFN increased Nrf2 gene expression compared to that in the HFD group ($^{\#}P < 0.05$ and $^{\#\#}P < 0.01$, Figure 6).

3.5. LGZGD, YCHD, and YCLGZGD Regulated Hepatic NQO1 Protein and NQO1 mRNA Expression in HFD-Fed Rats. The HFD group showed higher NQO1 expression than the control group did ($P < 0.01$). Similarly, LGZGD, YCLGZGD, and SFN groups had a higher NQO1 expression than the HFD group did ($P < 0.05$, Figure 7). The expression of NQO1 gene was similar to the tendency of protein among the four tested groups.

3.6. LGZGD, YCHD, and YCLGZGD Treatment Increased Hepatic HO-1 Protein and HO-1 mRNA Expression in HFD-Fed Rats. We investigated whether YCLGZGD had a regulatory effect on HO-1 expression in the liver. HO-1 levels in the liver significantly increased in the HFD group ($P < 0.05$) compared to that in the control group. LGZGD, YCLGZGD, and SFN treatment resulted in a sharp increase in HO-1 expression ($P < 0.05$ and $P < 0.01$ versus the HFD group).

Furthermore, HO-1 gene expression was measured to confirm the effects of YCLGZGD on the liver. As shown in Figure 8, HFD group had a significantly higher hepatic Nrf2 gene expression than the control group did ($P < 0.05$). LGZGD, YCLGZGD, and SFN treatment groups showed an

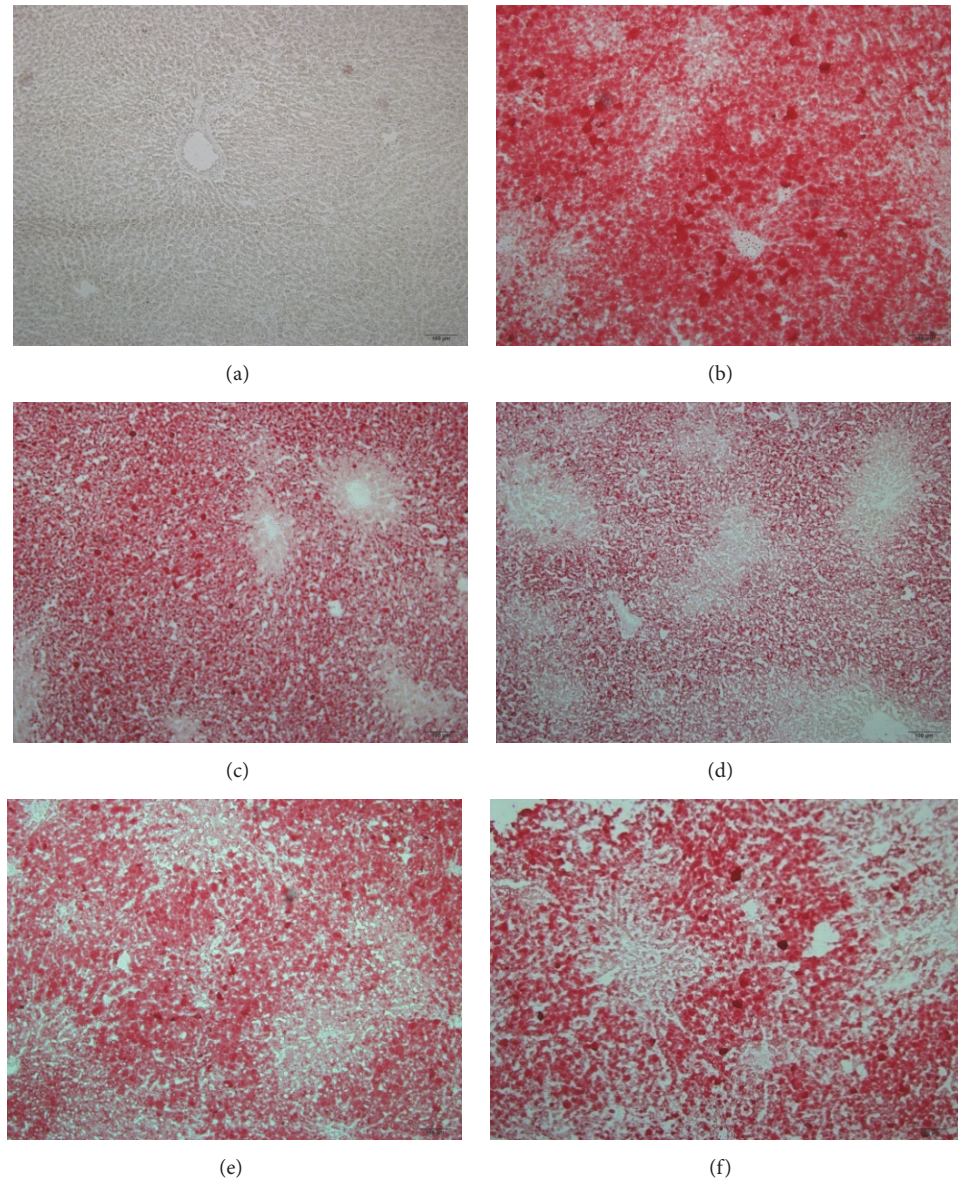

Figure 4: Oil Red O-stained sections, ×100. The red blots show lipid drops in hepatocytes. (a) Control fed rat, (b) HFD model rats, (c) LGZGD treatment rats, (d) YCHD treatment rats, (e) YCLGZGD treatment rats, and (f) SFN treatment rats.

increased Nrf2 gene expression compared to that in the HFD group ($^{\#\#}P < 0.01$, Figure 8).

4. Discussion

NAFLD, a multifactorial disorder caused by various genetic and environmental factors, is considered to be closely associated with hepatic metabolic disorders, resulting in overaccumulation of fatty acids/TGs and cholesterol. The presence of steatosis is closely associated with chronic hepatic inflammation [21], which is mainly caused by oxidative stress and lipid peroxidation (LPO) during the second hit. Free fatty acid oxidation results in production of copious amounts of reactive oxygen species, promoting oxidative stress through several mitochondria-centered pathways. The Nrf2/ARE signaling pathway is involved in this process.

Nrf2 is a key transcription factor that combats cellular oxidative stress. However, whether Nrf2 plays a role in hepatic lipotoxicity is still uncertain. Moreover, the molecular mechanism responsible for the regulation of Nrf2-mediated lipid accumulation remains elusive. Nrf2-null mice exhibited higher lipid accumulation, elevated hepatic fatty acid levels, and oxidative stress after feeding an HFD [22]. Furthermore, the livers of Nrf2-knockout mice fed methionine- and choline-deficient diets exhibited relatively high oxidative stress and inflammation, suggesting that impaired Nrf2 activity might be a risk factor for NAFLD [23–25].

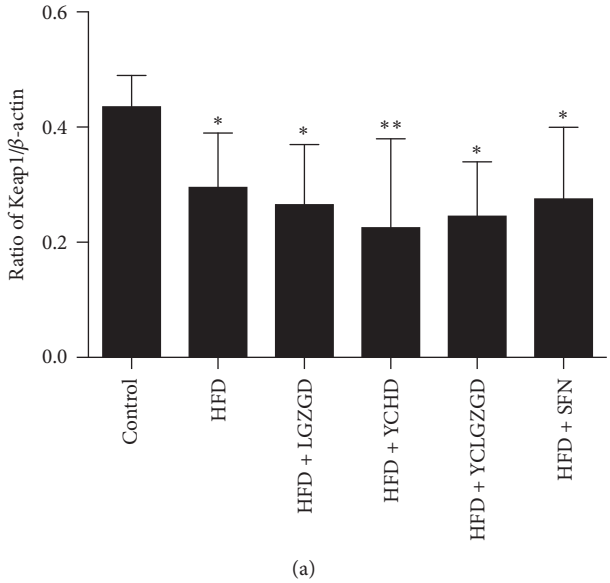

(a)

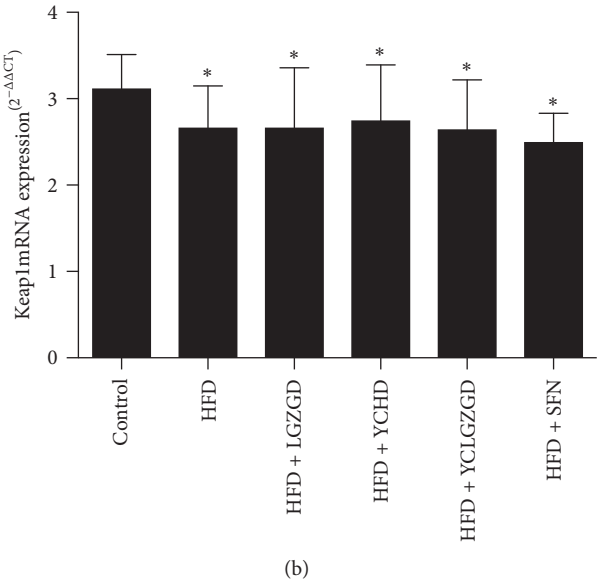

(b)

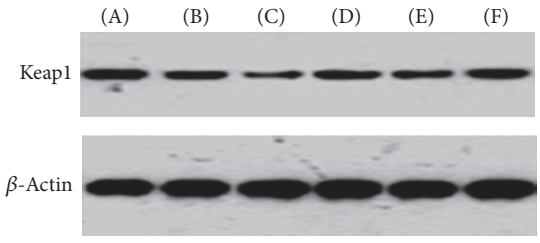

(A) Control
(B) HFD
(C) HFD + LGZGD
(D) HFD + YCHD
(E) HFD + YCLGZGD
(F) HFD + SFN

(c)

Figure 5: LGZGD, YCHD, and YCLGZGD regulated the hepatic Keap1 protein ((a), (b)) and Keap1 mRNA (c) expression in HFD-fed rats. Control: blank control group; HFD: HFD-fed group; LGZGD: LGZGD treatment group; YCHD: YCHD treatment group; YCLGZGD: YCLGZGD treatment group; and SFN: sulforaphane treatment group. $^{**}P < 0.01$ and $^{*}P < 0.05$ versus control group ($n = 10$/group).

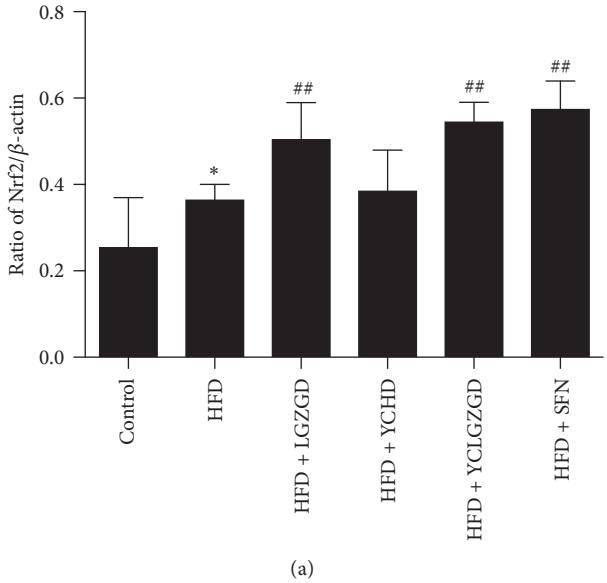

(a)

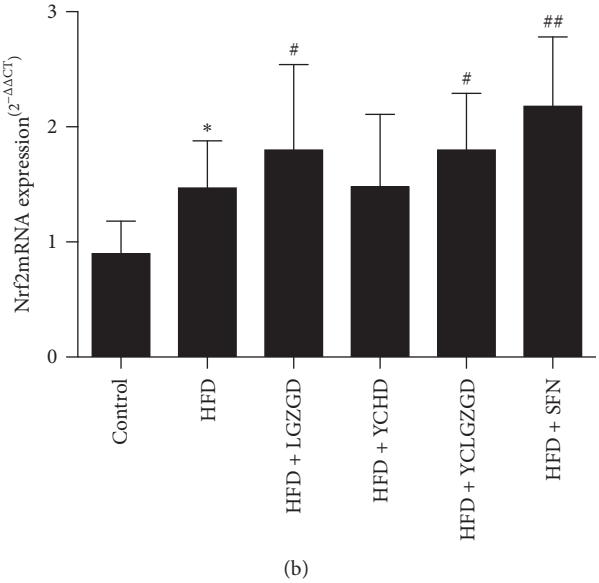

(b)

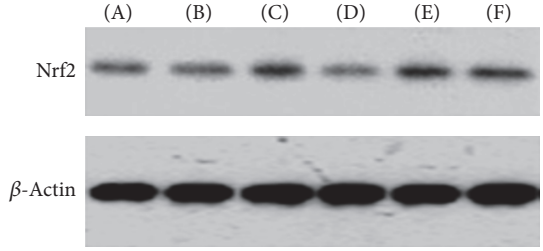

(A) Control
(B) HFD
(C) HFD + LGZGD
(D) HFD + YCHD
(E) HFD + YCLGZGD
(F) HFD + SFN

(c)

Figure 6: YCLGZGD increased hepatic Nrf2 protein ((a), (b)) and Nrf2 mRNA (c) expression in HFD-fed rats. Control: blank control group; HFD: HFD-fed group; LGZGD: LGZGD treatment group; YCHD: YCHD treatment group; YCLGZGD: YCLGZGD treatment group; and SFN: sulforaphane treatment group. $^{*}P < 0.05$ versus control group; $^{\#}P < 0.05$ and $^{\#\#}P < 0.01$ versus HFD group ($n = 10$/group).

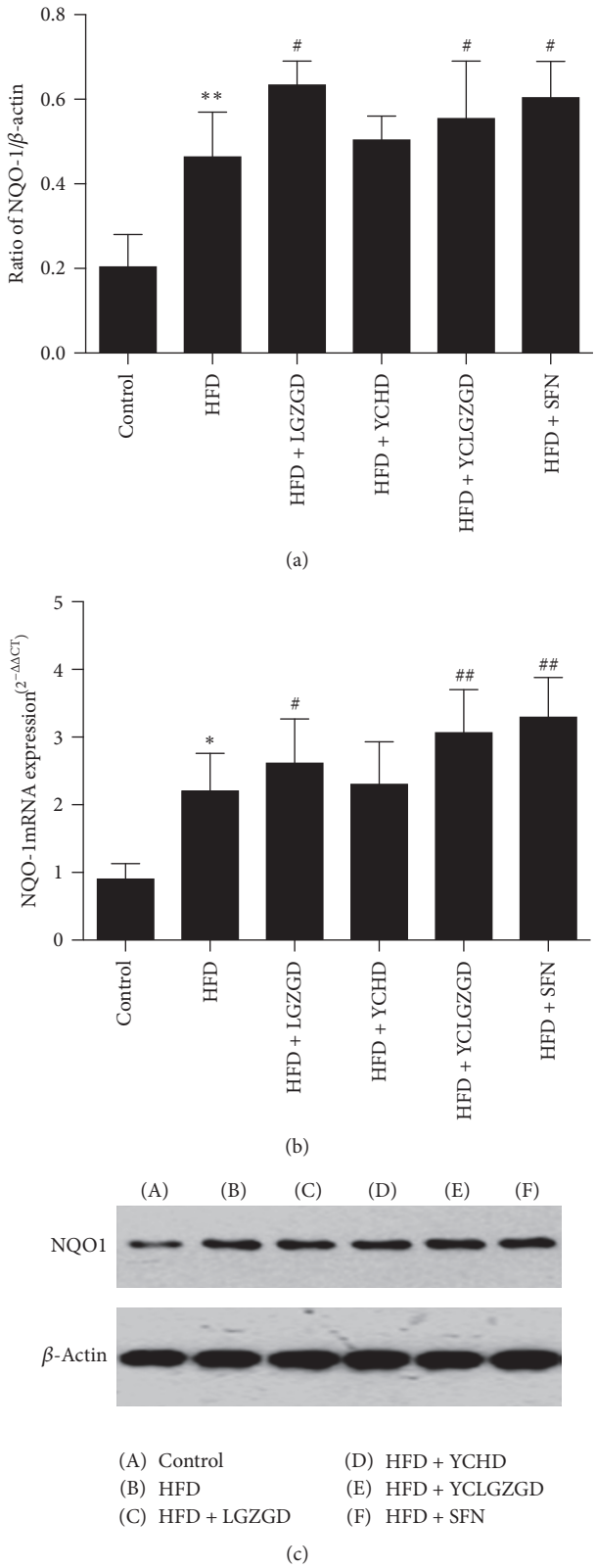

Figure 7: YCLGZGD increased hepatic NQO1 protein ((a), (b)) and NQO1 mRNA expression (c) in HFD-fed rats. Control: blank control group; HFD: HFD-fed group; LGZGD: LGZGD treatment group; YCHD: YCHD treatment group; YCLGZGD: YCLGZGD treatment group; and SFN: sulforaphane treatment group. $^{*}P < 0.05$ versus control group; $^{**}P < 0.01$ versus control group; $^{\#}P < 0.05$ and $^{\#\#}P < 0.01$ versus HFD group ($n = 10$/group).

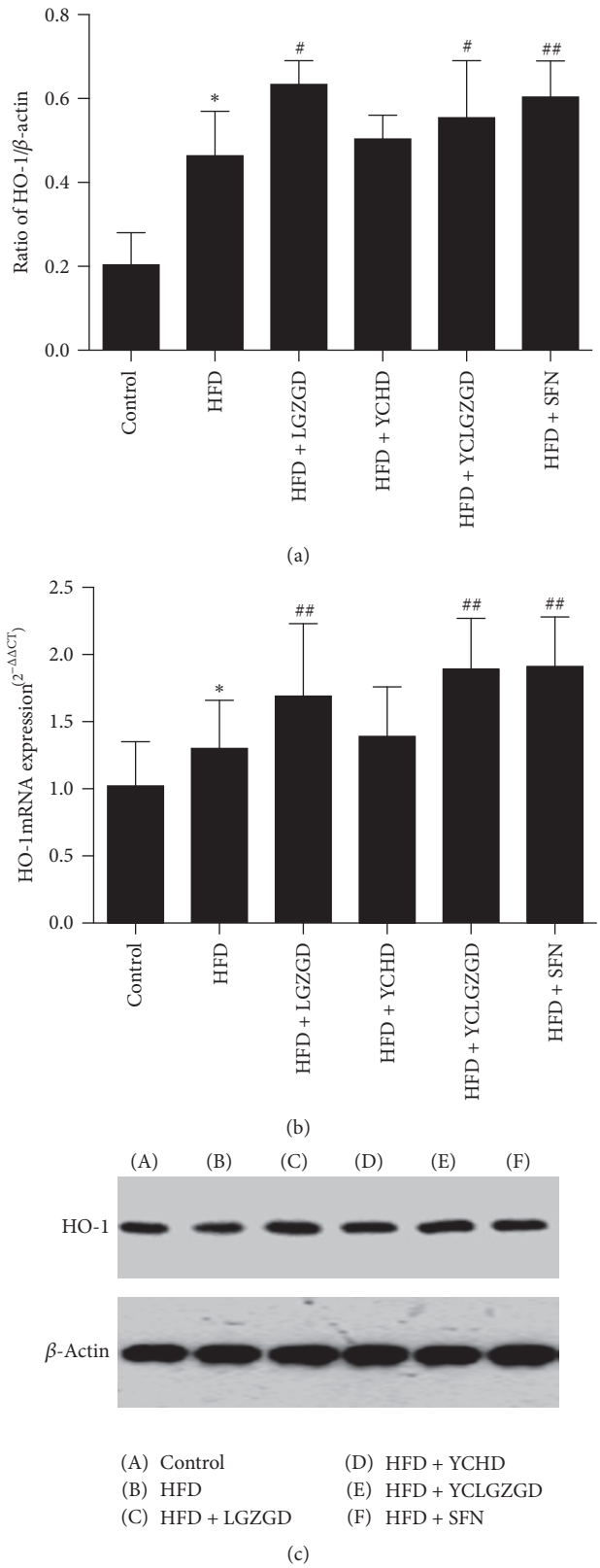

Figure 8: YCLGZGD treatment increased hepatic HO-1 protein ((a), (b)) and HO-1 mRNA (c) expression in HFD-fed rats. Control: blank control group; HFD: HFD-fed; LGZGD: LGZGD treatment group; YCHD: YCHD treatment group; YCLGZGD: YCLGZGD treatment group; and SFN: sulforaphane treatment group. $^{*}P < 0.05$ versus control group; $^{\#}P < 0.05$ and $^{\#\#}P < 0.01$ versus HFD group ($n = 10$/group).

ARE is a nucleotide motif sequence that exists in 5′-upstream promoter region of genes with antioxidative stress. It is widely accepted that Nrf2 is responsible for ARE-dependent gene activation, which can upregulate phase II detoxification and antioxidant enzymes, such as HO-1, NQO1, and superoxide dismutase (SOD).

Keap1 has been shown to interact with the Neh2 (Nrf2-ECH homology domain 2) degron domain of Nrf2 [26]. It is an adaptor subunit of a cullin-3- (CUL3-) based ubiquitin E3 ligase [27]. Under unstressed conditions, Keap1 binds to Nrf2 in the cytoplasm and promotes the ubiquitination and proteasomal degradation of Nrf2. Upon exposure to chemicals (often electrophiles) or reactive oxygen species, the ubiquitin E3 ligase activity of the Keap1–CUL3 complex decreases, and Nrf2 is stabilized. The stabilized Nrf2 accumulates in the nucleus and activates its target genes.

HFD-induced NAFLD animal models have been widely used to identify the pathogenesis and evaluate new treatments [28, 29]. The results of the present study showed that 8 weeks of HFD feeding induced fatty liver disease in SD rats. The rats showed key biochemical features of NAFLD, including elevation of hepatic enzyme levels, hyperlipidemia associated with increased TG accumulation in the liver, histological changes such as steatosis, lobular, and portal inflammation, and hepatocyte injury, for example, ballooning; all of these are characteristics of metabolic syndrome [30]. Furthermore, the histological abnormalities observed in the H&E and ORO-stained liver samples in the HFD-fed rats were consistent with the previous reports [31].

Sulforaphane is an isothiocyanate compound most commonly obtained from cruciferous vegetables [32]. It is produced in plants as a xenobiotic response to predation via vesicular release of the hydrolytic enzyme myrosinase from damaged cells, which converts glucosinolates to isothiocyanates [33]. Over the last two decades, SFN has been extensively characterized for its reported anticancer, antioxidant, and antimicrobial properties [34]. These activities have been mainly attributed to the ability of SFN to modulate the Keap1-Nrf2-ARE signaling pathway.

In previous studies, some researches showed several chemicals which were contained in Chinese herbal medicine such as *Panax notoginseng* [35], *salviae miltiorrhizae* [36, 37], *Ligusticum wallichii* [38], and *Forsythia suspense* [39, 40] and have Nrf2 activating activities. Few components in YCHD and LGZGD were reported to join in this process except *licorice* [41]. However, the effects of a kind of compound in the formula are not equal to it alone. Formula has the advantage of the whole regulation in different aspects such as improvement in liver enzymes, blood lipid, and symptoms in patients [42].

In the present study, we evaluated the therapeutic efficacy of different treatments in an NASH rat model. Although all three CHM treatments showed therapeutic effects on NASH in rats fed on HFD, the rats in the YCLGZGD group showed more therapeutic improvement, especially in TG and HDL level, than the rats in other two groups did, indicating that LGZGD in combination with YCHD has synergistic effects. We also measured the expression of proteins and genes involved in the Nrf2/ARE signaling pathway. The expression of Nrf2, NQO1, and HO-1 proteins and genes in LGZGD and YCLGZGD treatment groups was similar to that in the SFN group, whereas Keap1 expression was similar between the treatment and HFD groups. This indicates that LGZGD and YCLGZGD regulate the Nrf2/ARE signaling pathway without decreasing Keap1 expression. However, we did not observe obvious effects of YCHD on the proteins and genes in the Nrf2/ARE signaling pathway. YCHD may take advantage of other mechanisms in treating NASH, which need to be explored in the future.

Taken together, the results of the present study showed that YCLGZGD alleviated NAFLD by attenuating oxidative stress and improving lipid regulation, thus providing data to support its clinical use. Because the medicinal herbs present in YCLGZGD have been used in TCM for thousands of years, YCLGZGD is considered safe and tolerable. In conclusion, YCLGZGD can be an optimal approach for NAFLD management given its capacity to regulate oxidative stress, lipid metabolism, inflammatory response, and histological abnormalities via the Nrf2/ARE signaling pathway.

Conflicts of Interest

The authors declare that there are no conflicts of interest regarding the publication of this paper.

Authors' Contributions

Yi Guo and Jun-xiang Li contributed equally to this work.

Acknowledgments

This study was supported by the National Science Foundation of China (Grant no. 81503549), the Specialized Research Fund for the Doctoral Program of Higher Education of China (Grant no. 20130013110007), and the self-selected topic of the Beijing University of Chinese Medicine (Grant no. 2015-JYB-JSMS-110).

References

[1] D. A. Sass, P. Chang, and K. B. Chopra, "Nonalcoholic fatty liver disease: a clinical review," *Digestive Diseases and Sciences*, vol. 50, no. 1, pp. 171–180, 2005.

[2] M. Charlton, "Nonalcoholic fatty liver disease: a review of current understanding and future impact," *Clinical Gastroenterology and Hepatology*, vol. 2, no. 12, pp. 1048–1058, 2004.

[3] R. Vuppalanchi and N. Chalasani, "Nonalcoholic fatty liver disease and nonalcoholic steatohepatitis: selected practical issues in their evaluation and management," *Hepatology*, vol. 49, no. 1, pp. 306–317, 2009.

[4] J.-H. Ryoo, Y. J. Suh, H. C. Shin, Y. K. Cho, J.-M. Choi, and S. K. Park, "Clinical association between non-alcoholic fatty liver disease and the development of hypertension," *Journal of Gastroenterology and Hepatology (Australia)*, vol. 29, no. 11, pp. 1926–1931, 2014.

[5] J.-H. Ryoo, W. T. Ham, J.-M. Choi et al., "Clinical significance of non-alcoholic fatty liver disease as a risk factor for prehypertension," *Journal of Korean Medical Science*, vol. 29, no. 7, pp. 973–979, 2014.

[6] N. Katsiki, D. P. Mikhailidis, and C. S. Mantzoros, "Non-alcoholic fatty liver disease and dyslipidemia: An update," *Metabolism: Clinical and Experimental*, vol. 65, no. 8, pp. 1109–1123, 2016.

[7] J. K. Dowman, J. W. Tomlinson, and P. N. Newsome, "Pathogenesis of non-alcoholic fatty liver disease," *QJM*, vol. 103, no. 2, pp. 71–83, 2010.

[8] M. Enjoji, K. Yasutake, M. Kohjima, and M. Nakamuta, "Nutrition and nonalcoholic fatty liver disease: the significance of cholesterol," *International Journal of Hepatology*, vol. 2012, 6 pages, 2012.

[9] G. F. Watts, "Nutrition and metabolism: nutritional therapy for disordered triglyceride metabolism and nonalcoholic fatty liver disease," *Current Opinion in Lipidology*, vol. 21, no. 6, pp. 545–547, 2010.

[10] D. B. Andrews and J. E. Lavine, "Medical therapy for nonalcoholic fatty liver disease in children and adolescents," *Expert Review of Gastroenterology and Hepatology*, vol. 6, no. 1, pp. 1–3, 2012.

[11] C. Eckard, R. Cole, J. Lockwood et al., "Prospective histopathologic evaluation of lifestyle modification in nonalcoholic fatty liver disease: a randomized trial," *Therapeutic Advances in Gastroenterology*, vol. 6, no. 4, pp. 249–259, 2013.

[12] L. Tock, A. R. Dâmaso, A. de Piano et al., "Long-term effects of metformin and lifestyle modification on nonalcoholic fatty liver disease obese adolescents," *Journal of Obesity*, vol. 2010, Article ID 831901, 6 pages, 2010.

[13] R. C. Smith, "Metformin as a treatment for antipsychotic drug side effects: special focus on women with schizophrenia," *The American Journal of Psychiatry*, vol. 169, no. 8, pp. 774–776, 2012.

[14] Z. Du H, L. Luo, J. Hou Y et al., "study on HPLC fingerprints of Yinchenhao decoction and attributive analysis of common peaks," *Journal of Nan Jing University of Tcm*, vol. 31, no. 4, pp. 380–384, 2015.

[15] Z. Song H, D. Feng, J. Xu B et al., "Study on the compatibility and therapeutic basis of composite herbal medicines of Linguizhugan Decoction," *Chinese Traditional Patent Medicine*, vol. 25, no. 2, pp. 132–137, 2003.

[16] M. Tang-you, G. Kang-li, Z. Wei-han et al., "Experimental study of "Wenyun Qingli" method on DAG-PKCε signal pathway in liver tissue of NASH rats," *Global Traditional Chinese Medicine*, vol. 9, no. 8, pp. 908–913, 2016.

[17] Z. Dan, S. Ting-ting, C. Lan-yu et al., "Treatment of nonalcoholic fatty liver disease in Jingui Yaolue," *Journal of Changchun University of Chinese Medicine*, vol. 32, no. 2, pp. 423–425, 2016.

[18] M. Bahabadi, A. Mohammadalipour, J. Karimi et al., "Hepatoprotective effect of parthenolide in rat model of nonalcoholic fatty liver disease," *Immunopharmacology & Immunotoxicology*, vol. 39, no. 4, pp. 233–242, 2017.

[19] D. Lee H, D. Han H, K. Nam T et al., "Ezetimibe, an NPC1L1 inhibitor, is a potent Nrf2 activator that protects mice from diet-induced nonalcoholic steatohepatitis," *Free Radical Biology & Medicine*, vol. 10, no. 99, pp. 520–532, 2016.

[20] J. Du, M. Zhang, J. Lu et al., "Osteocalcin improves nonalcoholic fatty liver disease in mice through activation of Nrf2 and inhibition of JNK," *Endocrine*, vol. 53, no. 3, pp. 701–709, 2016.

[21] D. Cai, M. Yuan, D. F. Frantz et al., "Local and systemic insulin resistance resulting from hepatic activation of IKK-β and NF-κB," *Nature Medicine*, vol. 11, no. 2, pp. 183–190, 2005.

[22] Y. Tanaka, L. M. Aleksunes, R. L. Yeager et al., "NF-E2-related factor 2 inhibits lipid accumulation and oxidative stress in mice fed a high-fat diet," *Journal of Pharmacology and Experimental Therapeutics*, vol. 325, no. 2, pp. 655–664, 2008.

[23] S. Chowdhry, M. H. Nazmy, P. J. Meakin et al., "Loss of Nrf2 markedly exacerbates nonalcoholic steatohepatitis," *Free Radical Biology and Medicine*, vol. 48, no. 2, pp. 357–371, 2010.

[24] H. Sugimoto, K. Okada, J. Shoda et al., "Deletion of nuclear factor-E2-related factor-2 leads to rapid onset and progression of nutritional steatohepatitis in mice," *American Journal of Physiology: Gastrointestinal and Liver Physiology*, vol. 298, no. 2, pp. G283–G294, 2010.

[25] Y.-K. J. Zhang, R. L. Yeager, Y. Tanaka, and C. D. Klaassen, "Enhanced expression of Nrf2 in mice attenuates the fatty liver produced by a methionine- and choline-deficient diet," *Toxicology and Applied Pharmacology*, vol. 245, no. 3, pp. 326–334, 2010.

[26] K. Itoh, N. Wakabayashi, Y. Katoh et al., "Keap1 represses nuclear activation of antioxidant responsive elements by Nrf2 through binding to the amino-terminal Neh2 domain," *Genes & Development*, vol. 13, no. 1, pp. 76–86, 1999.

[27] A. Kobayashi, M. Kang, H. Okawa et al., "Oxidative stress sensor Keap1 functions as an adaptor for Cul3-based E3 ligase to regulate proteasomal degradation of Nrf2," *Molecular and Cellular Biology*, vol. 24, no. 16, pp. 7130–7139, 2004.

[28] R. Barbuio, M. Milanski, M. B. Bertolo, M. J. Saad, and L. A. Velloso, "Infliximab reverses steatosis and improves insulin signal transduction in liver of rats fed a high-fat diet," *Journal of Endocrinology*, vol. 194, no. 3, pp. 539–550, 2007.

[29] V. T. Samuel, Z.-X. Liu, X. Qu et al., "Mechanism of hepatic insulin resistance in non-alcoholic fatty liver disease," *The Journal of Biological Chemistry*, vol. 279, no. 31, pp. 32345–32353, 2004.

[30] K.-X. Gan, C. Wang, J.-H. Chen, C.-J. Zhu, and G.-Y. Song, "Mitofusin-2 ameliorates high-fat diet-induced insulin resistance in liver of rats," *World Journal of Gastroenterology*, vol. 19, no. 10, pp. 1572–1581, 2013.

[31] J. C. Fraulob, R. Ogg-Diamantino, C. Fernandes-Santos, M. B. Aguila, and C. A. Mandarim-de-Lacerda, "A mouse model of metabolic syndrome: insulin resistance, fatty liver and Non-Alcoholic Fatty Pancreas Disease (NAFPD) in C57BL/6 mice fed a high fat diet," *Journal of Clinical Biochemistry and Nutrition*, vol. 46, no. 3, pp. 212–223, 2010.

[32] Y. Zhang, P. Talalay, C. G. Cho, and G. H. Posner, "A major inducer of anti-carcinogenic protective enzymes from broccoli: isolation and elucidation of structure," in *Proceedings of the National Academy of Sciences of the United States of America USA*, vol. 89, pp. 2399–2403, 1992.

[33] E. Smirnova, L. Griparic, D.-L. Shurland, and A. M. van der Bliek, "Dynamin-related protein Drp1 is required for mitochondrial division in mammalian cells," *Molecular Biology of the Cell*, vol. 12, no. 8, pp. 2245–2256, 2001.

[34] Y. Zhang and L. Tang, "Discovery and development of sulforaphane as a cancer chemopreventive phytochemical," *Acta Pharmacologica Sinica*, vol. 28, no. 9, pp. 1343–1354, 2007.

[35] J. Fan, D. Liu, C. He, X. Li, and F. He, "Inhibiting adhesion events by Panax notoginseng saponins and Ginsenoside Rb1 protecting arteries via activation of Nrf2 and suppression of p38 – VCAM-1 signal pathway," *Journal of Ethnopharmacology*, vol. 192, pp. 423–430, 2016.

[36] X. Liu, C. Xavier, J. Jann, and H. Wu, "Salvianolic acid B (Sal B) protects retinal pigment epithelial cells from oxidative stress-induced cell death by activating glutaredoxin 1 (Grx1)," *International Journal of Molecular Sciences*, vol. 17, no. 11, article no. 1835, 2016.

[37] H. Li, F. Song, L.-R. Duan et al., "Paeonol and danshensu combination attenuates apoptosis in myocardial infarcted rats by inhibiting oxidative stress: Roles of Nrf2/HO-1 and PI3K/Akt pathway," *Scientific Reports*, vol. 6, Article ID 23693, 2016.

[38] J. Li, J. Yu, H. Ma et al., "Intranasal Pretreatment with Z-Ligustilide, the Main Volatile Component of Rhizoma Chuanxiong, Confers Prophylaxis against Cerebral Ischemia via Nrf2 and HSP70 Signaling Pathways," *Journal of Agricultural and Food Chemistry*, vol. 65, no. 8, pp. 1533–1542, 2017.

[39] C.-W. Pan, G.-Y. Zhou, W.-L. Chen et al., "Protective effect of forsythiaside A on lipopolysaccharide/d-galactosamine-induced liver injury," *International Immunopharmacology*, vol. 26, no. 1, pp. 80–85, 2015.

[40] J. Bao, R. DIng, L. Zou et al., "Forsythiae Fructus Inhibits B16 Melanoma Growth Involving MAPKs/Nrf2/HO-1 Mediated Anti-Oxidation and Anti-Inflammation," *American Journal of Chinese Medicine*, vol. 44, no. 5, pp. 1043–1061, 2016.

[41] S. Ji, Z. Li, W. Song et al., "Bioactive Constituents of Glycyrrhiza uralensis (Licorice): Discovery of the Effective Components of a Traditional Herbal Medicine," *Journal of Natural Products*, vol. 79, no. 2, pp. 281–292, 2016.

[42] Z. Chen, X. Ma, Y. Zhao et al., "Yinchenhao decoction in the treatment of cholestasis: A systematic review and meta-analysis," *Journal of Ethnopharmacology*, vol. 168, pp. 208–216, 2015.

Hindawi
Evidence-Based Complementary and Alternative Medicine
Volume 2017, Article ID 9208314, 13 pages
https://doi.org/10.1155/2017/9208314

Research Article

Extracts of Salvia-Nelumbinis Naturalis Ameliorate Nonalcoholic Steatohepatitis via Inhibiting Gut-Derived Endotoxin Mediated TLR4/NF-κB Activation

Xiangbing Shu,[1] Miao Wang,[1] Hanchen Xu,[1] Yang Liu,[1] Jie Huang,[1] Zemin Yao,[2] and Li Zhang[1]

[1]*Institute of Digestive Diseases, China-Canada Center of Research for Digestive Diseases (ccCRDD), Longhua Hospital, Shanghai University of Traditional Chinese Medicine, Shanghai 200032, China*
[2]*Department of Biochemistry, Microbiology & Immunology, Ottawa Institute of Systems Biology, University of Ottawa, Ottawa, ON, Canada K1H 8M5*

Correspondence should be addressed to Li Zhang; zhangli.hl@163.com

Received 10 March 2017; Revised 1 June 2017; Accepted 18 June 2017; Published 31 July 2017

Academic Editor: H. Balaji Raghavendran

Nonalcoholic steatohepatitis (NASH) is featured by the presence of hepatic steatosis combined with inflammation and hepatocellular injury. Gut-derived endotoxin plays a crucial role in the pathogenesis of NASH. Salvia-Nelumbinis naturalis (SNN), a formula of Traditional Chinese Medicine, has been identified to be effective for NASH, but the mechanisms were not thoroughly explored. In the present study, a NASH model was generated using C57BL/6 mice fed a high fat diet (HFD) supplemented periodically with dextran sulfate sodium (DSS) in drinking water for 12 weeks. Mice fed HFD alone (without DSS) or chow diet were used as controls. The NASH mice were given the SNN extracts in the following 4 weeks, while control mice were provided with saline. Mice fed HFD developed steatosis, and DSS supplementation resulted in NASH. The SNN extracts significantly improved metabolic disorders including obesity, dyslipidemia, and liver steatosis and reduced hepatic inflammation, circulating tumor necrosis factor-α (TNF-α), and lipopolysaccharide (LPS) levels. The beneficial effect of the SNN extracts was associated with restoration of intestinal conditions (microbiota, integrity of intestinal barrier) and inhibition of TLR4/NF-κB activation. These results suggest that the SNN extracts ameliorate NASH progression, possibly through blocking endotoxin related TLR4/NF-κB activation.

1. Introduction

Nonalcoholic fatty liver disease (NAFLD) is a main cause of chronic liver diseases, and the global prevalence is approximately 24% [1]. The progressive form of NAFLD has been referred to as nonalcoholic steatohepatitis (NASH). Although NASH represents the minority (10–20%) of patients with NAFLD, it can potentially progress to advanced liver disease leading to cirrhosis, liver-related mortality, and hepatocellular carcinoma (HCC) [2]. Since simple fatty liver is considered to be benign, determination of the risks factors of disease progression is of vital importance. Histological studies identified that the degree of inflammation is the strongest and independent predictor for NAFLD progression [3]. Our current understanding of the pathophysiology of NASH is that excessive fat accumulation coexists with inflammation and cell injury in the liver. Thus, ideal pharmaceutical therapy for NASH should both improve metabolic conditions and target the mechanisms of hepatic cell injury.

NASH is characterized by Kupffer cell activation, and dysbiosis-driven inflammatory plays a vital role [4]. Intestinal microorganisms (endotoxin) produced by opportunistic pathogen in the intestine could enter liver directly through portal vein. These highly conserved molecules known as "pathogen associated molecular patterns" (PAMPs) can be recognized specifically by pattern recognition receptors (PRRs), such as toll-like receptors (TLRs). Studies demonstrated that intraperitoneally injection of LPS, the major component of the outer membrane of Gram-negative bacteria, can exaggerate liver inflammation in high fat diet (HFD) or

high calorie diet feeding animals, further indicating the role of gut-derived endotoxin in promoting NASH development [5, 6]. The LPS sensor TLR4 could subsequently trigger a cascade of molecules leading to activation of nuclear factor κB (NF-κB) and production of proinflammatory cytokines and chemokines [7]. In addition, activation of TLRs also attracts other immune cells to the infected sites, thus contributing to the development of NASH.

Prevention and treatment of NASH still confront great obstacles currently. Diet and lifestyle modification are recommended as the first-line therapy. However, these measures cannot be implemented efficiently or maintained in the long run. The need for specific pharmacotherapy is urgent, yet the options available are limited. Recently, natural products have attracted increasing interest in preventing and treating NASH [8]. Herbal medicines derived from Traditional Chinese Medicine (TCM) theories have been applied for treating liver diseases for thousands of years in China. The extracts of Salvia-Nelumbinis naturalis (SNN) formula, initially called Jiangzhi Granula and designed entirely based on TCM theories, have been used to treat NAFLD. We have shown that the SNN extracts can ameliorate NAFLD and related metabolic disorders in patients in a multicenter, randomized, double-blind, placebo-controlled clinical trial [9]. Both in vivo and in vitro experiments in our previous studies confirmed beneficial effects of SNN or its ingredients on insulin resistance and lipid accumulation [10]. Using methionine/choline deficient (MCD) diet-induced NASH model, we have found that the SNN extracts can protect the liver from server damage through improving hepatic antioxidant capability [11]. However, whether SNN extracts can exert a beneficial effect on liver injury related to gut-derived endotoxin has not been determined.

In the present study, we applied NASH mice induced by HFD supplemented with dextran sulfate sodium (DSS) and determined the role of endotoxin in NASH development. With these animals, we assessed the efficacy and potential mechanisms of the SNN extracts in treating of NASH.

2. Materials and Methods

2.1. Preparation of SNN Extracts. The SNN extracts were prepared as previously described [8]. Briefly, the medicinal materials, 1.5 portion of *Salviae*, 1 portion of *Nelumbinis*, 2.5 portion of *Rhizoma Polygoni Cuspidati,* and 1.5 portion of *Herba Artemisiae Scopariae*, were triturated and blended to powder and then mixed with water/methanol (5 : 95, V/V) for sonication, filtration, and vacuum condensation to obtain the extracts. Methanol was removed from the extracts to gain powder before animal experiments. The main chemical components of the extracts were compared with the previously established standard [12], and 1 g medicinal material can get 200 mg extracts.

2.2. Mouse Experiments. Male C57BL/6 mice, 6 weeks of age, were purchased from SLAC Animal Laboratories (Shanghai, China). After one-week acclimatization, the mice were divided into 3 groups: the chow group (n = 10) received standard control diet (SLAC Animal Laboratories, Shanghai, China); HFD group (n = 6) received HFD (60% of calories derived from fat, Research Diets, NJ, USA); the HF-DSS group (n = 26) received HFD supplemented with 1% DSS (MP Biomedicals, Solon, OH, USA) in drinking water. DSS was given in cycles; each cycle consisted of a 7-day DSS administration followed by a 10-day interval with normal drinking water. After 12 weeks of feeding, HFD group mice and 6 mice from the HF-DSS group were sacrificed to evaluate the model. The remaining HF-DSS mice were further divided into 2 groups: HF-DSS group (n = 10) remained on HF-DSS diet, while mice in treatment group (n = 10) were given the SNN extracts (750 mg/kg) for 4 weeks by gavage.

The body weight and food intake of the mice were recorded at every DSS treatment cycle. The animal protocols were performed in accordance with the guidelines with approval of the Animal Experiment Ethics Committee at Shanghai University of Traditional Chinese Medicine.

2.3. Serum Biochemical and Immunological Analysis. After 12 h fasting, mice were anaesthetized with sodium pentobarbital (100 mg/kg) and sacrificed. Blood was collected, and serum triglyceride (TG), total cholesterol (TC), low density lipoprotein cholesterol (LDL-c), high density lipoprotein cholesterol (HDL-c), alanine transaminase (ALT), aspartate transaminase (AST), alkaline phosphatase (ALP), and lactate dehydrogenase (LDH) were analyzed using the Hitachi full-automatic system. Serum LPS and tumor necrosis factor-α (TNF-α) were detected by ELISA kits (Westang Testmart) according to the manufacturer's instructions.

2.4. Hepatic Lipid Content Analysis. Hepatic TG and TC contents were qualified as described previously [8]. Briefly, liver tissue (200 mg) was homogenized in 3 ml of ethanol-acetone (1 : 1) mixture. The homogenate was extracted over night at 4°C and centrifuged for 15 min at 3,000 rpm at 4°C. The organic layer was collected, and TG and TC were qualified using commercial kits (Jiancheng tech, Nanjing, China).

2.5. Histology and Immunohistochemistry Analysis. The liver and colon tissues were fixed in 10% formaldehyde, and paraffin-embedded sections (4 μm thickness) were prepared for H&E staining. Frozen liver sections (8 μm thickness) were fixed with 10% paraformaldehyde at room temperature for 30 min and stained with Oil Red O (Sigma, St. Louis, MO) for 60 min. Immunohistochemical staining (IHC) with F4/80 (1 : 200, Abcam, Cambridge, UK) was performed on 4 μm thick paraffin-embedded liver sections following the manufacturer's protocol. Images were captured using Olympus IX71 Inverted microscope (Tokyo, Japan).

2.6. Fecal DNA Extraction, Pyrosequencing, and Bioinformatics Statistics. Fresh feces were collected from the ileocecal region of the mice, and genomic DNA was extracted by QIAamp DNA stool mini kit (Qiagen, Germany) as previously described [13]. Purity was determined and concentration was calculated. The extracted DNA was used as the template to amplify the V3 region of 16S rDNA genes. PCR reaction, pyrosequence, and quality control were performed

Table 1: Sequences of the primers used for PCR.

Genes	Forward primer	Reverse primer
TNFα	CCCTCCAGAAAAGACACCATG	CACCCCGAAGTTCAGTAGACAG
IL1β	GCTTCAGGCAGGCAGTATCA	TGCAGTTGTCTAATGGGAACG
IL-6	GGGACTGATGCTGGTGACAAC	CAACTCTTTTCTCATTTCCACGA
MCP-1	GCTGACCCCAAGAAGGAATG	TTGAGGTGGTTGTGGAAAAGG
TLR2	TTCACCACTGCCCGTAGATG	GGTACAGTCGTCGAACTCTACCTC
TLR4	TTACACGTCCATCGGTTGATC	TACACCTGCCAGAGACATTGC
GAPDH	GTGCCGCCTGGAGAAACC	GGTGGAAGAGTGGGAGTTGC

as described previously [13]. The high-quality valid reads were clustered into operational taxonomic units (OTUs) using Mothur (http://www.mothur.org/). Rarefaction curve analysis and Shannon diversity index were analyzed according to the representative sequences of OTUs. A heat map was generated by R software (http://www.R-project.org). Taxonomy-based analysis was performed using the Ribosomal Database Project (RDP) classifier.

2.7. Cell Culture and Treatment. Kupffer cells were isolated from pathogen-free male C57/BL6 mice (6–8 weeks, weighing 20 ± 0.5 g) as previously described [14], and their identity was authenticated by the engulfment of immunofluorescence beads. After a 24 h recovery period from isolation, the primary Kupffer cells were cultured in the absence or presence of 50, 100, and 200 ng/ml of LPS (Sigma, St. Louis, MO) for 1, 2, and 4 h.

2.8. Quantitative Real-Time PCR. Total RNA was extracted from the liver or LPS treated Kupffer cells using a TRIzol reagent (Invitrogen Corp, Carlsbad, CA, USA) and reversely transcribed into cDNA using reverse transcription kits (Promega, Madison, WI, USA). Sequences of the primers (obtained from Shine Gene, Shanghai, China) used in the experiments were shown in Table 1. Quantitative real-time PCR (qRT-PCR) was performed using the SYBR Green PCR Master Mix kit (TOYOBO, Osaka, Japan) according to the manufacturer's protocol. Quantification of the mRNA concentrations was carried out using the AB StepOnePlus Real-Time PCR System (Applied Biosystems, Carlsbad, CA, USA). The relative mRNA levels were normalized using GAPDH as an internal control and expressed as fold change relative to the control.

2.9. Western Blot Analysis. Primary antibodies used for Western blot analysis were anti-zonula occludens 1 (ZO-1), anti-occludin, anti-claudin-1 (Thermo Scientific, Rockford, USA), anti-phosphorylated p65, anti-phosphorylated IκB, anti-p65, anti-IκB (Cell Signaling Technology, Danvers, USA), anti-TIRAP (Toll-interleukin 1 receptor domain containing adaptor protein), anti-IRAK1 (interleukin-1 receptor-associated kinase 1), anti-IRAK4 (Proteintech, Wuhan, China), anti-TRAF6 (TNF receptor-associated factor 6), anti-TLR4 (Abcam, Cambridge, MA, USA), anti-β-actin, and anti-Histone H3 (Hua'an Biological Technology, Hangzhou, China). The antibody-antigen complexes were visualized by using the ECL (Electrochemiluminescence) kit (Millipore, Billerica, USA). The intensity of the immunoreactive bands was semiquantified using the GeneTools (SynGene, Frederick, USA).

Table 2: The change of body weight, liver weight, and food intake of the mice.

Parameters	Control	HF-DSS	SNN
Body weight (g)	28.5 ± 0.64	32.5 ± 1.51**	27.9 ± 1.56$^{\#}$
Liver weight (g)	1.3 ± 0.03	1.5 ± 0.04**	1.2 ± 0.07$^{\#\#}$
Liver/body weight (%)	4.6 ± 0.06	4.5 ± 0.15	4.0 ± 0.10$^{\#}$
Food intake (g/d)	11.9 ± 0.23	7.9 ± 0.38***	8.0 ± 1.07

$n = 10$ per group, $^{**}P < 0.01$, $^{***}P < 0.001$ versus control group; $^{\#}P < 0.05$, $^{\#\#}P < 0.01$ versus HF-DSS group.

2.10. Statistical Analysis. SPSS 18.0 and GraphPad Prism 5 were used for data analysis. Data were expressed as means ± standard error (SE). One-way analysis of variance (ANOVA) with Tukey's correction was applied for differences between two groups, and $P < 0.05$ was accepted as statistically significant.

3. Results

3.1. Intestinal Damage Promotes Steatohepatitis. Male C57Bl/6 mice fed 12-week HFD exhibited obvious hepatic steatosis but no sign of inflammation in liver sections (Figure 1(a)). Supplementation of HFD with DSS, however, resulted in damage in the intestinal barriers, which was associated with significant hepatic steatosis combined with inflammation foci (Figures 1(a) and 1(b)). While the liver TG contents were comparable between the two groups of mice (Figure 1(c)), the HF-DSS mice presented increased level of serum AST (Figure 1(d)) and ALP (Figure 1(e)), suggesting that intestinal damage might have contributed to the development of NASH.

3.2. The SNN Extracts Treatment Alleviated Hepatomegaly in NASH Mice. NASH mice developed hepatomegaly and exhibit increased body weight (Table 2); the ratio of liver/body weight of NASH mice was not different from that in control mice fed a normal chow diet (Table 2). After 4-week SNN treatment, body weight, liver weight, and liver/body weight ratio were all significantly decreased compared with those of untreated NASH mice (Table 2). Because food intake between untreated and SNN-treated groups was identical

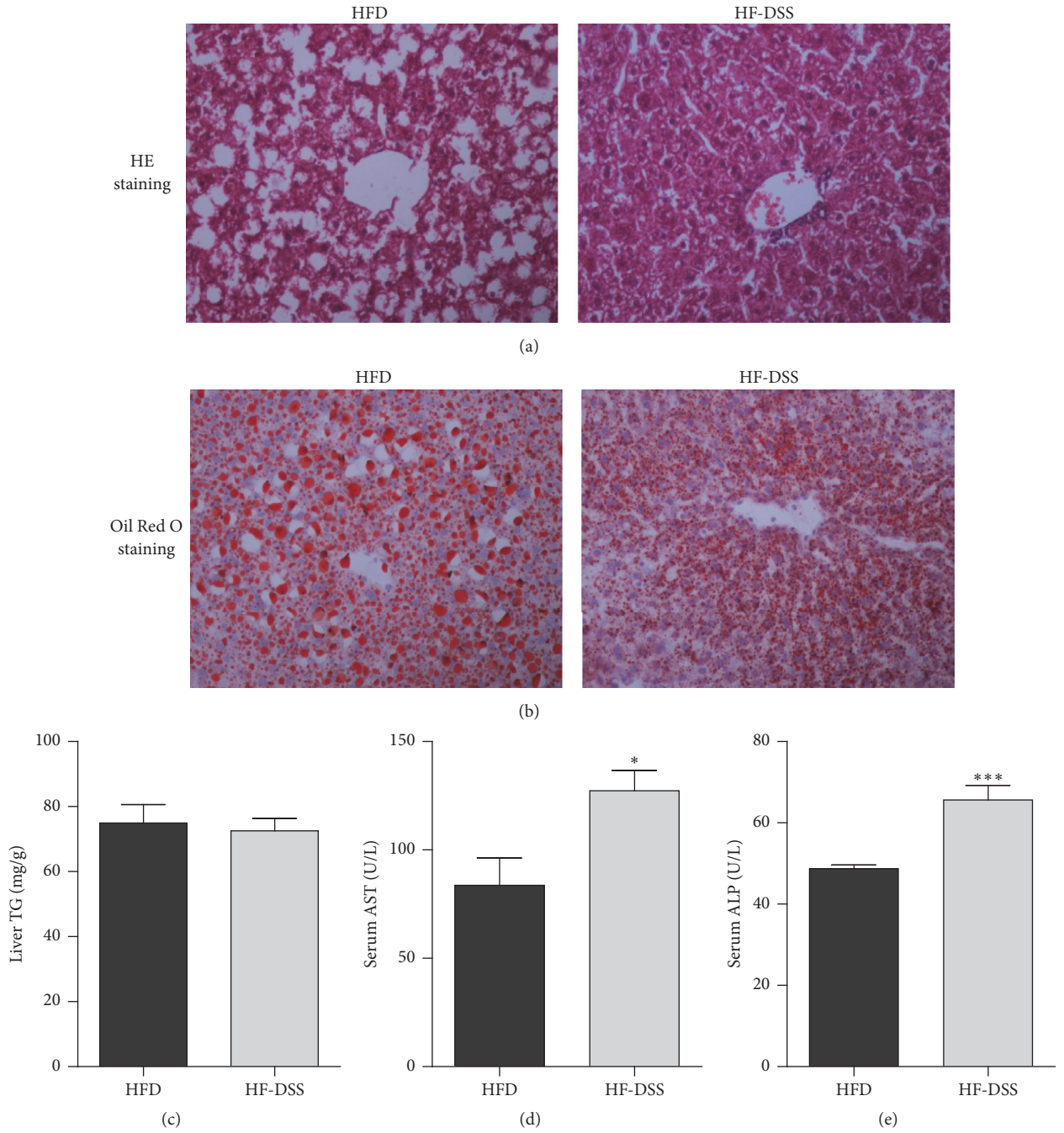

Figure 1: *DSS supplementation promotes steatohepatitis*. Male C57Bl/6 mice (7 weeks of age) were either fed HFD supplemented periodically with DSS in drinking water ($n = 6$) or HFD alone ($n = 6$) for 12 weeks. The mice were sacrificed, and liver tissue and serum were collected. Liver sections were stained with H&E (a) and Oil Red O (b). Image magnification ×200. TG contents in the liver (c), serum AST (d), and ALP (e) were analyzed. Data were present as mean ± SE, $^{*}P < 0.05$, $^{***}P < 0.001$ versus HFD mice.

(Table 2), the beneficial effect of the SNN extracts on body weight and liver weight was unlikely related to changes in satiety.

3.3. The SNN Extracts Improved Serum Lipid Profiles and Enzymes in NASH Mice. NASH mice developed hyperlipidemia after 16 weeks of HF-DSS feeding. Thus, the serum TC, TG, and LDL-c concentrations were increased as compared to that in chow diet fed controls (Figure 2). Treatment of mice with the SNN extracts for 4 weeks significantly reduced the serum TG concentration, whereas the serum TC concentration was restored to normal as compared to that in untreated NASH mice (Figures 2(a) and 2(b)). Unexpectedly, the level of HDL-c was significantly increased in NASH mice, while there were no differences in HDL-c between the SNN-treated and untreated groups (Figure 2(c)).

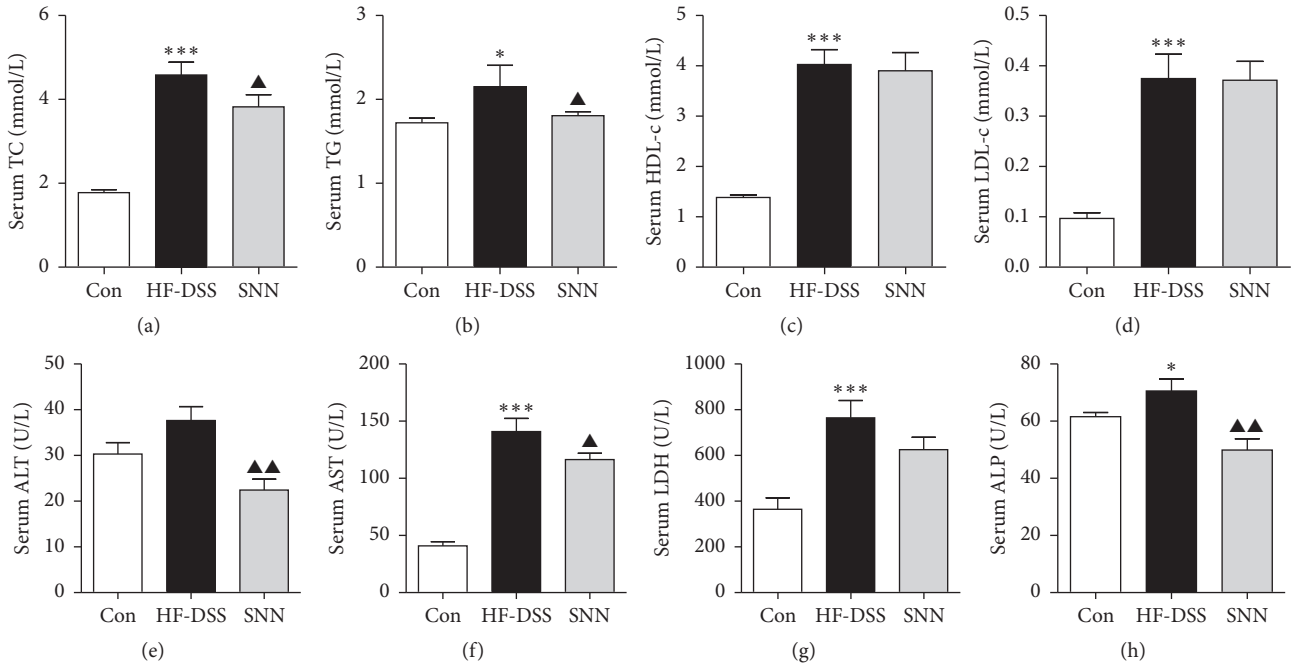

Figure 2: *The effect of SNN extracts on serum lipid profiles and enzymes*. Male C57Bl/6 mice (7 weeks of age) were fed HF-DSS diet for 12 weeks followed by either 4-week SNN ($n = 10$) or normal saline supplementation via gavage ($n = 10$), while chow diet mice were set as controls (Con, $n = 8$). The mice were sacrificed, blood was collected, and serum was separated. Serum TC (a), TG (b), HDL-c (c), and LDL-c (d) were analyzed; enzymes ALT (e), AST (f), LDH (g), and ALP (h) in serum were detected. Data were present as mean ± SE, $^{*}P < 0.05$, $^{***}P < 0.001$ versus Con mice; $^{\blacktriangle}P < 0.05$, $^{\blacktriangle\blacktriangle}P < 0.01$ versus HF-DSS (NASH) mice.

Liver enzymes (AST, ALP, and LDH) were significantly increased in mice fed HF-DSS diet, and the SNN extract treatment resulted in markedly decreased serum AST and ALP in these mice (Figures 2(f)–2(h)). There was no difference in serum ALT between NASH mice and chow diet fed mice. However, the SNN extract treated mice had lowered serum ALT compared with that in untreated NASH mice (Figure 2(e)).

3.4. The SNN Extracts Attenuated Hepatic Steatosis in NASH Mice. Upon HF-DSS dieting, mice developed obvious hepatic steatosis as demonstrated by histologic analysis using Oil Red O staining of the liver sections (Figure 3(a)). Increased hepatic TG and TC contents were in accordance with the observed histologic changes (Figures 3(b) and 3(c)). The hepatic steatosis was attenuated upon the SNN extracts treatment. Likewise, hepatic TG content was also markedly reduced in mice treated with the SNN extracts (Figure 3(b)). However, the SNN extracts treatment had no effect on hepatic TC concentration in NASH mice (Figure 3(c)).

3.5. SNN Treatment Ameliorated Liver Inflammation in NASH Mice. NASH mice developed hepatic steatosis and inflammation, and both of which were alleviated by the 4-week SNN extracts gavage (Figure 4(a)). Immunohistochemical (IHC) staining of liver sections of NASH mice showed that expression of F4/80, the membrane protein and an indicator of activated Kupffer cells, was decreased after the SNN extract treatment (Figure 4(b)). The mRNA concentrations of monocyte chemotactic protein 1 (MCP-1), IL-6, and TNF-α in the liver were significantly increased in NASH mice, and the increase was largely blocked by SNN extracts treatment (Figures 4(c)–4(e)).

3.6. Effect of the SNN Extracts Treatment on Gut Microbiota in NASH Mice. We performed 16s rDNA analysis using Illumine MiSeq and detected seven dominant phyla in the mouse feces, namely, Bacteroidetes, Firmicutes, Proteobacteria, Tenericutes, Deferribacteres, *TM7,* and Actinobacteria (Figure 5(a)). In NASH mice, the relative abundance of Firmicutes was significantly decreased and that of Bacteroidetes and Proteobacteria was significantly increased as compared to that in the control mice (Figures 5(b)–5(d)). Treatment with the SNN extracts for 4 weeks resulted in partial normalization of the decreased abundance of Firmicutes and increased abundance of Proteobacteria (Figures 5(b) and 5(d)). However, the bacterial diversity of the gut microbiota was not affected by the SNN extract treatment as suggested by the Shannon-Wiener curves (Figure 5(e)) and rarefaction curves (Figure 5(f)).

The major bacterial families identified in our analysis are shown in the hierarchical clustering heat map (Figure 5(g)). Altogether, 12 altered bacterial families were detected in NASH mice. With the SNN extract treatment, the relative abundance of Ruminococcaceae and Lachnospiraceae was increased, whereas the relative abundance of Desulfovibrionales and Campylobacterales was reduced in comparison to that in untreated NASH mice (Figure 5(g)).

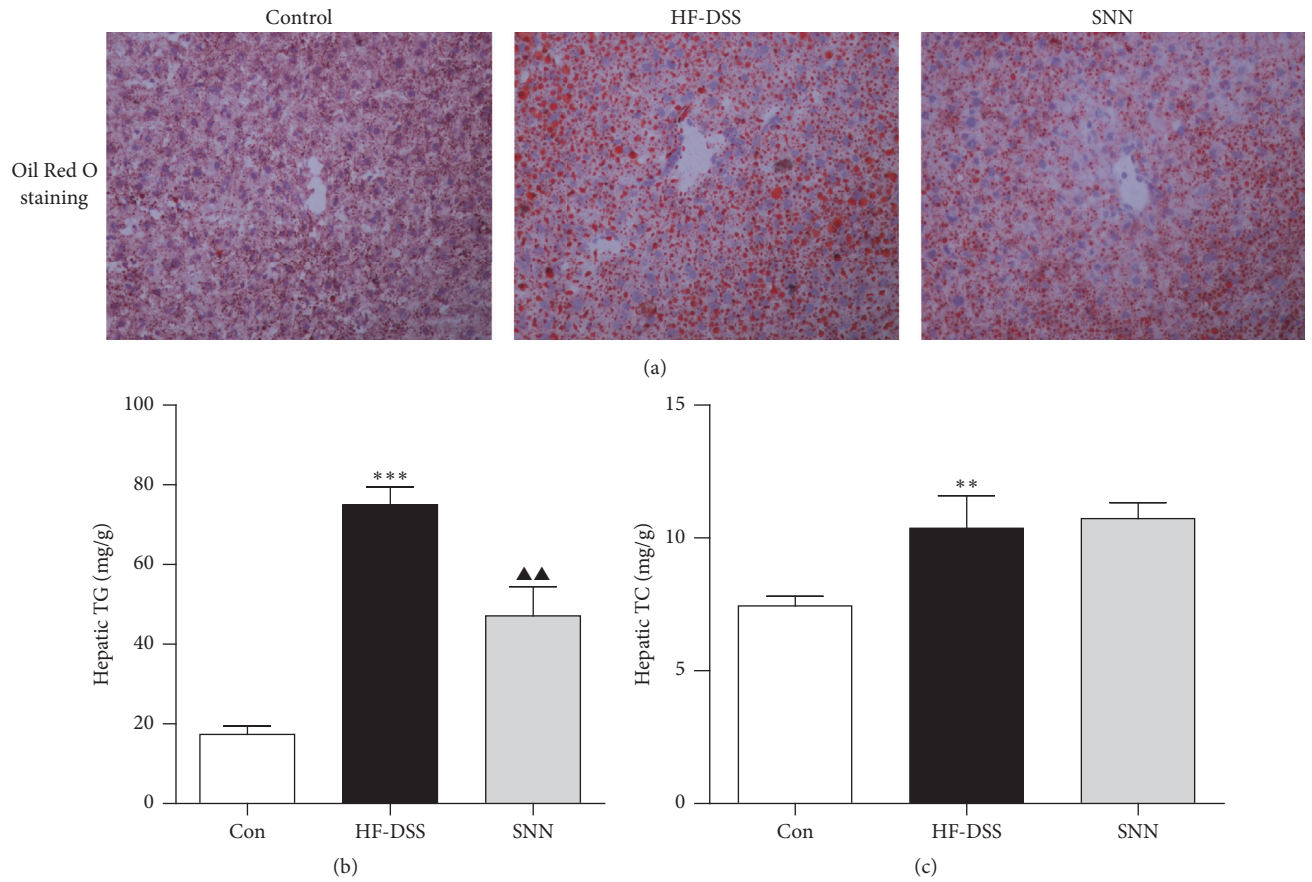

Figure 3: *The effect of SNN extracts on hepatic steatosis*. Male C57Bl/6 mice (7 weeks of age) were fed HF-DSS diet for 12 weeks followed by either 4-week SNN ($n = 10$) or normal saline supplementation via gavage ($n = 10$), while chow diet mice were set as controls (Con, $n = 8$). The mice were sacrificed, and liver tissues were collected and stained with Oil Red O (a). Image magnification ×200. Hepatic TG (b) and TC (c) were analyzed. Data were present as mean ± SE, $^{**}P < 0.01$, $^{***}P < 0.001$ versus Con mice; $^{▲▲}P < 0.01$ versus HF-DSS (NASH) mice.

3.7. The SNN Extracts Reduced Intestinal Injury and Blocked LPS Release. Gut-derived endotoxin may enter the circulation through damaged intestinal barrier. We next examined the integrity of the colon in NASH mice. Significant colon shortening was observed in these mice (Figure 6(a)), and architectural disruption of the crypts, increased severity of epithelial damage, and increased inflammation were detected in the colon sections (Figure 6(b)). Remarkably, the SNN extracts treatment was shown to protect the colons from this damage (Figures 6(a) and 6(b)). Further determination of proteins responsible for the integrity of intestinal barrier showed that the SNN extract treatment significantly increased the levels of ZO1, occludin, and claudin-1 (Figure 6(c)). Moreover, the elevated LPS and TNF-α levels observed in the NASH mice could be significantly attenuated by the SNN extracts treatment (Figures 6(d) and 6(e)).

3.8. LPS Aroused Inflammation in Kupffer Cells. We performed additional in vitro experiments to ascertain that LPS is responsible for the inflammatory response of hepatic macrophages. To this end, Kupffer cells were isolated from the mouse liver, and their phagocytic activity was validated by engulfment of fluorescently labeled beads (Figure 7(a)). Incubation Kupffer cells with LPS resulted in marked increase in TNF-α and IL-β mRNA, in a dose- (Figures 7(b) and 7(c)) and time-dependent (Figures 7(d) and 7(e)) manner. These in vitro data provide indirect support to the above in vivo observation (Figure 4) and suggest that gut-derived endotoxin may elicit proinflammatory response in the liver (through Kupffer cells).

3.9. SNN Treatment Regulated the TLR Signaling Pathway. Among the twelve functional TLRs present in mice, TLR2 and TLR4 are abundantly expressed in the liver. The mRNA of TLR2 and TLR4 was significantly increased in NASH mice. The TLR4 mRNA (Figure 8(a)) was decreased in the SNN extract treated mice, whereas the TLR2 mRNA was unchanged (Figure 8(b)). These results suggested that the SNN extracts might diminish the endotoxin effect.

Finally, we determined the effect of SNN extracts on the levels of key molecules involved in the TLR4/NF-κB pathway, namely, TLR4, TIRAP, IRAK1/4, and TRAF6. We found that the SNN extracts almost completely (e.g., TIRAP, TRAF6) or partially (e.g., TLR4, IRAK1, and IRAK4) restored the altered protein concentrations that occurred in the NASH mice (Figure 8(c)). Further analysis of members of the

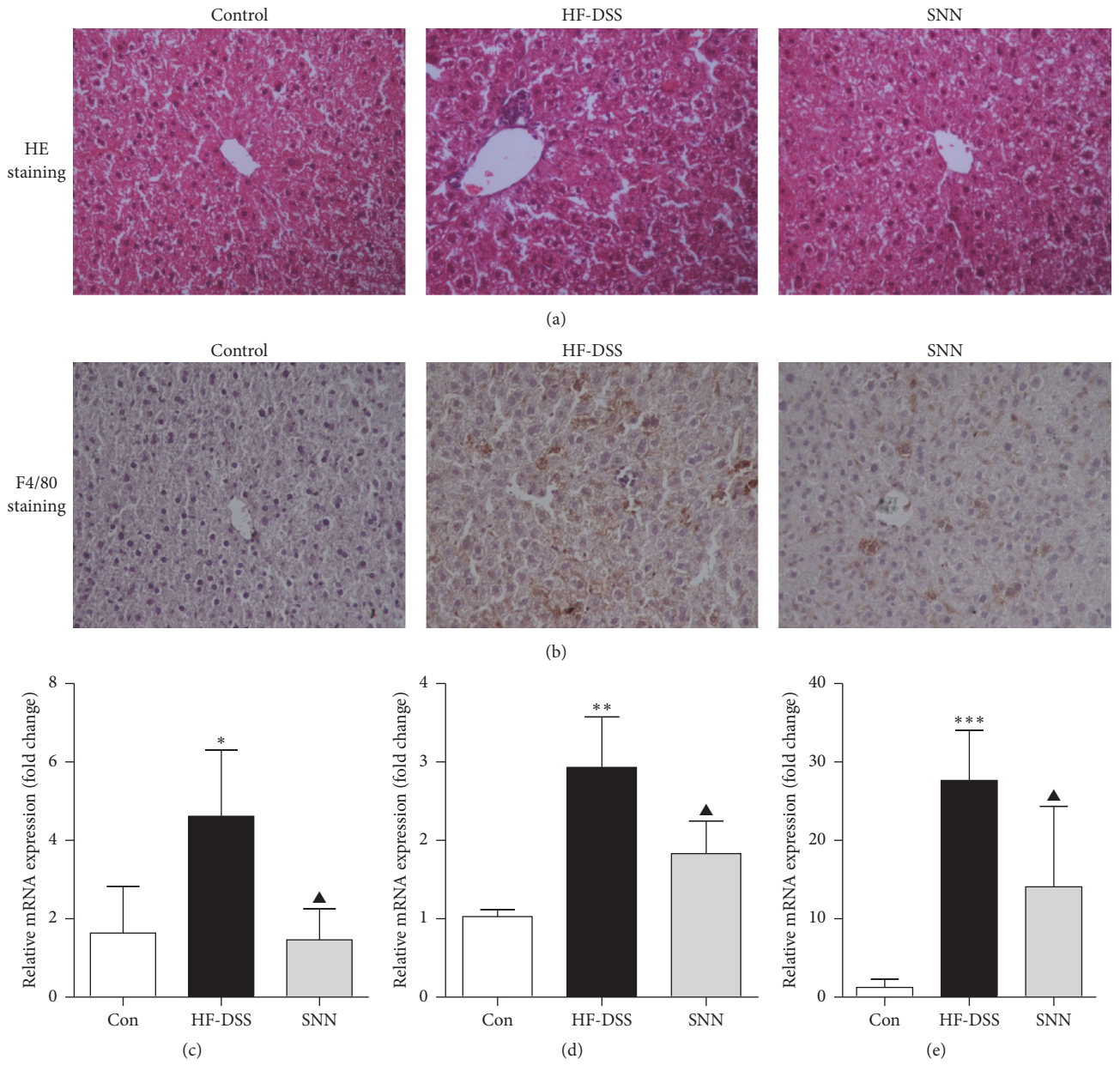

Figure 4: *The effect of SNN extracts on liver inflammation*. Male C57Bl/6 mice (7 weeks of age) were fed HF-DSS diet for 12 weeks followed by either 4-week SNN ($n = 10$) or normal saline supplementation via gavage ($n = 10$), while chow diet mice were set as controls (Con, $n = 8$). The mice were sacrificed, liver tissues were collected and stained with HE (a), and Kupffer cell activation was indicated by the F4/80 IHC (b). Image magnification ×200. Hepatic IL-6 (c), MCP-1 (d), and TNFα (e) mRNA was qualified by qRT-PCR. Data were present as mean ± SE, $^{*}P < 0.05$, $^{**}P < 0.01$, and $^{***}P < 0.001$ versus Con mice; $^{\blacktriangle}P < 0.05$ versus HF-DSS (NASH) mice.

NF-κB transcription factor family (such as p65) and their phosphorylate status showed increased phosphorylation of IκB and p65 in the livers of NASH mice, and the SNN extracts blunted IκB and p65 phosphorylation (Figure 8(d)). These results together suggest that the SNN extracts can inhibit TLR4/NF-κB activation.

4. Discussion

NASH is becoming the leading cause of chronic liver diseases and could result in an increase in the overall and liver-related mortality. In the present study, we demonstrated that the herbal medicine formula SNN inhibited the release of gut-derived endotoxin and blocked TLR4 mediated NF-κB activation in a mouse model of NASH, thus demonstrating the protective effect of SNN on NAFLD progression.

Accumulating evidence indicates that gut microbiota is associated with the development of NASH [15, 16]. It is reported that NAFLD patients, and in particular those with NASH, are more likely to have increased intestinal permeability compared with healthy controls [17]. Intervention of intestinal microbiota with antibiotic or prebiotics has

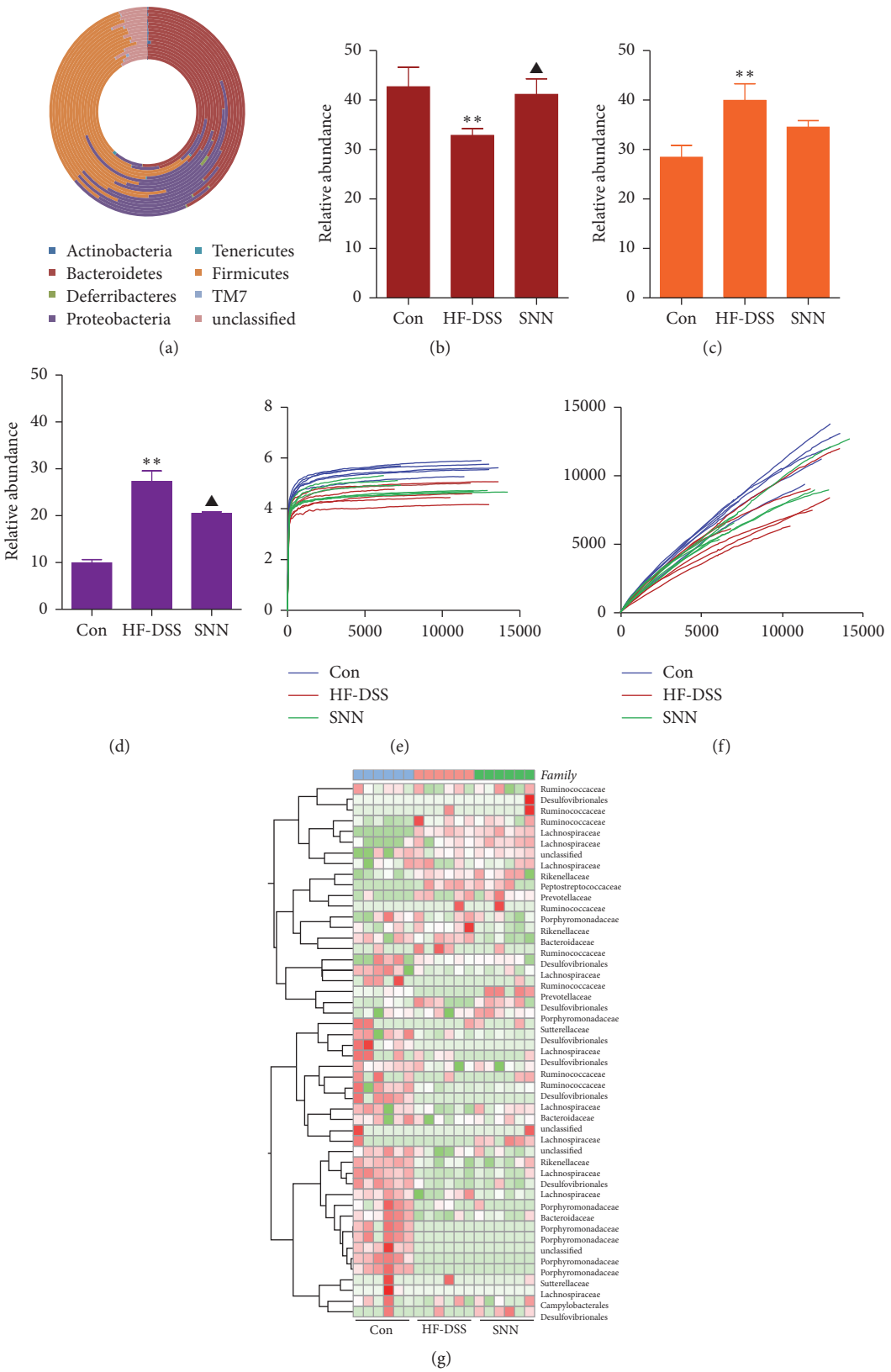

FIGURE 5: *The effect of SNN on the composition of gut microbiota*. Fresh feces were collected from the ileocecal region of the mice, and taxonomic structure of 16s rRNA gene was assessed using the Illumina MiSeq platform ($n = 6$ per group) and the species at phylum level were demonstrated (a); the alterations of Firmicutes (b), Bacteroidetes (c), and Proteobacteria (d) were indicated. Bacterial diversity was shown by Shannon curves (e) and Refraction curves (f). Key OTUs indicating genus-level changes based on the genus composition and abundance were generated (g). The relative abundance of each genus was indicated by a gradient of color from green (low abundance) to red (high abundance). Data were present as mean ± SE, $^{**}P < 0.01$ versus Con mice; $^{▲}P < 0.05$ versus HF-DSS (NASH) mice.

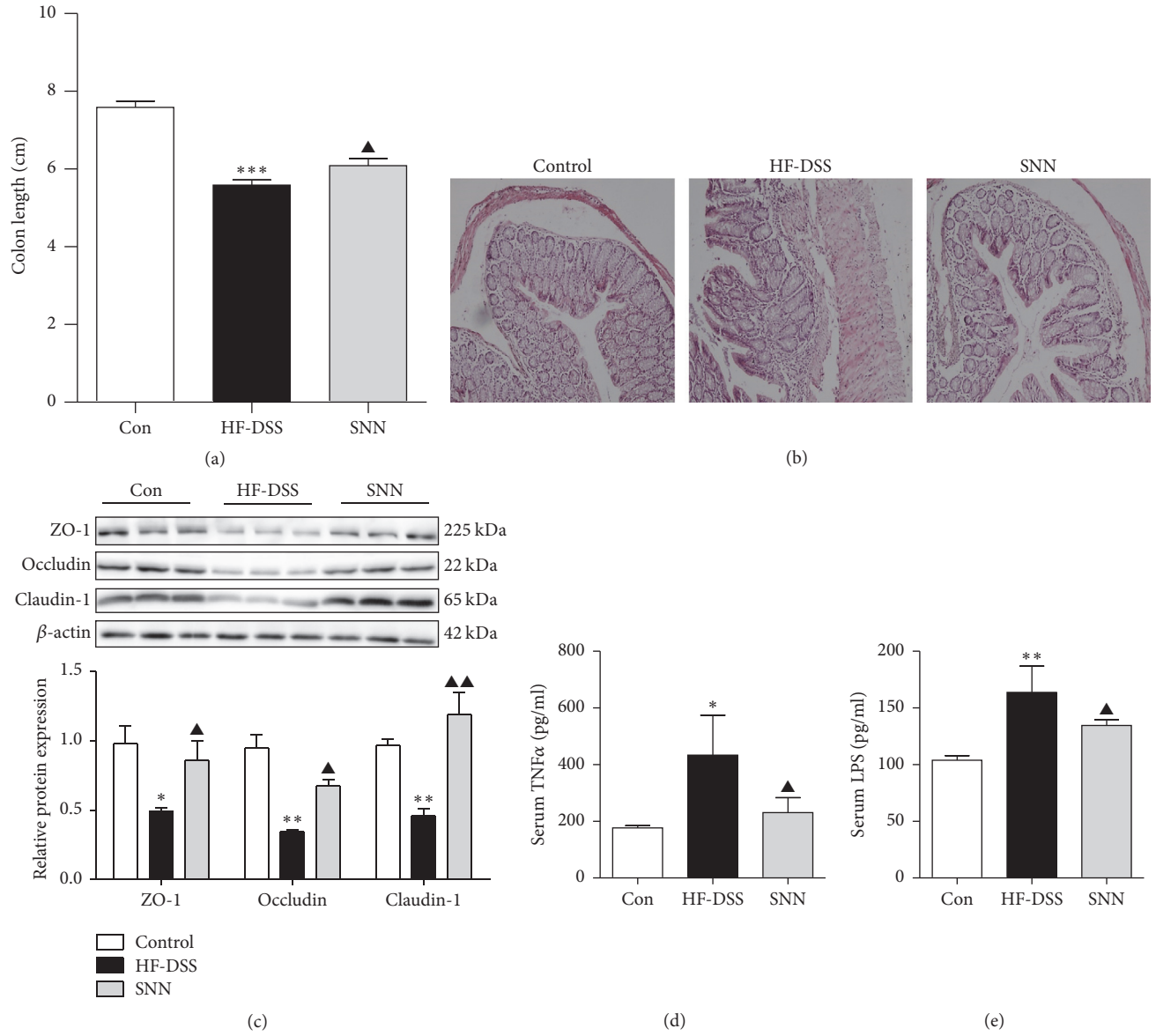

Figure 6: *The effect of SNN on intestinal injury and LPS release*. The colons of the mice were collected, the length was recorded (a), and the colon sections were further stained with HE (b). TJ proteins including ZO1, Occludin, and Claudin 1 were analyzed by Western blot (c). Circulating TNFα (d) and LPS (e) levels were detected by ELISA kits. Original magnification of representative images, ×200; data were present as mean ± SE, $^{*}P < 0.05$, $^{**}P < 0.01$, and $^{***}P < 0.001$ versus Con mice; $^{\blacktriangle}P < 0.05$, $^{\blacktriangle\blacktriangle}P < 0.01$ versus HF-DSS (NASH) mice.

been proved to be beneficial for NAFLD/NASH patients, indicating that the change of intestinal environment could affect NAFLD development and progression [18, 19]. Imbalances in the structure of the gut microbiota induced by HFD consumption may impair the integrity of gut barrier and increase the levels of endotoxin in liver through the portal vein [20]. Therefore, the gut microbiota represents a potential target of therapeutic drugs or nutritional interventions. We have identified SNN which acted on restoring the increase of opportunistic pathogens. Prebiotics or probiotics are reported to selectively modulate of the structure of gut microbiota, thus contributing to the improvement of intestinal function. The natural product berberine has been proved to prevent metabolic conditions (i.e., obesity, insulin resistance, and type 2 diabetes) in animals and patients, and gut microbiota modulation is thought to be the key mechanism.

Intestinal permeability is regulated by tight junctions (TJ); among the identified TJ, the transmembrane proteins occludin, claudins, and cytoplasmic proteins zonula occludens 1 (ZO-1) are considered crucial in regulating intestinal permeability [21]. Dysfunction of intestinal barrier can facilitate the hepatic entrance of intestinal microorganisms including LPS [6]. LPS is a component of the outer wall of Gram-negative bacteria, and itself can induce the intestinal barrier dysfunction and epithelial cells injury. We have compared 12-week HF-DSS diet with HFD feeding to the mice and confirmed that increased intestinal permeability accelerates

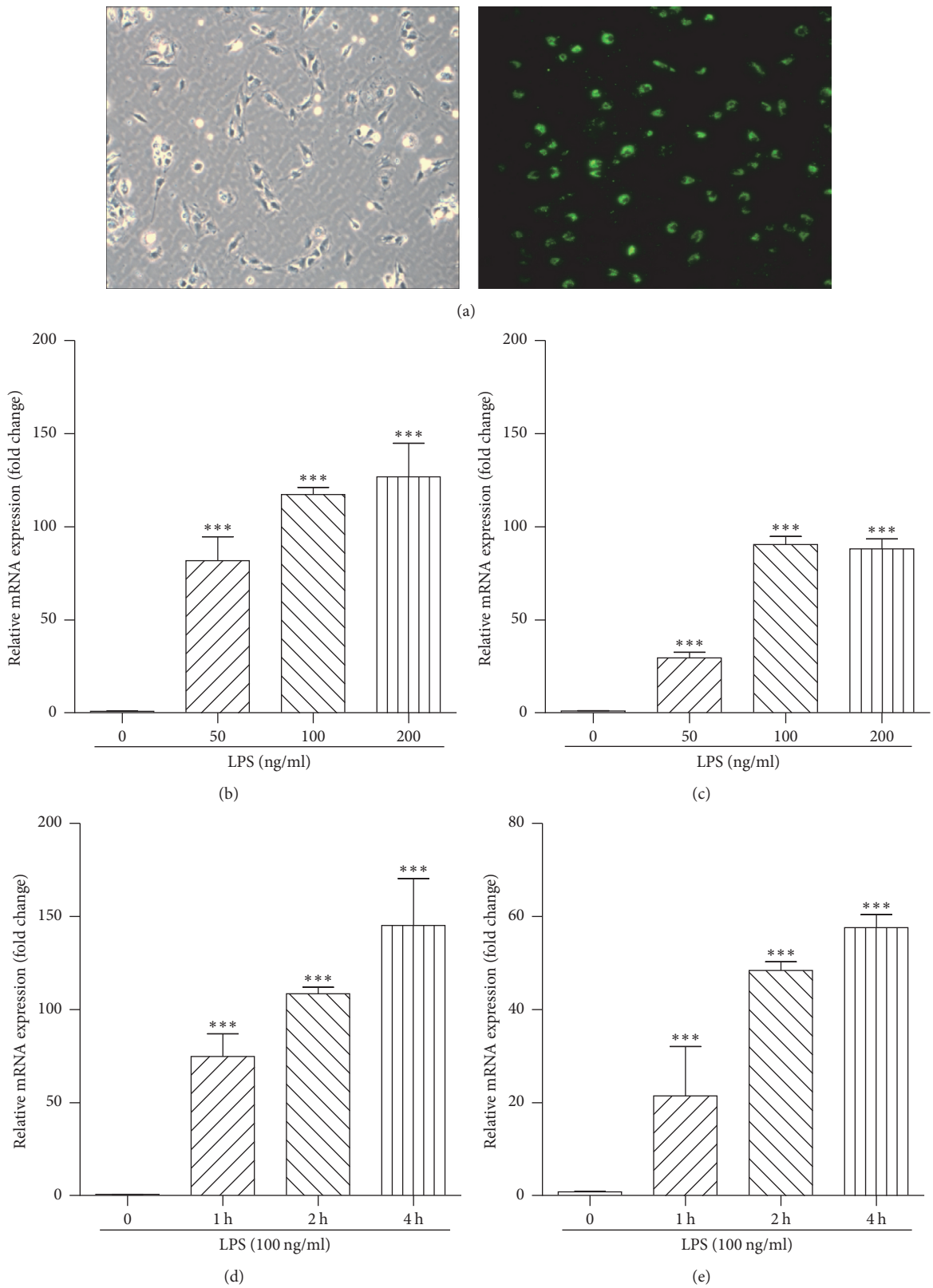

Figure 7: *LPS induced inflammation in Kupffer cells*. Kupffer cells were isolated from C57BL/6 mice and identified by fluorescently labeled beads (a). Kupffer cells were treated with LPS (50, 100, and 200 ng/ml) for 2 h, and mRNA expression of TNFα (b) and IL-β (c) in the cells was qualified by qRT-PCR. Kupffer cells were treated with LPS (100 ng/ml), and the cells were collected at different time points (1 h, 2 h, and 4 h). Cellular TNFα (d) and IL-β (e) mRNA expression was analyzed by qRT-PCR. Original magnification of representative images, ×200; data were present as mean ± SE, $^{***}P < 0.001$ versus cells cultured with routine medium.

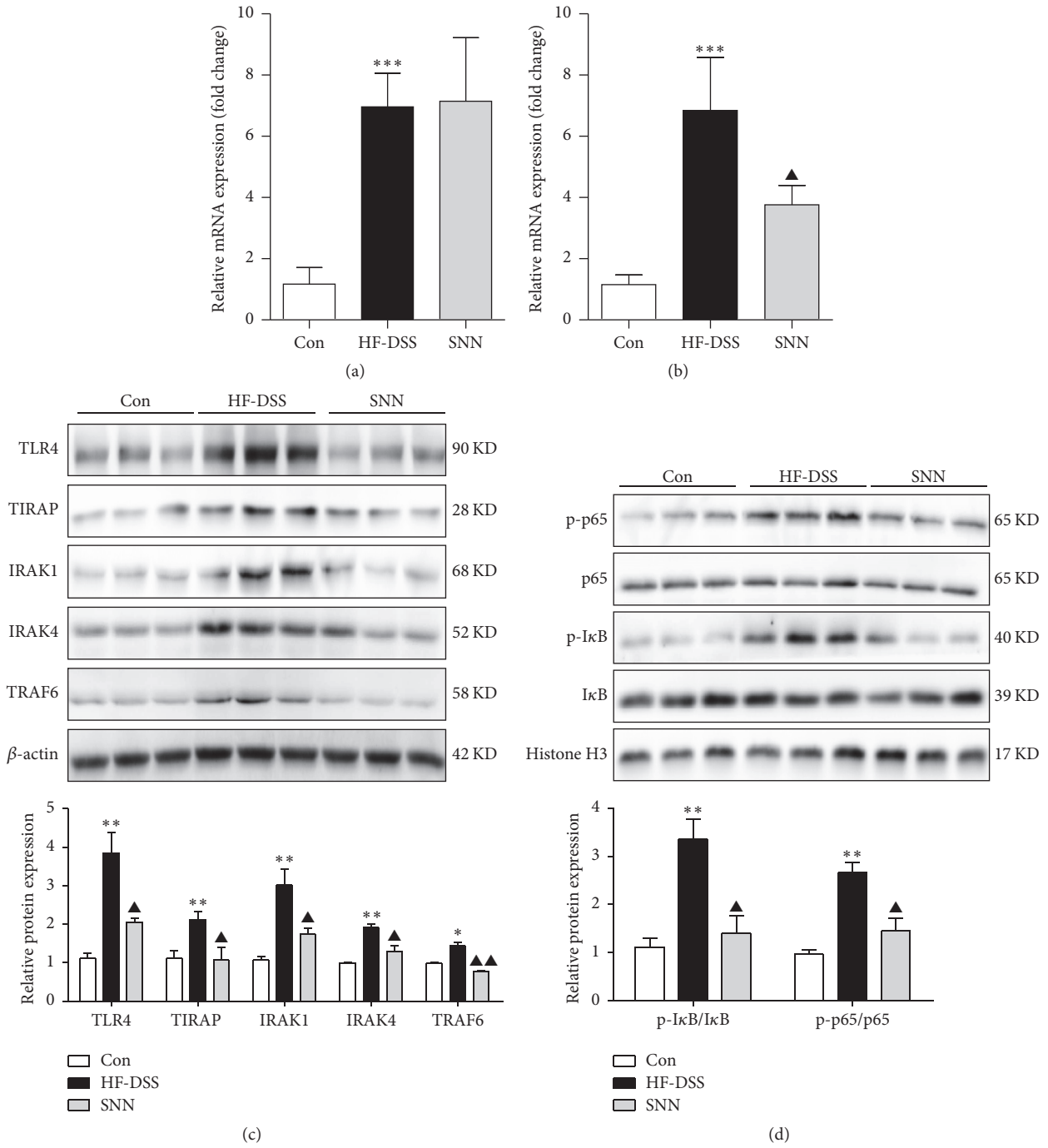

Figure 8: *The effect of SNN on TLR4 mediated NF-κB activation*. The livers of the mice were collected, and the mRNA expressions of hepatic TLR2 (a) and TLR4 (b) were analyzed by qRT-PCR, and the key molecules in TLR4/NF-κB pathway were detected by Western blot (c and d). Data were presented as mean ± SE, $n = 3$–6, $^{*}P < 0.05$, $^{**}P < 0.01$, and $^{***}P < 0.001$ versus Con mice; $^{\blacktriangle}P < 0.05$, $^{\blacktriangle\blacktriangle}P < 0.01$ versus HF-DSS (NASH) mice.

the development of NASH, indicating that endotoxin release to liver was a potential risk factor for liver inflammation.

Circulating levels of gut-derived LPS are increased in NAFLD patients [22]. We have isolated Kupffer cells from the mice, incubated the cells along with LPS, and detected increased TNF-α and IL-1β expression in time and dose dependent manner. Our results were consistent with reports which showed that injection of LPS to mice can induce inflammatory response in the liver [23, 24].

The innate immune response provides the first line of host defense against invading pathogens. This response is triggered by the activation of PRRs. Among the growing family of PRRs, TLRs play a fundamental role in the primary response against invaders [7]. The specific detection of PAMPs and

DAMPs by host receptors drives a cascade of signaling that converges at NF-κB and induces the secretion of proinflammatory cytokines. The activation of NF-κB typically involves phosphorylation of IκB by the inhibitor of nuclear factor-κB kinase (IKK) complex. The phosphorylation of IκB leads to its ubiquitylation and subsequent degradation, which allows the release of NF-κB and its translocation to the nucleus. The most common heterodimer of NF-κB is P65/P50 complex; subsequent to its translocation, P65 undergoes site-specific posttranslational modifications to further enhance the function [25]. We have analyzed the key molecules in the cascade pathway and found that SNN could inhibit the protein expression of TLR4, TIRAP, IRAK1/4, and TRAF6, which facilitate the phosphorylation of IκB and activation of NF-κB. These changes were consistent with the alteration of cytokines in both serum and liver tissues, further indicating that SNN specifically blocks LPS related hepatic inflammation. Suppression of LPS/TLR4/NF-κB pathway has been reported to be beneficial for inflammatory diseases, and many natural products, such as berberine, curcumin, and resveratrol, have been identified to be potential inhibitors of such cascade [26–28].

TLRs act as a double-edged sword: deficient TLR signaling might render the organism vulnerable to exposure to pathogenic attack, while an excessive TLR response, such as activation of TLR4 on the Kupffer cells, results in uncontrolled release of a range of proinflammatory cytokines and chemokines [29]. SNN is a safe therapeutic agent because it has been used for decades in China. Our previous basic research and clinical trial also showed that SNN is safe and effective in treating rodents and patients with NAFLD [10, 11]. However, since gut microbiota alteration could induce LPS, while chemically intestinal damage accelerates LPS release to the liver, the restored TLR4/NF-κB pathway on the SNN extracts treatment might be secondary to the blockage of LPS release from the intestine.

5. Conclusions

In summary, we identified that intestinal damage could accelerate the development of NASH, and the herbal medicine formula, SNN, significantly attenuated liver steatosis and inflammation in experimental mice. By improving intestinal environment and hepatic endotoxin entrance, SNN acts on TLR4/NF-κB pathway associated with NASH pathological progression. Our findings supported a beneficial role of SNN and indicated that SNN might be an effective therapeutic strategy against NAFLD progression.

Conflicts of Interest

The authors declare that they have no conflicts of interest.

Acknowledgments

The authors' sincere gratitude is extended to Dr. Haiyan Song for her valuable suggestions. This study was supported by the National Nature Science Foundation of China (no. 81620108030), Shanghai Rising-Star Program (no. 17QA1404000), and Natural Science Foundation of Shanghai (no. 14ZR144160).

References

[1] Z. M. Younossi, A. B. Koenig, D. Abdelatif, Y. Fazel, L. Henry, and M. Wymer, "Global epidemiology of nonalcoholic fatty liver disease—meta-analytic assessment of prevalence, incidence, and outcomes," *Hepatology*, vol. 64, no. 1, pp. 73–84, 2015.

[2] R. J. Wong, M. Aguilar, R. Cheung et al., "Nonalcoholic steatohepatitis is the second leading etiology of liver disease among adults awaiting liver transplantation in the United States," *Gastroenterology*, vol. 148, no. 3, pp. 547–555, 2015.

[3] C. K. Argo, P. G. Northup, A. M. S. Al-Osaimi, and S. H. Caldwell, "Systematic review of risk factors for fibrosis progression in non-alcoholic steatohepatitis," *Journal of Hepatology*, vol. 51, no. 2, pp. 371–379, 2009.

[4] G. Ferrere, A. Leroux, L. Wrzosek et al., "Activation of kupffer cells is associated with a specific dysbiosis induced by fructose or high fat diet in mice," *PLoS ONE*, vol. 11, no. 1, Article ID e0146177, 2016.

[5] K. Imajo, K. Fujita, M. Yoneda et al., "Hyperresponsivity to low-dose endotoxin during progression to nonalcoholic steatohepatitis is regulated by leptin-mediated signaling," *Cell Metabolism*, vol. 16, no. 1, pp. 44–54, 2012.

[6] N. Matsushita, T. Osaka, I. Haruta et al., "Effect of lipopolysaccharide on the progression of non-alcoholic fatty liver disease in high caloric diet-fed mice," *Scandinavian Journal of Immunology*, vol. 83, no. 2, pp. 109–118, 2016.

[7] T. Sharifnia, J. Antoun, T. G. C. Verriere et al., "Hepatic TLR4 signaling in obese NAFLD," *American Journal of Physiology—Gastrointestinal and Liver Physiology*, vol. 309, no. 4, pp. G270–G278, 2015.

[8] J.-Y. Xu, L. Zhang, Z.-P. Li, and G. Ji, "Natural products on nonalcoholic fatty liver disease," *Current Drug Targets*, vol. 16, no. 12, pp. 1347–1355, 2015.

[9] J. Pan, M. Wang, H. Song, L. Wang, and G. Ji, "The efficacy and safety of Traditional Chinese Medicine (Jiang Zhi Granule) for nonalcoholic fatty liver: a multicenter, randomized, placebo-controlled study," *Evidence-Based Complementary and Alternative Medicine*, vol. 2013, Article ID 965723, 8 pages, 2013.

[10] L. Zhang, J. Xu, H. Song, Z. Yao, and G. Ji, "Extracts from Salvia-Nelumbinis naturalis alleviate hepatosteatosis via improving hepatic insulin sensitivity," *Journal of Translational Medicine*, vol. 12, no. 1, article 236, 2014.

[11] Y. Liu, H. Song, L. Wang et al., "Hepatoprotective and antioxidant activities of extracts from Salvia-Nelumbinis naturalis against nonalcoholic steatohepatitis induced by methionine- and choline-deficient diet in mice," *Journal of Translational Medicine*, vol. 12, no. 1, p. 315, 2014.

[12] Y.-L. Lu, M. Wang, L. Zhang et al., "Simultaneous determination of six components in the 'Jiang-Zhi' granule by UPLC-MS analysis," *Chinese Journal of Natural Medicines*, vol. 8, no. 6, pp. 449–455, 2010.

[13] M. Li, X. Shu, H. Xu et al., "Integrative analysis of metabolome and gut microbiota in diet-induced hyperlipidemic rats treated with berberine compounds," *Journal of Translational Medicine*, vol. 14, no. 1, article no. 237, 2016.

[14] X. Zhang, W.-P. Yu, L. Gao, K.-B. Wei, J.-L. Ju, and J.-Z. Xu, "Effects of lipopolysaccharides stimulated Kupffer cells on activation of rat hepatic stellate cells," *World Journal of Gastroenterology*, vol. 10, no. 4, pp. 610–613, 2004.

[15] J. S. Park, J. H. Seo, and H.-S. Youn, "Gut microbiota and clinical disease: obesity and nonalcoholic fatty liver disease," *Pediatric Gastroenterology, Hepatology and Nutrition*, vol. 16, no. 1, pp. 22–27, 2013.

[16] L. Zhu, R. D. Baker, and S. S. Baker, "Gut microbiome and nonalcoholic fatty liver diseases," *Pediatric Research*, vol. 77, pp. 245–251, 2015.

[17] L. Miele, V. Valenza, G. La Torre et al., "Increased intestinal permeability and tight junction alterations in nonalcoholic fatty liver disease," *Hepatology*, vol. 49, no. 6, pp. 1877–1887, 2009.

[18] F. Mofidi, H. Poustchi, Z. Yari et al., "Synbiotic supplementation in lean patients with non-alcoholic fatty liver disease: a pilot, randomised, double-blind, placebo-controlled, clinical trial," *British Journal of Nutrition*, vol. 117, no. 05, pp. 662–668, 2017.

[19] K. Celinski, P. C. Konurek, M. Slomka et al., "Effects of treatment with melatonin and tryptophan on liver enzymes, parameters of fat metabolism and plasma levels of cytokines in patients with non-alcoholic fatty liver disease - 14 months follow up," *Journal of Physiology and Pharmacology*, vol. 65, no. 1, pp. 75–82, 2014.

[20] K. M. Schneider, V. Bieghs, F. Heymann et al., "CX3CR1 is a gatekeeper for intestinal barrier integrity in mice: limiting steatohepatitis by maintaining intestinal homeostasis," *Hepatology*, vol. 62, no. 5, pp. 1405–1416, 2015.

[21] R.-Y. Lu, W.-X. Yang, and Y.-J. Hu, "The role of epithelial tight junctions involved in pathogen infections," *Molecular Biology Reports*, vol. 41, no. 10, pp. 6591–6610, 2014.

[22] V. W.-S. Wong, G. L.-H. Wong, H.-Y. Chan et al., "Bacterial endotoxin and non-alcoholic fatty liver disease in the general population: a prospective cohort study," *Alimentary Pharmacology and Therapeutics*, vol. 42, no. 6, pp. 731–740, 2015.

[23] S. Ceccarelli, N. Panera, M. Mina et al., "LPS-induced TNF-α factor mediates pro-inflammatory and pro-fibrogenic pattern in non-alcoholic fatty liver disease," *Oncotarget*, vol. 6, no. 39, pp. 41434–41452, 2015.

[24] J. H. Guo, D. W. Han, L. i. XQ, Y. Zhang, and Y. C. Zhao, "The impact of small doses of LPS on NASH in high sucrose and high fat diet induced rats," *Eur Rev Med Pharmacol Sci*, vol. 18, no. 18, pp. 2742–2747, 2014.

[25] O. Morris, X. Liu, C. Domingues et al., "Signal Integration by the IκB Protein Pickle Shapes Drosophila Innate Host Defense," *Cell Host and Microbe*, vol. 20, no. 3, pp. 283–295, 2016.

[26] M.-Y. Gao, L. Chen, L. Yang, X. Yu, J.-P. Kou, and B.-Y. Yu, "Berberine inhibits LPS-induced TF procoagulant activity and expression through NF-κB/p65, Akt and MAPK pathway in THP-1 cells," *Pharmacological Reports*, vol. 66, no. 3, pp. 480–484, 2014.

[27] W. Zhong, K. Qian, J. Xiong, K. Ma, A. Wang, and Y. Zou, "Curcumin alleviates lipopolysaccharide induced sepsis and liver failure by suppression of oxidative stress-related inflammation via PI3K/AKT and NF-κB related signaling," *Biomedicine and Pharmacotherapy*, vol. 83, pp. 302–313, 2016.

[28] H. Zhang, Q. Sun, T. Xu et al., "Resveratrol attenuates the progress of liver fibrosis via the Akt/nuclear factor-κB pathways," *Molecular Medicine Reports*, vol. 13, no. 1, pp. 224–230, 2016.

[29] D. Ye, F. Y. L. Li, K. S. L. Lam et al., "Toll-like receptor-4 mediates obesity-induced non-alcoholic steatohepatitis through activation of X-box binding protein-1 in mice," *Gut*, vol. 61, no. 7, pp. 1058–1067, 2012.

Hindawi
Evidence-Based Complementary and Alternative Medicine
Volume 2017, Article ID 7282653, 9 pages
https://doi.org/10.1155/2017/7282653

Research Article

Hesperidin Protects against Acute Alcoholic Injury through Improving Lipid Metabolism and Cell Damage in Zebrafish Larvae

Zhenting Zhou,[1] Weichao Zhong,[1,2] Haiyan Lin,[1] Peng Huang,[1] Ning Ma,[3] Yuqing Zhang,[3] Chuying Zhou,[1] Yuling Lai,[1] Shaohui Huang,[1] Shiying Huang,[1] Lei Gao,[1,4] and Zhiping Lv[1]

[1]*School of Traditional Chinese Medicine, Southern Medical University, Guangzhou, Guangdong, China*
[2]*Department of Liver Diseases, Shenzhen Traditional Chinese Medicine Hospital, Shenzhen, Guangdong, China*
[3]*Key Laboratory of Zebrafish Modeling and Drug Screening for Human Diseases of Guangdong Higher Education Institutes, Department of Developmental Biology, Institute of Genetic Engineering, School of Basic Medical Sciences, Southern Medical University, Guangzhou, Guangdong, China*
[4]*The Key Laboratory of Molecular Biology, State Administration of Traditional Chinese Medicine, School of Traditional Chinese Medicine, Southern Medical University, Guangzhou, Guangdong, China*

Correspondence should be addressed to Lei Gao; rayg@foxmail.com and Zhiping Lv; lzp48241@126.com

Received 22 December 2016; Revised 3 April 2017; Accepted 18 April 2017; Published 17 May 2017

Academic Editor: Elzbieta Janda

Alcoholic liver disease (ALD) is a series of abnormalities of liver function, including alcoholic steatosis, steatohepatitis, and cirrhosis. Hesperidin, the major constituent of flavanone in grapefruit, is proved to play a role in antioxidation, anti-inflammation, and reducing multiple organs damage in various animal experiments. However, the underlying mechanism of resistance to alcoholic liver injury is still unclear. Thus, we aimed to investigate the protective effects of hesperidin against ALD and its molecular mechanism in this study. We established an ALD zebrafish larvae model induced by 350 mM ethanol for 32 hours, using wild-type and transgenic line with liver-specific eGFP expression *Tg (lfabp10α:eGFP)* zebrafish larvae (4 dpf). The results revealed that hesperidin dramatically reduced the hepatic morphological damage and the expressions of alcohol and lipid metabolism related genes, including *cyp2y3*, *cyp3a65*, *hmgcra*, *hmgcrb*, *fasn, and fads2* compared with ALD model. Moreover, the findings demonstrated that hesperidin alleviated hepatic damage as well, which is reflected by the expressions of endoplasmic reticulum stress and DNA damage related genes (*chop*, *gadd45αa,* and *edem1*). In conclusion, this study revealed that hesperidin can inhibit alcoholic damage to liver of zebrafish larvae by reducing endoplasmic reticulum stress and DNA damage, regulating alcohol and lipid metabolism.

1. Introduction

Hepatic steatosis is the early stage of alcoholic liver disease (ALD) induced by alcoholic consumption. ALD is an important component of liver diseases [1]. ALD involves the processes of hepatic pathological states, from simple hepatic steatosis to progressive fibrosis, cirrhosis, and even liver cancer [2]. Given that the prevalence of ALD worldwide is rising these years, exploring an effective treatment is of great importance.

Hesperidin, a kind of citrus bioflavonoid and abundant in citrus plants, including grapefruits, oranges, and lemons, is proved to play a role in antioxidation, anti-inflammation, and cardiovascular protection [3]. In addition, hesperidin regulates hepatic cholesterol synthesis by inhibiting the activity of 3-hydroxy-3-methyl-glutaryl-CoA (HMG-CoA) reductase [4, 5]. Recently, it is confirmed that hesperidin protects against fatty liver induced by high-cholesterol diet through mediating the mRNA expressions of *rbp*, *c-fabp*, and *h-fabp*, inhibiting synthesis and absorption of cholesterol [6]. Hesperidin is also capable of attenuating liver fibrosis by mitigating oxidative stress and modulating proinflammatory and profibrotic signals [7]. However, the effects of hesperidin on alcohol-induced hepatic steatosis need

further investigation and its underlying mechanisms remain unknown.

Taking into consideration findings mentioned above, we investigated the protective role of hesperidin in alcohol-induced liver injury of zebrafish larvae in the present study. We revealed the underlying mechanism of hesperidin against dyslipidemia and hepatocytes damage in ALD by evaluating the expression of some key genes related to alcohol and lipid metabolism. Furthermore, morphological observation of the whole bodies and livers of zebrafish larvae also showed the protective role of hesperidin in pathological changes caused by alcohol. First, we investigated the regulation of hesperidin on both alcohol metabolism and lipid homeostasis in zebrafish larvae ALD model and further drew the conclusion that hesperidin could resist to alcohol-induced metabolic abnormalities. Collectively, the results proved the abilities of hesperidin to reduce lipid accumulation and further demonstrated it could improve alcohol and lipid metabolism as well as hepatic steatosis. In a word, we hypothesize that citrus flavonoids are an effective treatment of ALD-related metabolic pathways through the ability of regulation of hesperidin on alcohol metabolism, lipid homeostasis, and liver damage.

2. Material and Methods

2.1. Animal Care and Treatment. Wild-type (WT) AB strain zebrafish and *Tg (lfabp10α:eGFP)* transgenics, obtained from Key Laboratory of Zebrafish Modeling and Drug Screening for Human Diseases of Guangdong Higher Education Institutes, Southern Medical University and School of Life Science, Southwest University, respectively, were cultured on a 14 h light/10 h dark cycle at 28°C following established protocols *(Westerfield M 2000 The Zebrafish Book: A Guide for the Laboratory Use of Zebrafish (Danio rerio). Eugene: Univ. of Oregon Press)*. The Institutional Animal Care and Use Committee of Southern Medical University approved all the protocols of zebrafish operations.

96–98 hours after fertilization (hpf) zebrafish larvae were first randomly divided into two groups, a control group treated with system water (water out of the water system of culture facility for zebrafish) only and a model group exposed to 350 mM ethanol for 32 h [8]. Subsequently, the control larvae were randomly divided into two groups (n = 40 in each group): a control group (treated with system water) and a hesperidin control group (treated with 25 μg/mL hesperidin). Simultaneously, the model larvae were randomly assigned into several groups as followed equally (n = 40 in each group): a model group (treated with system water) and 3 hesperidin treated groups (25 μg/mL, 12.5 μg/mL, and 6.25 μg/mL). Hesperidin monomer was dissolved in 0.1% DMSO (diluted in system water). After being incubated for 48 h, larvae were collected for further detection. The experimental plan for zebrafish is shown in Figure 1.

2.2. Oil Red O Staining. Zebrafish larvae of each group were collected and fixed with 4% paraformaldehyde (PFA) overnight at 4°C, washed 3 times with phosphate-buffered saline (PBS), and infiltrated sequentially with 20%, 40%, 80%, and 100% propylene glycol (Sigma, USA) at room temperature for 15 min, respectively. Subsequently, the larvae were stained with 0.5% Oil Red O (Sigma, USA) in 100% propylene glycol in the dark for 1 h at 65°C. Then the samples were destained by soak sequentially in 100%, 80%, 40%, and 20% propylene glycol for 30 min, respectively, and washed 3 times with PBS, followed by storing in 70% glycerol (Sigma, USA) [9]. The hepatic morphology and lipid droplets in liver were observed and imaged with microscope (Olympus szx10, Tokyo, Japan). In this study, staining shade and liver size were quantized into gray values by Image J software in order to reflect the degree of hepatic steatosis.

2.3. Nile Red Staining. The procedures were performed as previously described [10, 11]. Zebrafish larvae were fixed with 4% PFA as described previously and incubated in citric acid with 0.1% Triton (Sigma, USA) for 2 hours at 65°C after being washed with PBS 3 times. DAPI (Solarbio Life Science, China) was counterstained in the dark for 10 minutes at room temperature to stain the nuclei. Subsequently Nile Red dye (0.5 μg/mL in acetone, Sigma, USA) was used to stain the lipid droplets in liver, incubated in the dark for 50 minutes at room temperature, and washed 3 times with PBS. The stained larvae were imaged with Confocal Laser Scanning Microscope (Nikon C2plus, Tokyo, Japan).

2.4. Histologic Analysis. Zebrafish larvae were fixed with 4% PFA overnight, penetrated with ethanol and xylene respectively, embedded in paraffin, cut into 4 μm thick sections, stained with H&E, and observed with microscope (Nikon Eclipse Ni-U, Tokyo, Japan).

2.5. Quantitative Real-Time PCR. The procedure was performed according to the previous study [12]. Total RNA was extracted from 10 zebrafish larvae using Trizol reagent (Invitrogen, USA) following the standard procedures and subsequently reverse-transcribed with qScript cDNA using PrimeScript™ RT-PCR Kit (Takara). qPCR was carried out on Light Cycler 96 (Roche, Switzerland) using a SYBR Green kit (Takara Biotechnology, Inc.). The detailed protocol outlined by the manufacturer's instructions was followed. The levels of target genes were calculated by the comparative CT method and normalized to the reference gene *rpp0* (ribosomal protein P0). Primers for each gene are listed in Table 1.

2.6. Statistical Analysis. All data are presented as mean ± standard error of the mean (SEM). Statistical analysis was carried by SPSS (version 20.0). Statistical differences were evaluated by Student's t-test and one-way ANOVA test. Value of $P < 0.05$ was considered to be statistically significant. GraphPad Prism 5 software was used to plot graph.

3. Results

3.1. Alcoholic Fatty Liver Model Was Established in Zebrafish Larvae. 96–98 hpf zebrafish larvae were chosen to be exposed to ethanol during a window, which was the stage from the formation of liver to the full utilization of yolk

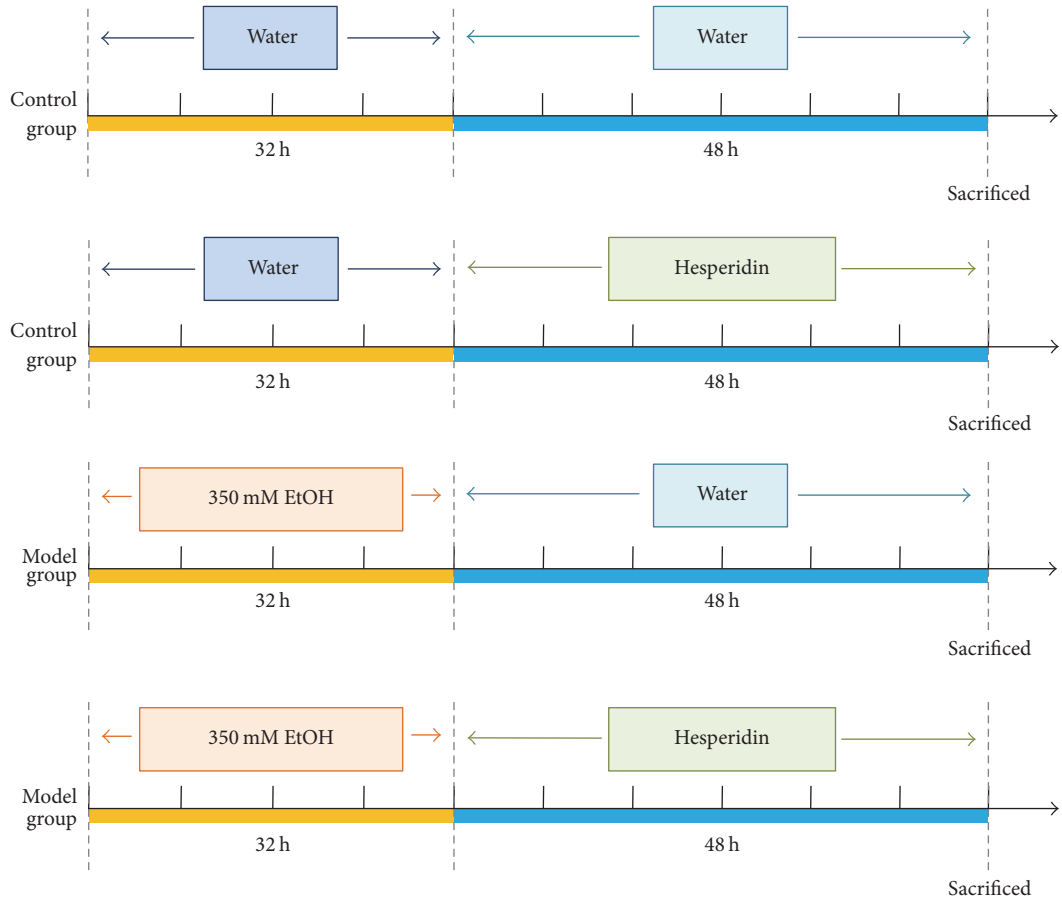

Figure 1: Experimental plan for zebrafish.

Table 1: Primers used to quantify mRNA levels.

Gene	FP sequence (5′-3′)	RP sequence (5′-3′)
cyp2y3	tattcccatgctgcactctg	aggagcgtttacctgcagaa
cyp3a65	aaaccctgatgagcatggac	caagtctttggggatgagga
hmgcra	ctgaggctctggtggacgtg	gatagcagctacgatgttggcg
hmgcrb	cctgttagccgtcagtgga	tctttgaccactcgtgccg
hmgcs	ctcactcgtgtggacgagaa	gatacggggcatcttcttga
fasn	gagaaagcttgccaaacagg	gagggtcttgcaggagacag
fads2	tcatcgtcgctgttattctgg	tgaagatgttgggtttagcgtg
chop	aggaaagtgcaggagctgac	ctccacaagaagaatttcctcc
gadd45αa	tggctttgtttgtgggactt	tggaaaacagtccactgaga
edem1	gacagcagaaaccctcaagc	catggccctcatcttgactt
rpp0	ctgaacatctcgcccttctc	tagccgatctgcagacacac

(5.5–6 dpf). During this period the metabolic effects of fasting could be avoided [13]. The acute alcoholic exposure time of zebrafish larvae was set to 32 hours, which is used to distinguish it from chronic exposure in alcoholics.

Taking previous studies into account, we discovered that morphological phenotypes, hepatomegaly, and behavioral abnormalities occurred in most of the larvae after having been treated with 350 mM ethanol for 32 hours [14, 15]. Histologic examinations of liver stained with H&E and Oil Red O revealed that severe lipid deposited in the liver tissues after 32 hours of exposure to 350 mM ethanol (Figures 2(a) and 2(b)). Furthermore, we discovered that 350 mM ethanol could lead to hepatic steatosis in zebrafish larvae after 32 hours of treatment, by quantification of Oil Red O staining in the liver, performed by Image J software (Figure 2(c)).

3.2. Hesperidin Reduced Hepatic Steatosis in Zebrafish Larvae Induced by Alcohol. As descried above, there existed severe lipid deposits in the liver tissues in larvae after alcoholic exposure. However, it was interesting that hesperidin could dose-dependently alleviate hepatic steatosis in larvae induced by alcohol (Figure 3(a)). The development of hepatic steatosis was quantified into gray level according to the results of Oil Red O staining by Image J software. The assessment of gray level further showed that hesperidin could reduce the development of hepatic steatosis with a dose-dependent correlation. The dose of 12.5 μg/mL and 25 μg/mL almost reversed the alcoholic lipid deposition in larvae (Figure 3(b)). On the other hand, using the Nile Red staining, a selective fluorescent dye for intracellular lipid droplets, we investigated whether hesperidin had a protective effect on liver of *Tg (lfabp10α:eGFP)* larvae after alcoholic exposure. Consistent with the results of Oil Red O staining, hesperidin (12.5 μg/mL, 48 hours) significantly alleviated hepatic lipid droplets

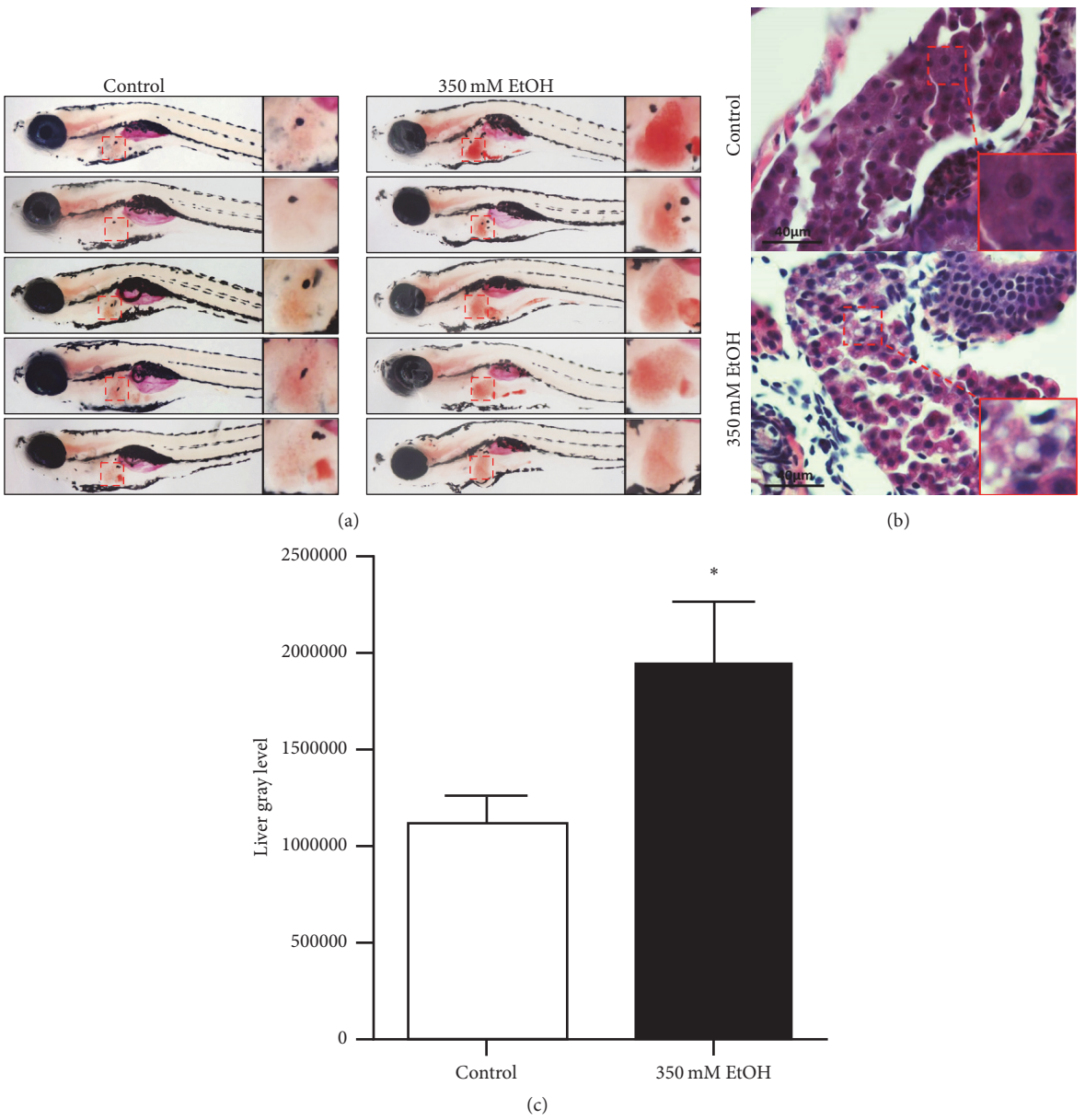

Figure 2: *Alcoholic fatty liver model was established in zebrafish larvae*. (a) Oil Red O staining for whole body of zebrafish larvae. (b) H&E staining for liver sections of zebrafish larvae. (c) Quantitative analysis for the results of Oil Red O staining (n = 20/group, three experiments). The data are presented as the means ± SEM ($^*P < 0.05$ versus control group).

induced by alcohol in larvae (Figure 3(c)). Furthermore, paraffin sections of larvae stained with H&E also confirmed the liver pathological changes consistently (Figure 3(d)). Additionally, Oil Red O staining and H&E staining showed that hesperidin does not have any substantial effects on livers of control zebrafish (Figures 3(a), 3(b), and 3(d)).

3.3. Hesperidin Improved Alcohol Metabolism in Zebrafish Larvae. We further investigated the effects of hesperidin on alcohol metabolism. Cytochrome P450 family 2 subfamily E member 1 *(cyp2e1)*, a crucial enzyme in regulation of oxidative stress response in alcohol metabolism process, is considered to be responsible for alcoholic liver injury in mammals. Cytochrome P450 family 2 subfamily Y polypeptide 3 *(cyp2y3)*, a gene homolog of cyp2e1, is essential for alcohol metabolism in liver of zebrafish [13]. Liver injury is dramatically increased due to the increase of *cyp2y3*, which could speed up the rate of alcohol metabolism and accumulation of acetaldehyde [13]. As showed in Table 2, the expression of *cyp2y3* mRNA was significantly increased compared with the control larvae. Interestingly, hesperidin intervention normalized the level of *cyp2y3* mRNA in larvae. Moreover, a similar change of the expression of cytochrome P450 family 3 subfamily A polypeptide 65 *(cyp3a65)* occurred, which is a homo gene of cytochrome P450 family 3 subfamily A *(cyp3a)* primarily in the liver and crucial to the metabolisms of both endogenous and exogenous substances [16]. These findings indicated that hesperidin might improve alcohol metabolism

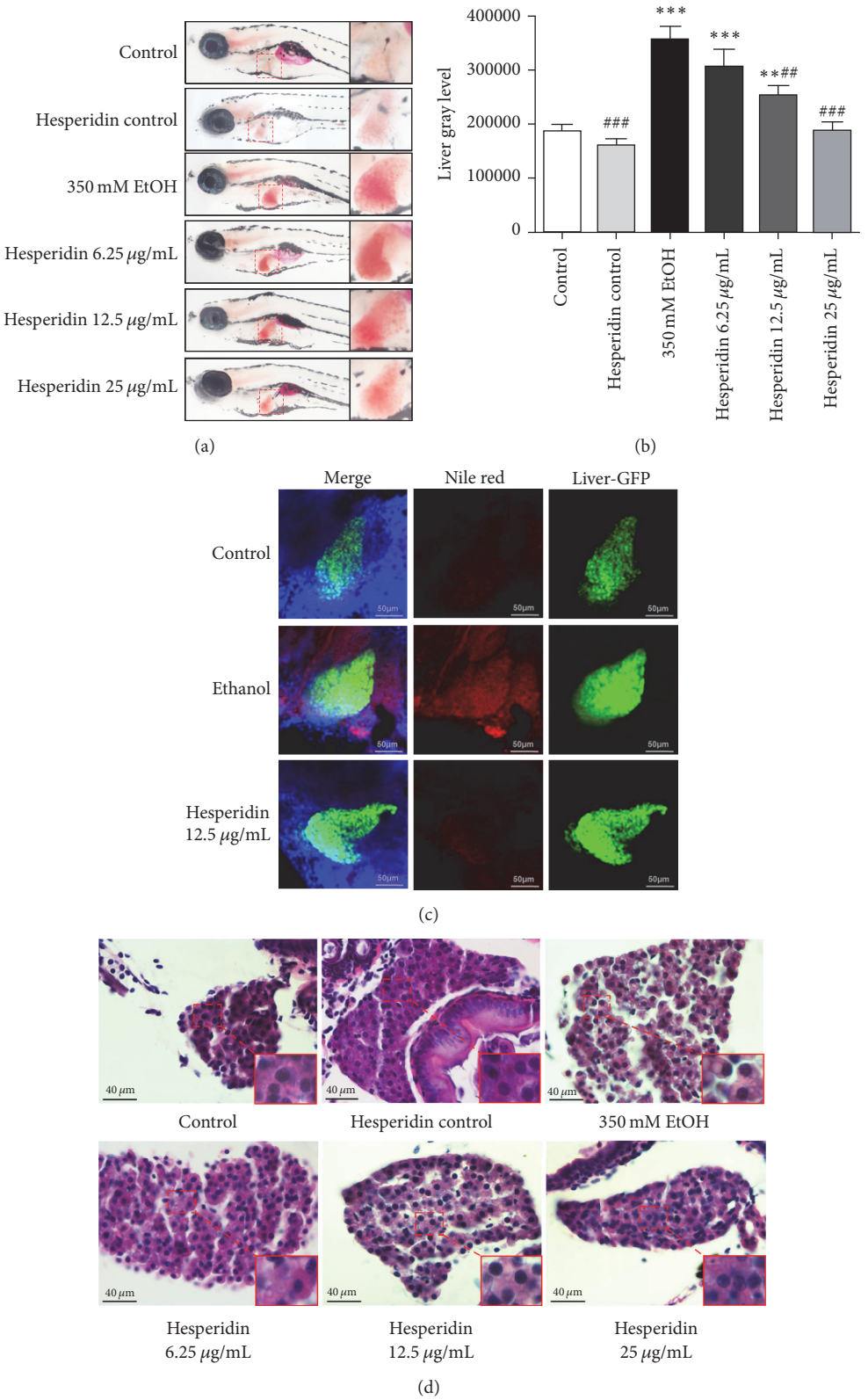

Figure 3: *Hesperidin reduced hepatic steatosis in zebrafish larvae induced by alcohol.* (a) Oil Red O staining for whole body of zebrafish larvae. (b) Quantitative analysis for the results of Oil Red O staining (n = 20/group, three experiments). (c) Nile Red staining for intracellular lipid droplets in liver tissues of zebrafish larvae. (d) H&E staining for liver sections of zebrafish larvae. The data are presented as the means ± SEM ($^{*}P < 0.05$ versus control group; $^{\#}P < 0.05$ versus 350 mM EtOH group).

Table 2: Hesperidin treatment improved alcohol metabolism in zebrafish larvae.

mRNA level (versus *rpp0*)	Group		
	Control	350 mM EtOH	Hesperidin (12.5 μg/mL)
cyp2y3	$1.659e-4 \pm 3.574e-5$	$3.04e-4 \pm 3.018e-5^{*}$	$1.677e-4 \pm 3.799e-5^{\#}$
cyp3a65	$1.565e-2 \pm 5.0e-5$	$1.77e-2 \pm 4.0e-4^{*}$	$1.135e-2 \pm 2.5e-4^{**\#\#\#}$

n = 20/group, three experiments; the data are presented as the means ± SEM ($^{*}P < 0.05$ versus control group; $^{\#}P < 0.05$ versus 350 mM EtOH group).

Table 3: Hesperidin treatment improved lipid metabolism in zebrafish larvae against alcoholic injury.

mRNA level (versus *rpp0*)	Group		
	Control	350 mM EtOH	Hesperidin (12.5 μg/mL)
hmgcra	$1.762e-4 \pm 8.408e-6$	$5.378e-4 \pm 1.006e-4^{***}$	$3.048e-4 \pm 2.663e-5^{\#}$
hmgcrb	$3.442e-4 \pm 7.15e-6$	$6.391e-4 \pm 1.011e-4^{*}$	$2.564e-4 \pm 3.55e-6^{\#}$
hmgcs	$1.575e-4 \pm 5.5e-6$	$1.87e-4 \pm 5.0e-6$	$1.305e-4 \pm 1.15e-5^{\#}$
fasn	$6.41e-4 \pm 3.1e-5$	$8.5e-4 \pm 6.0e-6^{**}$	$2.32e-4 \pm 1.0e-5^{**\#\#\#}$
fads2	$1.338e-4 \pm 3.525e-5$	$4.79e-4 \pm 4.8e-5^{*}$	$0.462e-4 \pm 1.04e-5^{\#\#}$

n = 20/group, three experiments; the data are presented as the means ± SEM ($^{*}P < 0.05$ versus control group; $^{\#}P < 0.05$ versus 350 mM EtOH group).

and reduce the accumulation of toxic substances in zebrafish larvae after exposure to ethanol.

3.4. Hesperidin Protected Zebrafish Larvae against Alcoholic Injury through Improving Lipid Metabolism. We further investigated some lipid metabolism related genes (*hmgcra*, *hmgcrb*, *hmgcs*, *fasn*, and *fads2*), which were related to cholesterol synthesis, fatty acid synthase, desaturase, and mitochondrial enzyme, in order to confirm whether hesperidin could protect against hepatic steatosis by reduction of lipid metabolism and improvement of lipid homeostasis [17–20]. The results of qPCR showed that the expressions of *hmgcra*, *hmgcrb*, *hmgcs*, *fasn*, and *fads2* mRNAs were significantly increased in larvae after treatment with alcohol. However, the intervention of hesperidin induced the levels of these mRNAs above to reversion (Table 3).

3.5. Hesperidin Reduced Endoplasmic Reticulum Stress and DNA Damage Induced by Alcohol in Zebrafish Larvae. Endoplasmic reticulum stress and DNA damage play key roles in various kinds of pathological liver damage induced by alcohol [21, 22]. We investigated the levels of mRNAs, DNA damage inducible transcript 3 *(chop)*, growth arrest, and DNA damage-inducible, α, a *(gadd45αa)* and endoplasmic reticulum degradation-enhancing α-mannosidase-like protein 1 *(edem1)*, which were related to endoplasmic reticulum stress and DNA damage [22–24]. The results of mRNAs levels also confirmed that hesperidin normalized the increased expressions of *chop*, *gadd45αa*, and *edem1* induced by alcohol (Table 4). Collectively, these evidences indicated that hesperidin suppressed endoplasmic reticulum stress and DNA damage.

4. Discussion

Hepatic steatosis, the earliest manifestation of alcoholism, can develop into some severe liver diseases [2]. Hepatocytes are susceptible to damage due to chronic hepatic steatosis, which is generally the early stage of steatohepatitis and cirrhosis [25]. Thus, further liver damage induced by alcohol can be prevented through the blockade of lipid accumulation. Moreover, it is reported that hesperidin in vivo can improve certain aspects of lipid homeostasis and reduce inflammation of adipose tissue [26]. However, there is no study about the effects of hesperidin on alcohol and metabolic abnormalities. To our knowledge, it is the first time that we investigated the effects of hesperidin on regulating alcohol metabolism, pathology, endoplasmic reticulum stress, and DNA damage in ALD on zebrafish. In this study, according to previous findings [14, 15], we successfully established an ALD zebrafish model by exposing zebrafish larvae to 350 mM ethanol for 32 hours. In addition, we discovered that the intervention of hesperidin could inhibit hepatic steatosis and endoplasmic reticulum stress of hepatocytes induced by acute alcoholic exposure.

The establishment of ALD zebrafish larvae is easy to operate and less time-consuming. Given that there exists difficulties of gaining liver tissues and blood from zebrafish larvae, we are not able to investigate the expressions of mRNAs and proteins of liver tissues or the serum levels of biochemical markers of liver injury directly. However, zebrafish larvae show more advantages on short growth cycle and transparent body, so we can obtain quantities of larvae in a short time and it is easier to get observation of the overall staining.

We discovered hesperidin protected against hepatic steatosis in zebrafish larvae after alcoholic exposure for the first time in this present study. Larvae stained with H&E and Oil Red O indicated that hesperidin could attenuate alcohol-induced hepatic steatosis and its therapeutic effect was dose-dependent. Moreover, the best and lowest treatment concentration is 12.5 μg/mL. Now that the antisteatosis effect of hesperidin was confirmed, we then investigated the possible effects of hesperidin against cell death and damage induced by alcohol. In addition, both *chop* and *gadd45αa* can inhibit cell growth while increasing cell damage [22, 23]. Transcription of lipid metabolism can be regulated by

Table 4: Hesperidin attenuates endoplasmic reticulum stress and DNA damage in zebrafish larvae with alcoholic injury.

mRNA level (versus *rpp0*)	Group		
	Control	350 mM EtOH	Hesperidin (12.5 μg/mL)
chop	$7.459e-3 \pm 2.27e-3$	$13.34e-3 \pm 5.576e-4^{*}$	$7.778e-3 \pm 1.029e-3^{\#}$
gadd45αa	$8.41e-4 \pm 3e-6$	$12.65e-4 \pm 4.5e-5^{**}$	$8.93e-4 \pm 2.8e-5^{\#\#}$
edem1	$1.739e-4 \pm 4.2e-6$	$3.007e-4 \pm 8.3e-6^{**}$	$1.427e-4 \pm 1.675e-5^{\#\#}$

$n = 20$/group, three experiments; the data are presented as the means ± SEM ($^{*}P < 0.05$ versus control group; $^{\#}P < 0.05$ versus 350 mM EtOH group).

chop, the upregulation of which can lead to abnormal lipid metabolism in the liver [27]. Moreover, *chop* is considered as a specific transcription factor of endoplasmic reticulum stress [22]. In another aspect, *edem1*, a gene essential for the unfolded protein response, was upregulated markedly with endoplasmic reticulum stress unbalance [24]. After exposure to alcohol, the expressions of *chop, gadd45αa*, and *edem1* were significantly increased in larvae, which indicated that the larvae were going through severe endoplasmic reticulum stress and DNA damage during that period. To the contrary, downregulation of chop, gadd45αa, and edem1 were induced in larvae after being treated with hesperidin. Collectively, we summed up that hesperidin could inhibit steatosis and damage of liver in zebrafish larvae after alcoholic exposure.

HMG-CoA reductases are key enzymes in lipid metabolism, including HMG Coenzyme A reductase a *(hmgcra),* HMG Coenzyme A reductase b *(hmgcrb)*, and 3-hydroxy-3-methylglutaryl-CoA synthase *(hmgcs)*, mainly regulating genes related to cholesterol synthesis [14, 17, 28]. Besides, synthesis and desaturation of fatty acid can be regulated by fatty acid synthase *(fasn)* [19]. Fatty acid desaturase 2 *(fads2)*, a gene related to dyslipidemia, primarily participates in metabolism of unsaturated fatty acids, affecting the concentrations of total cholesterol, low density lipoprotein cholesterol, high lipoprotein cholesterol, and triglyceride [18]. In our study, the expressions of *hmgcra*, *hmgcrb*, *hmgcs*, *fasn,* and *fads2* genes related to lipid metabolism were significantly increased in larvae after alcoholic exposure, which indicated that treatment with alcohol could cause lipid metabolism disorders in zebrafish larvae. However, hesperidin markedly ameliorated lipid metabolism through mediating the expressions of these genes above.

In another aspect, *cyp2y3* and *cyp3a65*, homologous genes of cytochrome P450 CYP2 *(cyp2)* and *cyp3a*, are essential for alcoholic metabolism mainly in liver of zebrafish. The closest homolog to *cyp2e1* in zebrafish is *cyp2y3*, which has a protein similarity of 43% [13]. Alcohol metabolism and oxidative stress can be decreased by blocking *cyp2* homologous genes. In addition, *cyp3a65* is crucial to metabolism of both endogenous and exogenous substances [16]. Interestingly, we found that the treatment of hesperidin could reduce the levels of *cyp2y3* and *cyp3a65* in larvae, which were upregulated by alcoholic exposure previously. The underlying mechanism of the therapeutical effect of hesperidin was likely to be related to the improvement of alcoholic metabolism and reduction of toxic substances. Taking all these evidences above, we discovered that alcohol-induced liver injury of zebrafish larvae was mainly caused by dysbolisms of lipid and alcohol. However, these dysbolisms could be improved by hesperidin, which resisted alcohol-induced steatosis and injury therefore. Finally, we summarized the protective effects of hesperidin in zebrafish larvae during acute alcoholic injury as showed in Figure 4.

In conclusion, we revealed that hesperidin inhibited hepatic steatosis and injury in zebrafish induced by alcohol, by ameliorating cell damage and regulating metabolism of alcohol and lipid. However, the pathways of effects of hesperidin on reducing cell damage and lipid metabolism still need further exploration. Hesperidin is abundant in citrus fruits and grape fruit [26], which indicates that hesperidin easily accumulates in the plasma and is available in vivo when humans intake hesperidin-containing food regularly. Thus, whether hesperidin is suitable for prevention of ALD and lipid metabolism syndrome needs further preclinical investigation.

Abbreviations

ALD: Alcoholic liver disease
PBS: Phosphate-buffered saline
PFA: Paraformaldehyde
H&E: Hematoxylin and eosin
qPCR: Real-time quantitative PCR
hpf: Hours after fertilization
dpf: Days after fertilization
rpp0: Ribosomal protein P0
cyp2e1: Cytochrome P450 family 2 subfamily E member 1
cyp2y3: Cytochrome P450, family 2, subfamily Y, polypeptide 3
cyp3a65: Cytochrome P450, family 3, subfamily A, polypeptide 65
cyp3a: Cytochrome P450, family 3, subfamily A
chop: DNA damage inducible transcript 3
gadd45αa: Growth arrest and DNA damage-inducible, alpha, a
hmgcra: HMG Coenzyme A reductase a
hmgcrb: HMG Coenzyme A reductase b
fasn: Fatty acid synthase
fads2: Fatty acid desaturase 2
fabp10α: Fatty acid binding protein 10a
edem1: Endoplasmic reticulum degradation-enhancing α-mannosidase-like protein 1.

Conflicts of Interest

The authors do not have any disclosures to report.

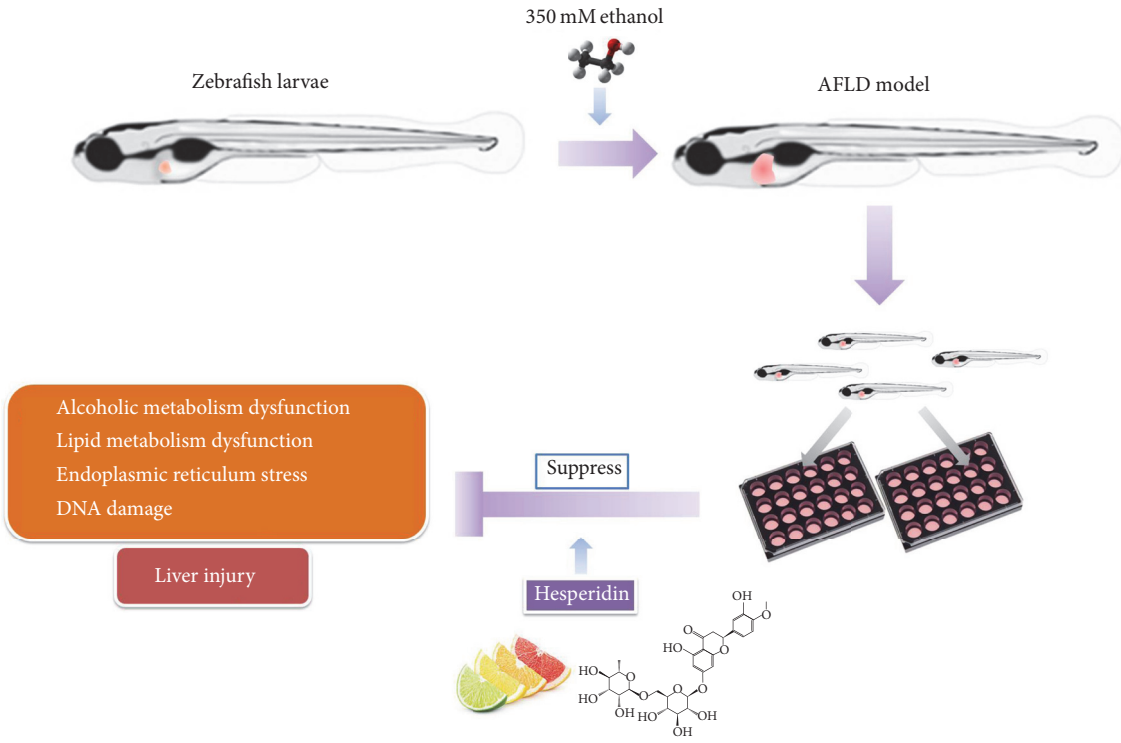

Figure 4: A model depicting the protective role of hesperidin in zebrafish larvae during acute alcoholic injury.

Authors' Contributions

Lei Gao and Zhiping Lv participated in conception and design of the study; Zhenting Zhou, Haiyan Lin, Peng Huang, Ning Ma, and Yuqing Zhang participated in generation, collection, assembly, and interpretation of data; Lei Gao, Weichao Zhong, and Shiying Huang participated in drafting and revision of the manuscript; Chuying Zhou and Yuling Lai participated in statistical analysis; Lei Gao, Zhiping Lv, and Shaohui Huang obtained funding; Zhiping Lv and Lei Gao participated in study supervision. Lei Gao and Zhiping Lv contributed equally to this work. Zhenting Zhou, Weichao Zhong, and Haiyan Lin contributed equally to this work and are co-first authors.

Acknowledgments

This work was supported by the National Natural Science Foundation of China (81603501 and 81302948), Science and Technology Planning Project of Guangzhou City (201508020014 and 201707010080), Science and Technology Planning Project of Guangdong Province (2014A020221097), China Postdoctoral Science Foundation (2016M592508), Administration of Traditional Chinese Medicine of Guangdong Province (20162087), and the Scientific Research Initiative Program of Southern Medical University (LX2015N003, PY2016N001). The authors thank Miss Haiyan An (Southern Medical University, Guangzhou, China) for technical assistance.

References

[1] H. Ni, A. Bhakta, S. Wang et al., "Role of hypoxia inducing factor-1β in alcohol-induced autophagy, steatosis and liver injury in mice," *PLoS ONE*, vol. 9, no. 12, Article ID e115849, 2014.

[2] E. S. Orman, G. Odena, and R. Bataller, "Alcoholic liver disease: pathogenesis, management, and novel targets for therapy," *Journal of Gastroenterology and Hepatology*, vol. 28, no. 1, pp. 77–84, 2013.

[3] A. Çetin, O. Çiftçi, and A. Otlu, "Protective effect of hesperidin on oxidative and histological liver damage following carbon tetrachloride administration in Wistar rats," *Archives of Medical Science*, vol. 12, no. 3, pp. 486–493, 2016.

[4] S. H. Bok, S. H. Lee, Y. B. Park et al., "Plasma and hepatic cholesterol and hepatic activities of 3-hydroxy-3-methyl-glutaryl-CoA reductase and acyl CoA: cholesterol transferase are lower in rats fed citrus peel extract or a mixture of citrus bioflavonoids," *The Journal of Nutrition*, vol. 129, no. 6, pp. 1182–1185, 1999.

[5] Y. B. Park, K. M. Do, S. H . Bok, M. K. Lee, T. S. Jeong, and M. S. Choi, "Interactive effect of hesperidin and vitamin E supplements on cholesterol metabolism in High cholesterol-fed rats," *International Journal for Vitamin and Nutrition Research*, vol. 71, no. 1, pp. 36–44, 2001.

[6] X. Wang, J. Hasegawa, Y. Kitamura et al., "Effects of hesperidin on the progression of hypercholesterolemia and fatty liver induced by high-cholesterol diet in rats," *Journal of Pharmacological Sciences*, vol. 117, no. 3, pp. 129–138, 2011.

[7] J. E. Pérez-Vargas, N. Zarco, M. Shibayama, J. Segovia, V. Tsutsumi, and P. Muriel, "Hesperidin prevents liver fibrosis

in rats by decreasing the expression of nuclear factor-κB, transforming growth factor-β and connective tissue growth factor," *Pharmacology*, vol. 94, pp. 80–89, 2014.

[8] D. L. Howarth, C. Yin, K. Yeh, and K. C. Sadler, "Defining hepatic dysfunction parameters in two models of fatty liver disease in zebrafish larvae," *Zebrafish*, vol. 10, no. 2, pp. 199–210, 2013.

[9] W. Dai, K. Wang, X. Zheng et al., "High fat plus high cholesterol diet lead to hepatic steatosis in zebrafish larvae: a novel model for screening anti-hepatic steatosis drugs," *Nutrition and Metabolism*, vol. 12, Article 42, 2015.

[10] P. Greenspan, E. P. Mayer, and S. D. Fowler, "Nile red: a selective fluorescent stain for intracellular lipid droplets," *Journal of Cell Biology*, vol. 100, no. 3, pp. 965–973, 1985.

[11] D. Pardal, M. Caro, I. Tueros, A. Barranco, and V. Navarro, "Resveratrol and piceid metabolites and their fat-reduction effects in zebrafish larvae," *Zebrafish*, vol. 11, no. 1, pp. 32–40, 2014.

[12] L. Gao, Y. Zhou, W. Zhong et al., "Caveolin-1 is essential for protecting against binge drinking-induced liver damage through inhibiting reactive nitrogen species," *Hepatology*, vol. 60, no. 2, pp. 687–699, 2014.

[13] O. Tsedensodnom, A. M. Vacaru, D. L. Howarth, C. Yin, and K. C. Sadler, "Ethanol metabolism and oxidative stress are required for unfolded protein response activation and steatosis in zebrafish with alcoholic liver disease," *Disease Models & Mechanisms*, vol. 6, no. 5, pp. 1213–1226, 2013.

[14] M. J. Passeri, A. Cinaroglu, C. Gao, and K. C. Sadler, "Hepatic steatosis in response to acute alcohol exposure in zebrafish requires sterol regulatory element binding protein activation," *Hepatology*, vol. 49, no. 2, pp. 443–452, 2009.

[15] D. L. Howarth, M. Passeri, and K. C. Sadler, "Drinks like a fish: using zebrafish to understand alcoholic liver disease," *Alcoholism: Clinical and Experimental Research*, vol. 35, no. 5, pp. 826–829, 2011.

[16] H.-P. Tseng, T.-H. Hseu, D. R. Buhler, W.-D. Wang, and C.-H. Hu, "Constitutive and xenobiotics-induced expression of a novel CYP3A gene from zebrafish larva," *Toxicology and Applied Pharmacology*, vol. 205, no. 3, pp. 247–258, 2005.

[17] S. Suganya, B. Nandagopal, and A. Anbarasu, "Natural Inhibitors of HMG-CoA Reductase-An Insilico Approach Through Molecular Docking and Simulation Studies," *Journal of Cellular Biochemistry*, vol. 18, no. 1, pp. 52–57, 2016.

[18] Y. Tian, W. Zhang, S. Zhao et al., "FADS1-FADS2 gene cluster confers risk to polycystic ovary syndrome," *Scientific Reports*, vol. 6, Article ID 21195, 2016.

[19] M. Zappaterra, M. Deserti, R. Mazza, S. Braglia, P. Zambonelli, and R. Davoli, "A gene and protein expression study on four porcine genes related to intramuscular fat deposition," *Meat Science*, vol. 121, pp. 27–32, 2016.

[20] T. S. Angeles and R. L. Hudkins, "Recent advances in targeting the fatty acid biosynthetic pathway using fatty acid synthase inhibitors," *Expert Opinion on Drug Discovery*, vol. 11, no. 12, pp. 1187–1199, 2016.

[21] Z. Ren, X. Wang, M. Xu et al., "Binge ethanol exposure causes endoplasmic reticulum stress, oxidative stress and tissue injury in the pancreas," *Oncotarget*, vol. 7, no. 34, pp. 54303–54316, 2016.

[22] H. Malhi and R. J. Kaufman, "Endoplasmic reticulum stress in liver disease," *Journal of Hepatology*, vol. 54, no. 4, pp. 795–809, 2011.

[23] X.-X. Zhao, Y.-B. Zhang, P.-L. Ni, Z.-L. Wu, Y.-C. Yan, and Y.-P. Li, "Protein arginine methyltransferase 6 (Prmt6) is essential for early zebrafish development through the direct suppression of gadd45αa stress sensor gene," *Journal of Biological Chemistry*, vol. 291, no. 1, pp. 402–412, 2016.

[24] J. Soeda, A. Mouralidarane, P. Cordero et al., "Maternal obesity alters endoplasmic reticulum homeostasis in offspring pancreas," *Journal of Physiology and Biochemistry*, pp. 1–11, 2016.

[25] D. L. Howarth, C. Lindtner, A. M. Vacaru et al., "Activating transcription factor 6 is necessary and sufficient for alcoholic fatty liver disease in zebrafish," *PLoS Genetics*, vol. 10, no. 5, Article ID e1004335, 2014.

[26] P. Selvaraj and K. V. Pugalendi, "Efficacy of hesperidin on plasma, heart and liver tissue lipids in rats subjected to isoproterenol-induced cardiotoxicity," *Experimental and Toxicologic Pathology*, vol. 64, no. 5, pp. 449–452, 2012.

[27] D. T. Rutkowski, J. Wu, S.-H. Back et al., "UPR pathways combine to prevent hepatic steatosis caused by ER stress-mediated suppression of transcriptional master regulators," *Developmental Cell*, vol. 15, no. 6, pp. 829–840, 2008.

[28] P. Cocci, G. Mosconi, and F. A. Palermo, "Partial cloning, tissue distribution and effects of epigallocatechin gallate on hepatic 3-hydroxy-3-methylglutaryl-CoA reductase mRNA transcripts in goldfish (Carassius auratus)," *Gene*, vol. 545, no. 2, pp. 220–225, 2014.